horizontal translation), q_{max} was at the heel of the wall with q_{min} at the toe. On November 27, 2001, when the height of the fill was 7.6 m (25 ft), q_{max} at the heel was about 140 kN/m^2 (2922 lb/ft^2), which was approximately equal to (γ_1)(height of fill) $=(18.9)(7.6) = 143.6$ kN/m^2. Also, at the toe, q_{min} was about 40 kN/m^2 (835 lb/ft^2), which suggests that the moment from lateral force had little effect on the vertical effective stress below the heel.

The lessons learned from this case study are the following:

a. Retaining walls may undergo lateral translation which will affect the variation of q_{max} and q_{min} along the base slab.
b. Initial lateral stress caused by compaction gradually decreases with time and lateral movement of the wall.

Mechanically Stabilized Retaining Walls

More recently, soil reinforcement has been used in the construction and design of foundations, retaining walls, embankment slopes, and other structures. Depending on the type of construction, the reinforcements may be galvanized metal strips, geotextiles, geogrids, or geocomposites. Sections 8.11 and 8.12 provide a general overview of soil reinforcement and various reinforcement materials.

Reinforcement materials such as metallic strips, geotextiles, and geogrids are now being used to reinforce the backfill of retaining walls, which are generally referred to as *mechanically stabilized retaining walls.* The general principles for designing these walls are given in the following sections.

8.11 Soil Reinforcement

The use of reinforced earth is a recent development in the design and construction of foundations and earth-retaining structures. *Reinforced earth* is a construction material made from soil that has been strengthened by tensile elements such as metal rods or strips, nonbiodegradable fabrics (geotextiles), geogrids, and the like. The fundamental idea of reinforcing soil is not new; in fact, it goes back several centuries. However, the present concept of systematic analysis and design was developed by a French engineer, H. Vidal (1966). The French Road Research Laboratory has done extensive research on the applicability and the beneficial effects of the use of reinforced earth as a construction material. This research has been documented in detail by Darbin (1970), Schlosser and Long (1974), and Schlosser and Vidal (1969). The tests that were conducted involved the use of metallic strips as reinforcing material.

Retaining walls with reinforced earth have been constructed around the world since Vidal began his work. The first reinforced-earth retaining wall with metal strips as reinforcement in the United States was constructed in 1972 in southern California.

The beneficial effects of soil reinforcement derive from (a) the soil's increased tensile strength and (b) the shear resistance developed from the friction at the soil-reinforcement interfaces. Such reinforcement is comparable to that of concrete structures. Currently, most reinforced-earth design is done with *free-draining granular soil only.* Thus, the effect of pore water development in cohesive soils, which, in turn, reduces the shear strength of the soil, is avoided.

8.12 Considerations in Soil Reinforcement

Metal Strips

In most instances, galvanized steel strips are used as reinforcement in soil. However, galvanized steel is subject to corrosion. The rate of corrosion depends on several environmental factors. Binquet and Lee (1975) suggested that the average rate of corrosion of galvanized steel strips varies between 0.025 and 0.050 mm/yr. So, in the actual design of reinforcement, allowance must be made for the rate of corrosion. Thus,

$$t_c = t_{\text{design}} + r \text{ (life span of structure)}$$

where

t_c = actual thickness of reinforcing strips to be used in construction
t_{design} = thickness of strips determined from design calculations
r = rate of corrosion

Further research needs to be done on corrosion-resistant materials such as fiberglass before they can be used as reinforcing strips.

Nonbiodegradable Fabrics

Nonbiodegradable fabrics are generally referred to as *geotextiles*. Since 1970, the use of geotextiles in construction has increased greatly around the world. The fabrics are usually made from petroleum products—polyester, polyethylene, and polypropylene. They may also be made from fiberglass. Geotextiles are not prepared from natural fabrics, because they decay too quickly. Geotextiles may be woven, knitted, or nonwoven.

Woven geotextiles are made of two sets of parallel filaments or strands of yarn systematically interlaced to form a planar structure. *Knitted geotextiles* are formed by interlocking a series of loops of one or more filaments or strands of yarn to form a planar structure. *Nonwoven geotextiles* are formed from filaments or short fibers arranged in an oriented or random pattern in a planar structure. These filaments or short fibers are arranged into a loose web in the beginning and then are bonded by one or a combination of the following processes:

1. *Chemical bonding*—by glue, rubber, latex, a cellulose derivative, or the like
2. *Thermal bonding*—by heat for partial melting of filaments
3. *Mechanical bonding*—by needle punching

Needle-punched nonwoven geotextiles are thick and have high in-plane permeability.

Geotextiles have four primary uses in foundation engineering:

1. *Drainage:* The fabrics can rapidly channel water from soil to various outlets, thereby providing a higher soil shear strength and hence stability.
2. *Filtration:* When placed between two soil layers, one coarse grained and the other fine grained, the fabric allows free seepage of water from one layer to the other. However, it protects the fine-grained soil from being washed into the coarse-grained soil.
3. *Separation:* Geotextiles help keep various soil layers separate after construction and during the projected service period of the structure. For example, in the construction of highways, a clayey subgrade can be kept separate from a granular base course.
4. *Reinforcement:* The tensile strength of geofabrics increases the load-bearing capacity of the soil.

Geogrids

Geogrids are high-modulus polymer materials, such as polypropylene and polyethylene, and are prepared by tensile drawing. Netlon, Ltd., of the United Kingdom was the first producer of geogrids. In 1982, the Tensar Corporation, presently Tensar International Corporation, introduced geogrids into the United States.

Geogrids generally are of two types: (a) uniaxial and (b) biaxial. Figures 8.22a and b shows these two types of geogrids, which are produced by Tensar International Corporation.

Commercially available geogrids may be categorized by manufacturing process, principally: extruded, woven, and welded. Extruded geogrids are formed using a thick sheet of polyethylene or polypropylene that is punched and drawn to create apertures and to enhance engineering properties of the resulting ribs and nodes. Woven geogrids are manufactured by grouping polymeric—usually polyester and polypropylene—and weaving them into a mesh pattern that is then coated with a polymeric lacquer. Welded geogrids are manufactured by fusing junctions of polymeric strips. Extruded geogrids have shown good performance when compared to other types for pavement reinforcement applications.

Uniaxial TENSAR grids are manufactured by stretching a punched sheet of extruded high-density polyethylene in one direction under carefully controlled conditions. The process aligns the polymer's long-chain molecules in the direction of draw and results in a product with high one-directional tensile strength and a high modulus. Biaxial TENSAR grids are manufactured by stretching the punched sheet of polypropylene in two orthogonal directions. This process results in a product with high tensile strength and a high modulus in two perpendicular directions. The resulting grid apertures are either square or rectangular.

The commercial geogrids currently available for soil reinforcement have nominal rib thicknesses of about 0.5 to 1.5 mm (0.02 to 0.06 in.) and junctions of about 2.5 to 5 mm (0.1 to 0.2 in.). The grids used for soil reinforcement usually have openings or apertures that are rectangular or elliptical. The dimensions of the apertures vary from about 25 to 150 mm (1 to 6 in.). Geogrids are manufactured so that the open areas of the grids are greater than 50% of the total area. They develop reinforcing strength at low strain levels, such as 2% (Carroll, 1988). Table 8.4 gives some properties of the TENSAR biaxial geogrids that are currently available commercially.

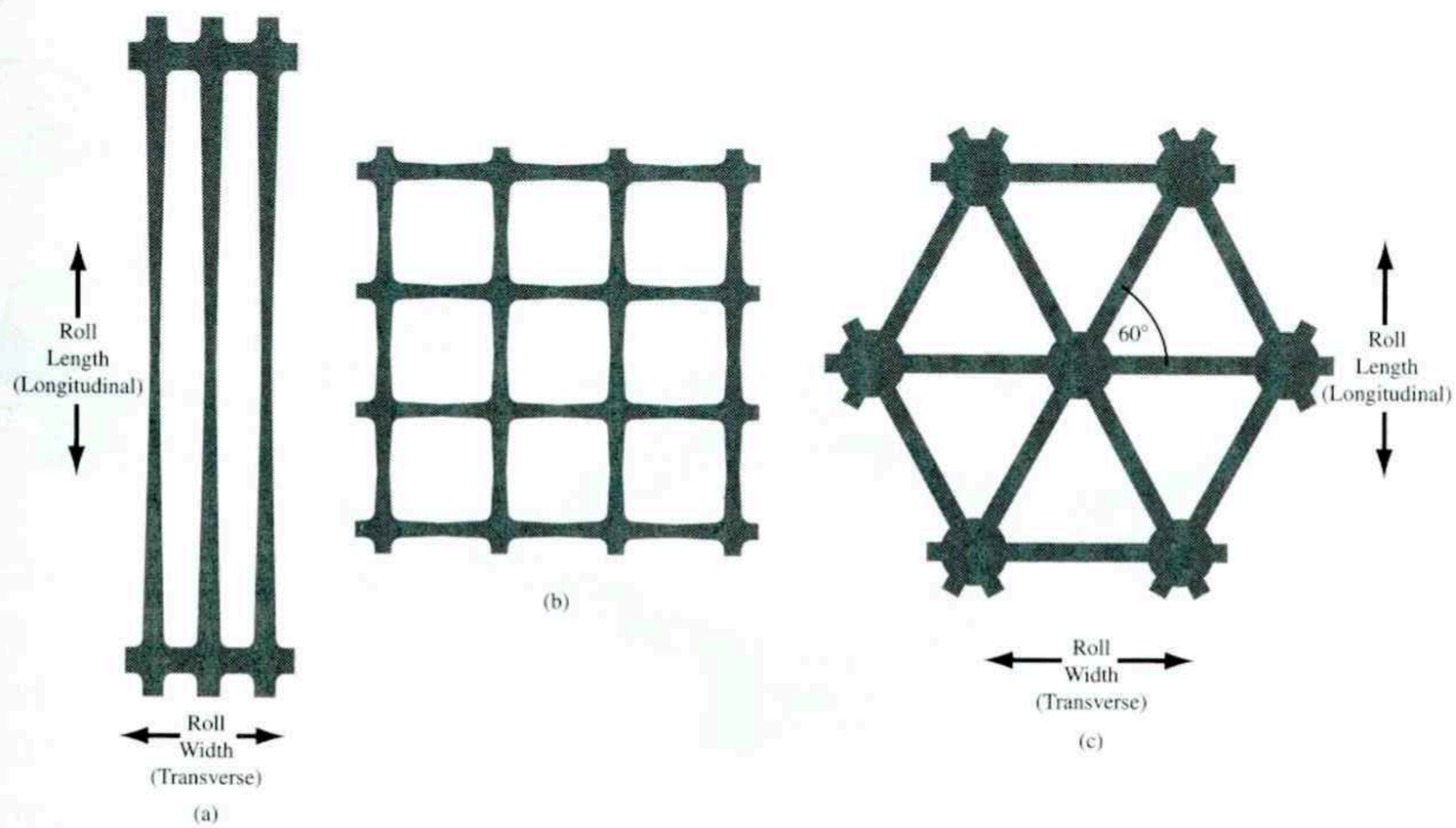

Figure 8.22 Geogrid: (a) uniaxial; (b) biaxial; (c) with triangular apertures (*Courtesy of Tensar International Corporation*)

Table 8.4 Properties of TENSAR Biaxial Geogrids

Property	Geogrid		
	BX1000	BX1100	BX1200
Aperture size			
Machine direction	25 mm (1 in.) (nominal)	25 mm (1 in.) (nominal)	25 mm (1 in.) (nominal)
Cross-machine direction	33 mm (1.3 in.) (nominal)	33 mm (1.3 in.) (nominal)	33 mm (1.3 in.) (nominal)
Open area	70% (minimum)	74% (nominal)	77% (nominal)
Junction			
Thickness	2.3 mm (0.09 in.) (nominal)	2.8 mm (0.11 in.) (nominal)	4.1 mm (0.16 in.) (nominal)
Tensile modulus			
Machine direction	182 kN/m (12,500 lb/ft) (minimum)	204 kN/m (14,000 lb/ft) (minimum)	270 kN/m (18,500 lb/ft) (minimum)
Cross-machine direction	182 kN/m (12,500 lb/ft) (minimum)	292 kN/m (20,000 lb/ft) (minimum)	438 kN/m (30,000 lb/ft) (minimum)
Material			
Polypropylene	97% (minimum)	99% (nominal)	99% (nominal)
Carbon black	2% (minimum)	1% (nominal)	1% (nominal)

The major function of geogrids is *reinforcement*. They are relatively stiff. The apertures are large enough to allow interlocking with surrounding soil or rock (Figure 8.23) to perform the function of reinforcement or segregation (or both). Sarsby (1985) investigated the influence of aperture size on the size of soil particles for maximum frictional efficiency (or efficiency against pullout). According to this study, the highest efficiency occurs when

$$B_{GG} > 3.5D_{50} \tag{8.30}$$

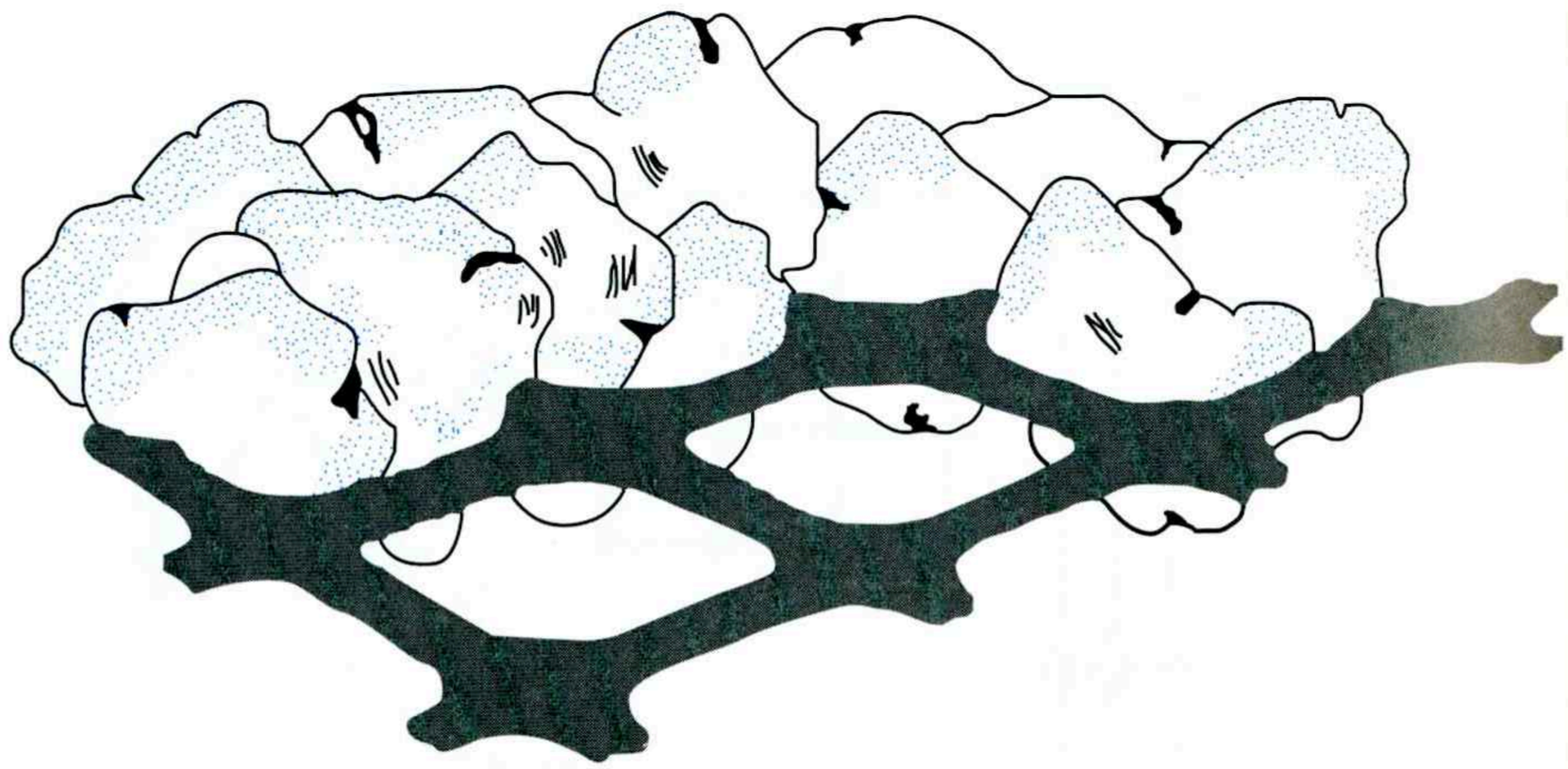

Figure 8.23 Geogrid apertures allowing interlocking with surrounding soil

where

B_{GG} = minimum width of the geogrid aperture
D_{50} = the particle size through which 50% of the backfill soil passes (i.e., the average particle size)

More recently, geogrids with triangular apertures (Figure 8.22c) have been introduced for construction purposes. TENSAR geogrids with triangular apertures are manufactured from a punched polypropylene sheet, which is then oriented in three substantially equilateral directions so that the resulting ribs shall have a high degree of molecular orientation. Table 8.5 gives some properties of TENSAR geogrids with triangular apertures.

Table 8.5 Properties of TENSAR Geogrids with Triangular Apertures

Geogrid	Property	Longitudinal	Diagonal	Transverse	General
TX 160	Rib pitch, mm (in.)	40 (1.60)	40 (1.60)	—	
	Mid-rib depth, mm (in.)	—	1.8 (0.07)	1.5 (0.06)	
	Mid-rib width, mm (in.)	—	1.1 (0.04)	1.3 (0.05)	
	Nodal thickness, mm (in.)				3.1 (0.12)
	Radial stiffness at low strain, kN/m @ 0.5% strain (lb/ft @ 0.5% strain)				430 (29,500)
TX 170	Rib pitch, mm (in.)	40 (1.60)	40 (1.60)	—	
	Mid-rib depth, mm (in.)	—	2.3 (0.09)	1.8 (0.07)	
	Mid-rib width, mm (in.)	—	1.2 (0.05)	1.3 (0.05)	
	Nodal thickness, mm (in.)				4.1 (0.16)
	Radial stiffness at low strain, kN/m @ 0.5% strain (lb/ft @ 0.5% strain)				475 (32,500)

8.13 General Design Considerations

The general design procedure of any mechanically stabilized retaining wall can be divided into two parts:

1. Satisfying *internal stability* requirements
2. Checking the *external stability* of the wall

The internal stability checks involve determining tension and pullout resistance in the reinforcing elements and ascertaining the integrity of facing elements. The external stability checks include checks for overturning, sliding, and bearing capacity failure (Figure 8.24). The sections that follow will discuss the retaining-wall design procedures for use with metallic strips, geotextiles, and geogrids.

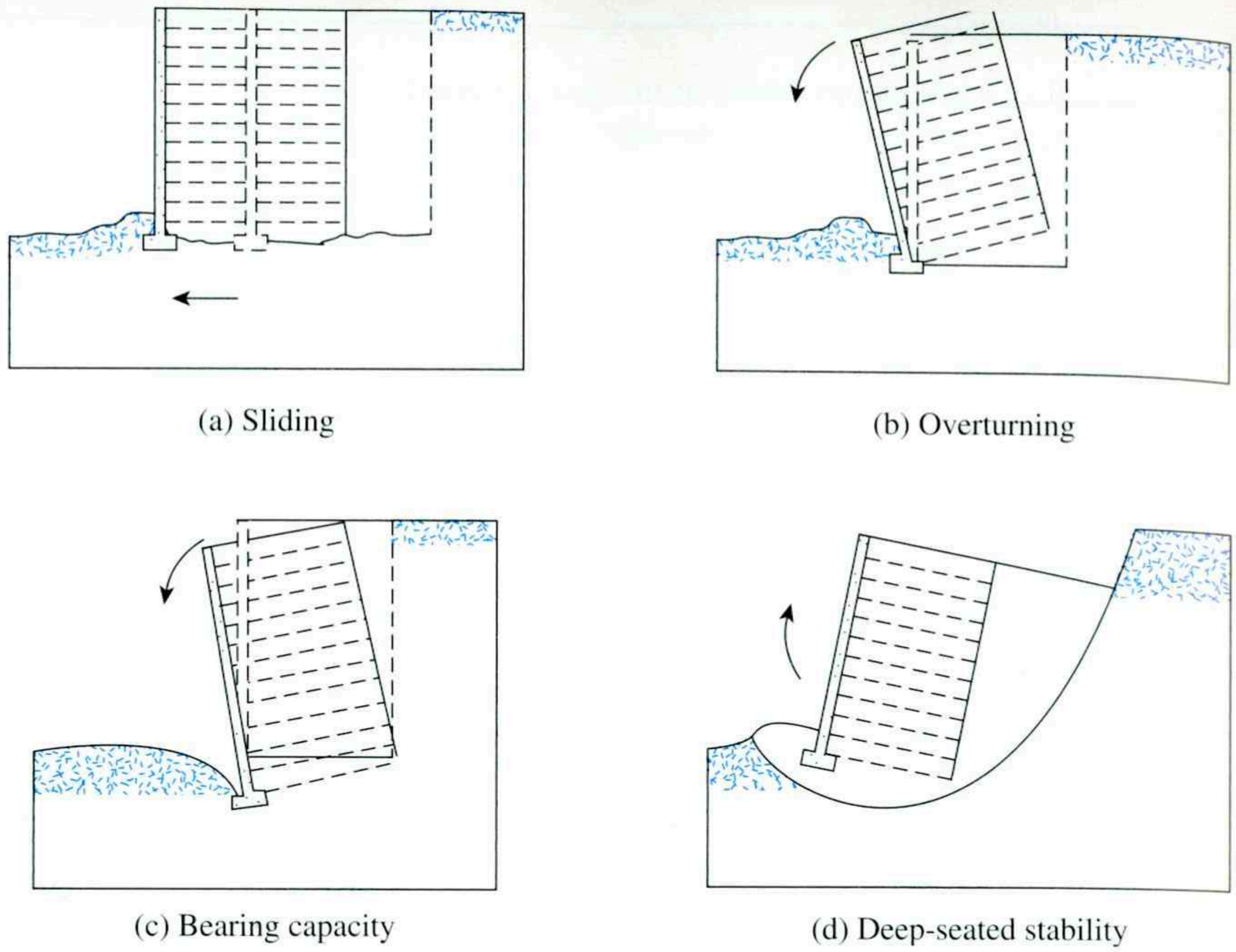

Figure 8.24 External stability checks (After Transportation Research Board, 1995) (From Transportation Research Circular 444: Mechanically Stabilized Earth Walls. Transportation Research Board, National Research Council, Washington, D.C., 1995, Figure 3, p. 7. Reproduced with permission of the Transportation Research Board.)

8.14 Retaining Walls with Metallic Strip Reinforcement

Reinforced-earth walls are flexible walls. Their main components are

1. *Backfill,* which is granular soil
2. *Reinforcing strips,* which are thin, wide strips placed at regular intervals, and
3. *A cover* or *skin,* on the front face of the wall

Figure 8.25 is a diagram of a reinforced-earth retaining wall. Note that, at any depth, the reinforcing strips or ties are placed with a horizontal spacing of S_H center to center; the vertical spacing of the strips or ties is S_V center to center. The skin can be constructed with sections of relatively flexible thin material. Lee et al. (1973) showed that, with a conservative design, a 5 mm-thick ($\approx$0.2 in.) galvanized steel skin would be enough to hold a wall about 14 to 15 m (45 to 50 ft) high. In most cases, precast concrete slabs can also be used as skin. The slabs are grooved to fit into each other so that soil cannot flow out between the joints. When metal skins are used, they are bolted together, and reinforcing strips are placed between the skins.

Figures 8.26 and 8.27 show a reinforced-earth retaining wall under construction; its skin (facing) is a precast concrete slab. Figure 8.28 shows a metallic reinforcement tie attached to the concrete slab.

The simplest and most common method for the design of ties is the *Rankine method.* We discuss this procedure next.

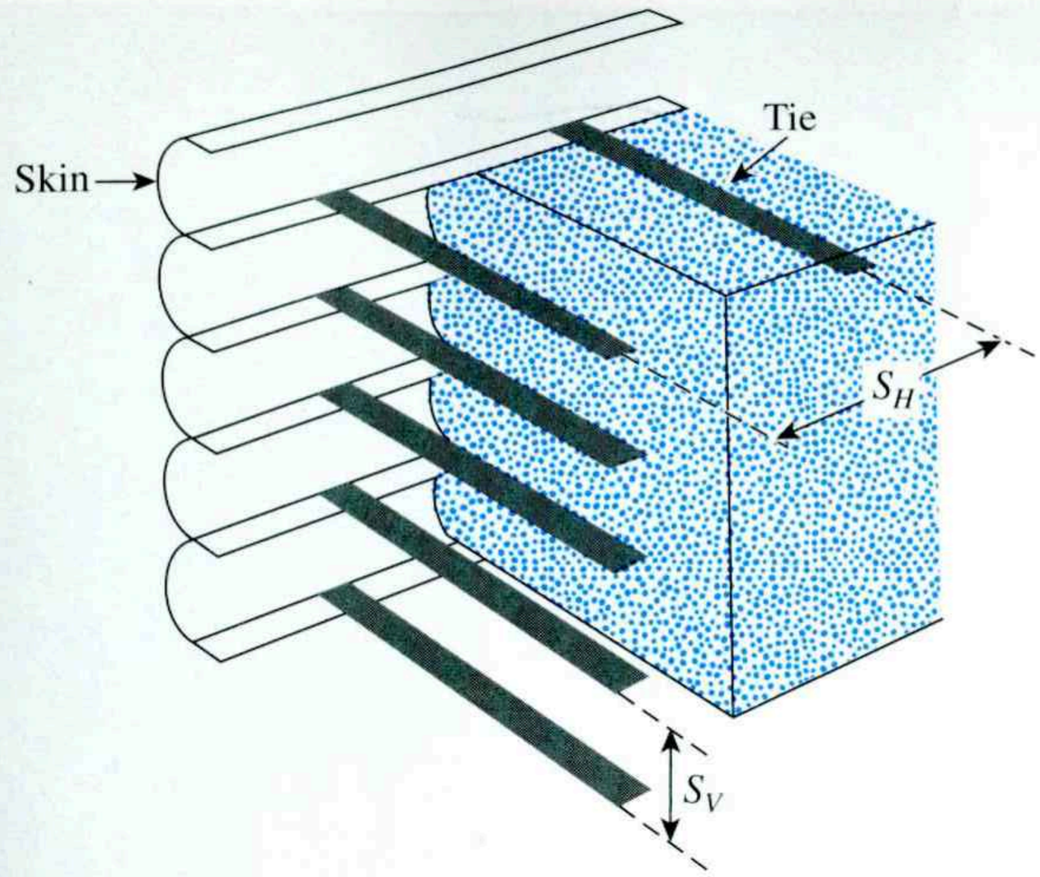

Figure 8.25 Reinforced-earth retaining wall

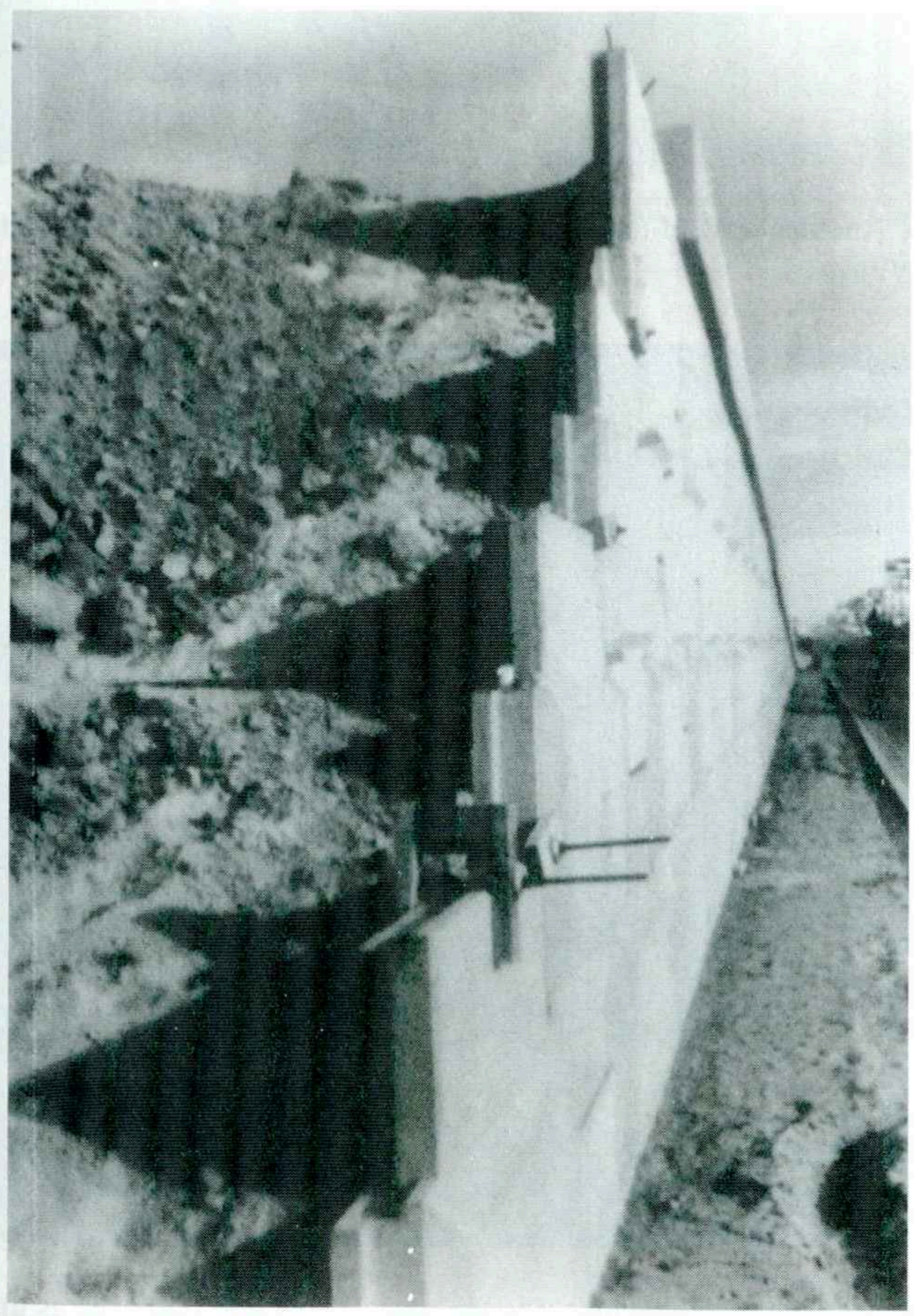

Figure 8.26 Reinforced-earth retaining wall (with metallic strip) under construction (*Courtesy of Braja M. Das, Henderson, NV*)

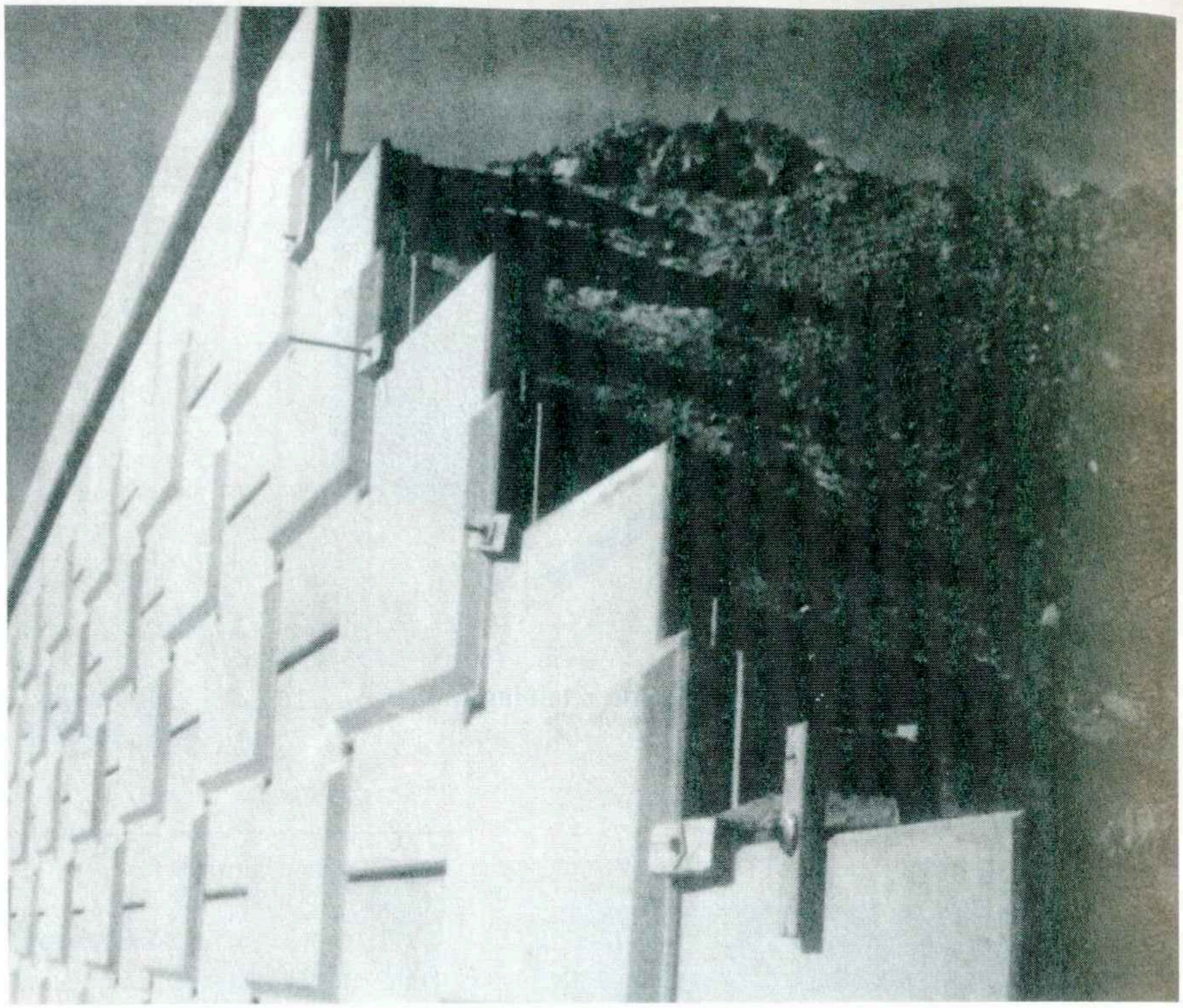

Figure 8.27 Another view of the retaining wall shown in Figure 8.26 (*Courtesy of Braja M. Das, Henderson, NV*)

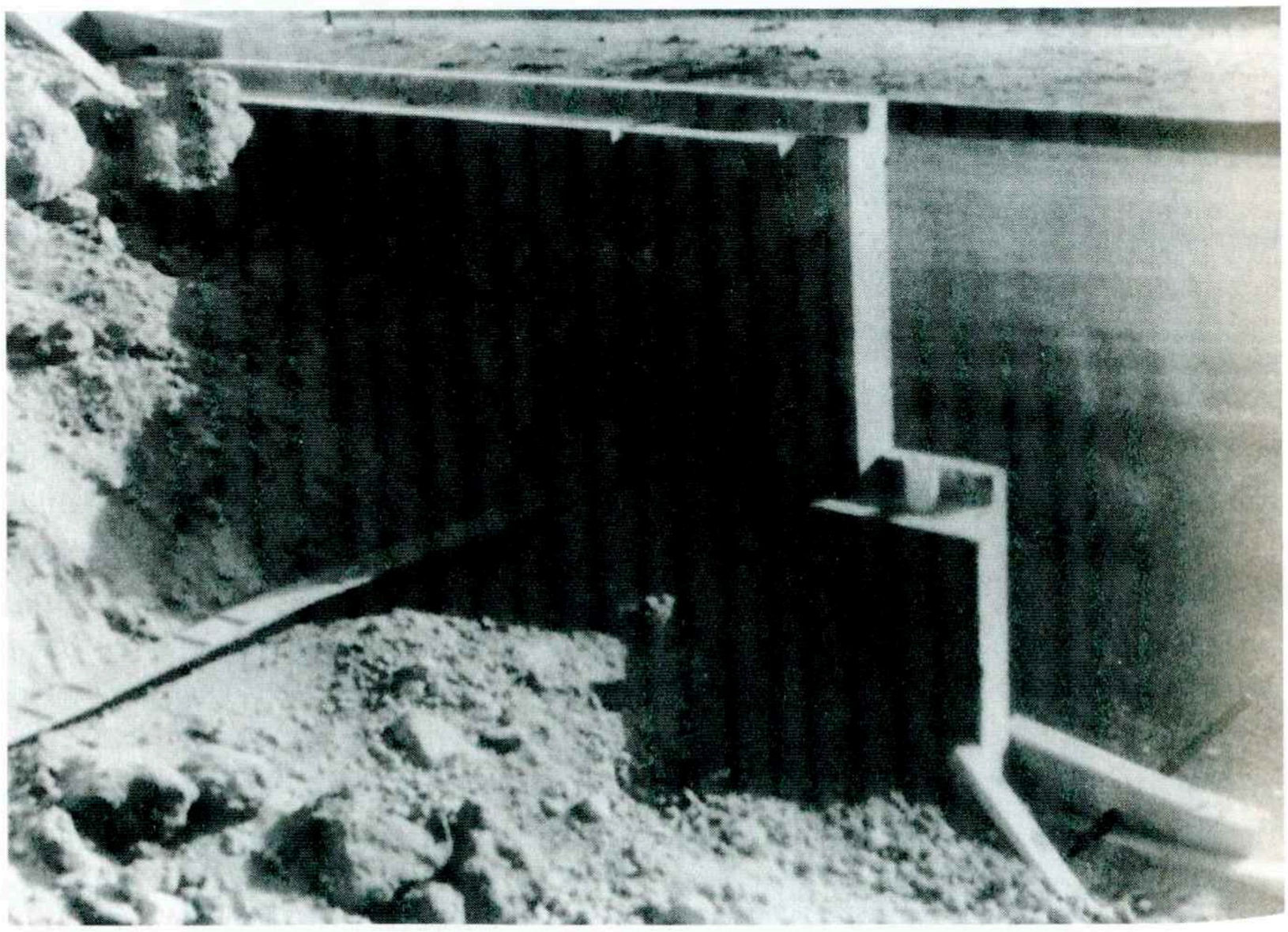

Figure 8.28 Metallic strip attachment to the precast concrete slab used as the skin (*Courtesy of Braja M. Das, Henderson, NV*)

Calculation of Active Horizontal and Vertical Pressure

Figure 8.29 shows a retaining wall with a granular backfill having a unit weight of γ_1 and a friction angle of ϕ'_1. Below the base of the retaining wall, the *in situ* soil has been excavated and recompacted, with granular soil used as backfill. Below the backfill, the *in situ* soil has a unit weight of γ_2, friction angle of ϕ'_2, and cohesion of c'_2. A surcharge having an intensity of q per unit area lies atop the retaining wall, which has reinforcement ties at depths $z = 0, S_V, 2S_V, \ldots, NS_V$. The height of the wall is $NS_V = H$.

According to the Rankine active pressure theory (Section 7.3)

$$\sigma'_a = \sigma'_o K_a - 2c'\sqrt{K_a}$$

where σ'_a = Rankine active pressure at any depth z.

For dry granular soils with no surcharge at the top, $c' = 0$, $\sigma'_o = \gamma_1 z$, and $K_a = \tan^2(45 - \phi'_1/2)$. Thus,

$$\sigma'_{a(1)} = \gamma_1 z K_a \tag{8.31}$$

When a surcharge is added at the top, as shown in Figure 8.29,

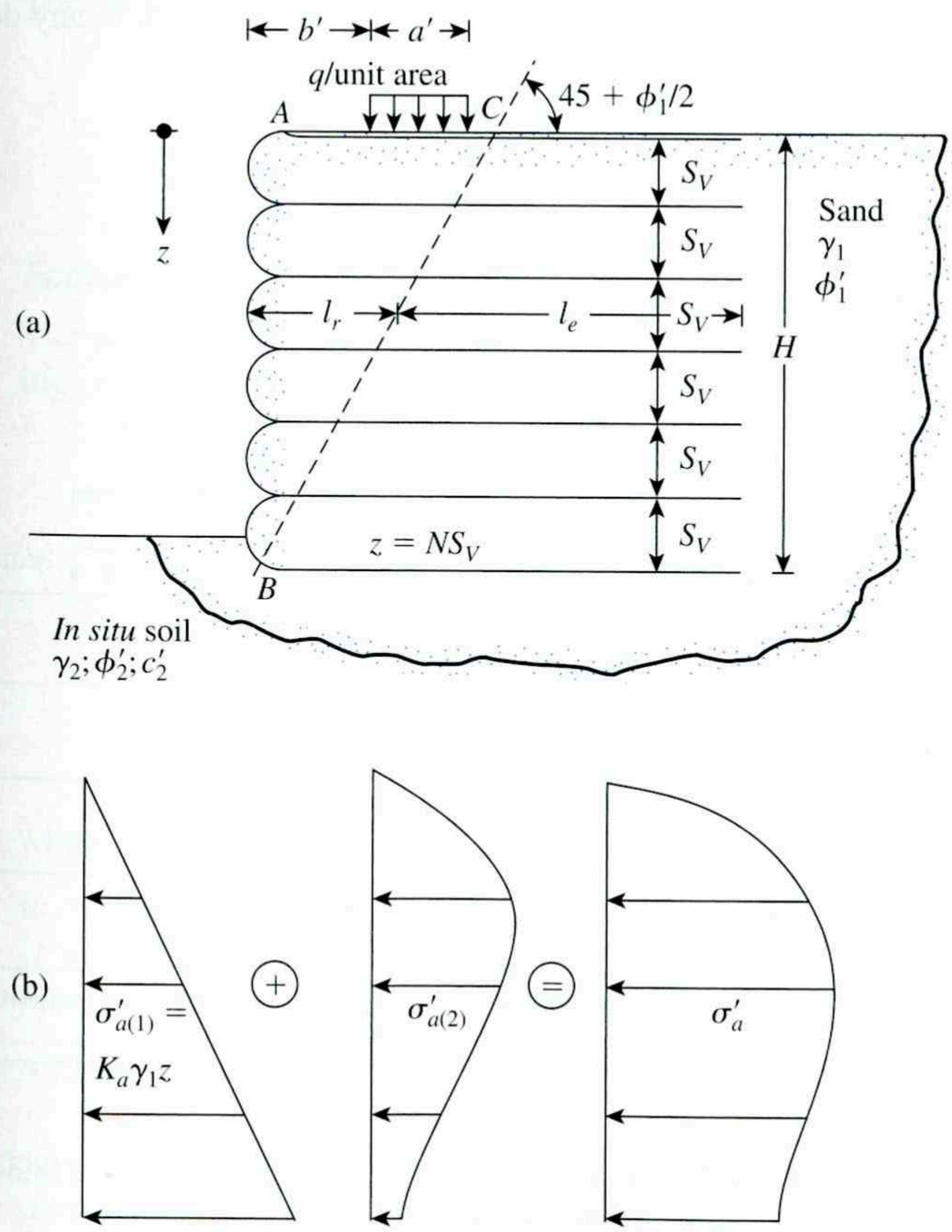

Figure 8.29 Analysis of a reinforced-earth retaining wall

$$\sigma'_o = \underset{\substack{\uparrow \\ = \gamma_1 z \\ \text{Due to} \\ \text{soil only}}}{\sigma'_{o(1)}} + \underset{\substack{\uparrow \\ \text{Due to the} \\ \text{surcharge}}}{\sigma'_{o(2)}} \tag{8.32}$$

The magnitude of $\sigma'_{o(2)}$ can be calculated by using the 2:1 method of stress distribution described in Eq. (5.14) and Figure 5.5. The 2:1 method of stress distribution is shown in Figure 8.30a. According to Laba and Kennedy (1986),

$$\sigma'_{o(2)} = \frac{qa'}{a' + z} \qquad (\text{for } z \leq 2b') \tag{8.33}$$

and

$$\sigma'_{o(2)} = \frac{qa'}{a' + \dfrac{z}{2} + b'} \qquad (\text{for } z > 2b') \tag{8.34}$$

Also, when a surcharge is added at the top, the lateral pressure at any depth is

$$\sigma'_a = \underset{\substack{\uparrow \\ = K_a \gamma_1 z \\ \text{Due to} \\ \text{soil only}}}{\sigma'_{a(1)}} + \underset{\substack{\uparrow \\ \text{Due to the} \\ \text{surcharge}}}{\sigma'_{a(2)}} \tag{8.35}$$

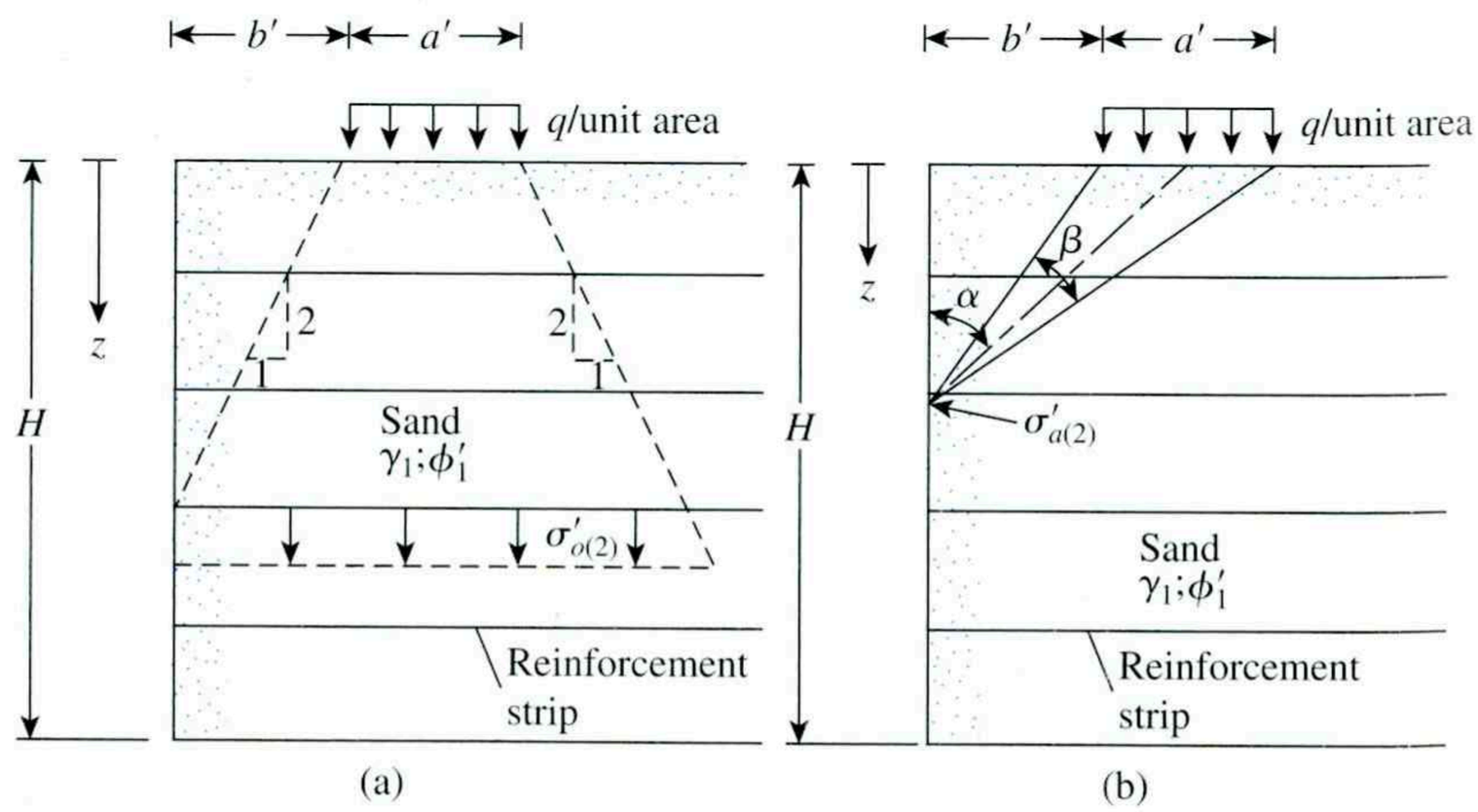

Figure 8.30 (a) Notation for the relationship of $\sigma'_{o(2)}$ in Eqs. (8.33) and (8.34); (b) notation for the relationship of $\sigma'_{a(2)}$ in Eqs. (8.36) and (8.37)

According to Laba and Kennedy (1986), $\sigma'_{a(2)}$ may be expressed (see Figure 8.30b) as

$$\sigma'_{a(2)} = M\left[\frac{2q}{\pi}(\underset{\substack{\uparrow \\ \text{(in radians)}}}{\beta} - \sin\beta\cos 2\alpha)\right] \tag{8.36}$$

where

$$M = 1.4 - \frac{0.4b'}{0.14H} \geq 1 \tag{8.37}$$

The net active (lateral) pressure distribution on the retaining wall calculated by using Eqs. (8.35), (8.36), and (8.37) is shown in Figure 8.29b.

Tie Force

The tie force *per unit length of the wall* developed at any depth z (see Figure 8.29) is

$$\begin{aligned} T &= \text{active earth pressure at depth } z \\ &\quad \times \text{ area of the wall to be supported by the tie} \\ &= (\sigma'_a)(S_V S_H) \end{aligned} \tag{8.38}$$

Factor of Safety against Tie Failure

The reinforcement ties at each level, and thus the walls, could fail by either (a) tie breaking or (b) tie pullout.

The factor of safety against *tie breaking* may be determined as

$$\begin{aligned} \text{FS}_{(B)} &= \frac{\text{yield or breaking strength of each tie}}{\text{maximum force in any tie}} \\ &= \frac{wtf_y}{\sigma'_a S_V S_H} \end{aligned} \tag{8.39}$$

where

w = width of each tie
t = thickness of each tie
f_y = yield or breaking strength of the tie material

A factor of safety of about 2.5 to 3 is generally recommended for ties at all levels.

Reinforcing ties at any depth z will fail by pullout if the frictional resistance developed along the surfaces of the ties is less than the force to which the ties are being subjected. The *effective length* of the ties along which frictional resistance is developed

may be conservatively taken as the length that extends *beyond the limits of the Rankine active failure zone,* which is the zone ABC in Figure 8.29. Line BC makes an angle of $45 + \phi_1'/2$ with the horizontal. Now, the maximum friction force that can be realized for a tie at depth z is

$$F_R = 2l_e w\sigma_o' \tan \phi_\mu' \tag{8.40}$$

where

l_e = effective length
σ_o' = effective vertical pressure at a depth z
ϕ_μ' = soil–tie friction angle

Thus, the factor of safety against *tie pullout* at any depth z is

$$\mathrm{FS}_{(P)} = \frac{F_R}{T} \tag{8.41}$$

Substituting Eqs. (8.38) and (8.40) into Eq. (8.41) yields

$$\mathrm{FS}_{(P)} = \frac{2l_e w\sigma_o' \tan \phi_\mu'}{\sigma_a' S_V S_H} \tag{8.42}$$

Total Length of Tie

The total length of ties at any depth is

$$L = l_r + l_e \tag{8.43}$$

where

l_r = length within the Rankine failure zone
l_e = effective length

For a given $\mathrm{FS}_{(P)}$ from Eq. (8.42),

$$l_e = \frac{\mathrm{FS}_{(P)}\sigma_a' S_V S_H}{2w\sigma_o' \tan\phi_\mu'} \tag{8.44}$$

Again, at any depth z,

$$l_r = \frac{(H - z)}{\tan\left(45 + \dfrac{\phi_1'}{2}\right)} \tag{8.45}$$

So, combining Eqs. (8.43), (8.44), and (8.45) gives

$$L = \frac{(H - z)}{\tan\left(45 + \dfrac{\phi_1'}{2}\right)} + \frac{\mathrm{FS}_{(P)}\sigma_a' S_V S_H}{2w\sigma_o' \tan\phi_\mu'} \tag{8.46}$$

8.15 Step-by-Step-Design Procedure Using Metallic Strip Reinforcement

Following is a step-by-step procedure for the design of reinforced-earth retaining walls.

General

Step 1. Determine the height of the wall, H, and the properties of the granular backfill material, such as the unit weight (γ_1) and the angle of friction (ϕ'_1).

Step 2. Obtain the soil–tie friction angle, ϕ'_μ, and the required value of $FS_{(B)}$ and $FS_{(P)}$.

Internal Stability

Step 3. Assume values for horizontal and vertical tie spacing. Also, assume the width of reinforcing strip, w, to be used.

Step 4. Calculate σ'_a from Eqs. (8.35), (8.36), and (8.37).

Step 5. Calculate the tie forces at various levels from Eq. (8.38).

Step 6. For the known values of $FS_{(B)}$, calculate the thickness of ties, t, required to resist the tie breakout:

$$T = \sigma'_a S_V S_H = \frac{wtf_y}{FS_{(B)}}$$

or

$$t = \frac{(\sigma'_a S_V S_H)[FS_{(B)}]}{wf_y} \tag{8.47}$$

The convention is to keep the magnitude of t the same at all levels, so σ'_a in Eq. (8.47) should equal $\sigma'_{a(\max)}$.

Step 7. For the known values of ϕ'_μ and $FS_{(P)}$, determine the length L of the ties at various levels from Eq. (8.46).

Step 8. The magnitudes of S_V, S_H, t, w, and L may be changed to obtain the most economical design.

External Stability

Step 9. Check for *overturning,* using Figure 8.31 as a guide. Taking the moment about B yields the overturning moment for the unit length of the wall:

$$M_o = P_a z' \tag{8.48}$$

Here,

$$P_a = \text{active force} = \int_0^H \sigma'_a dz$$

The resisting moment per unit length of the wall is

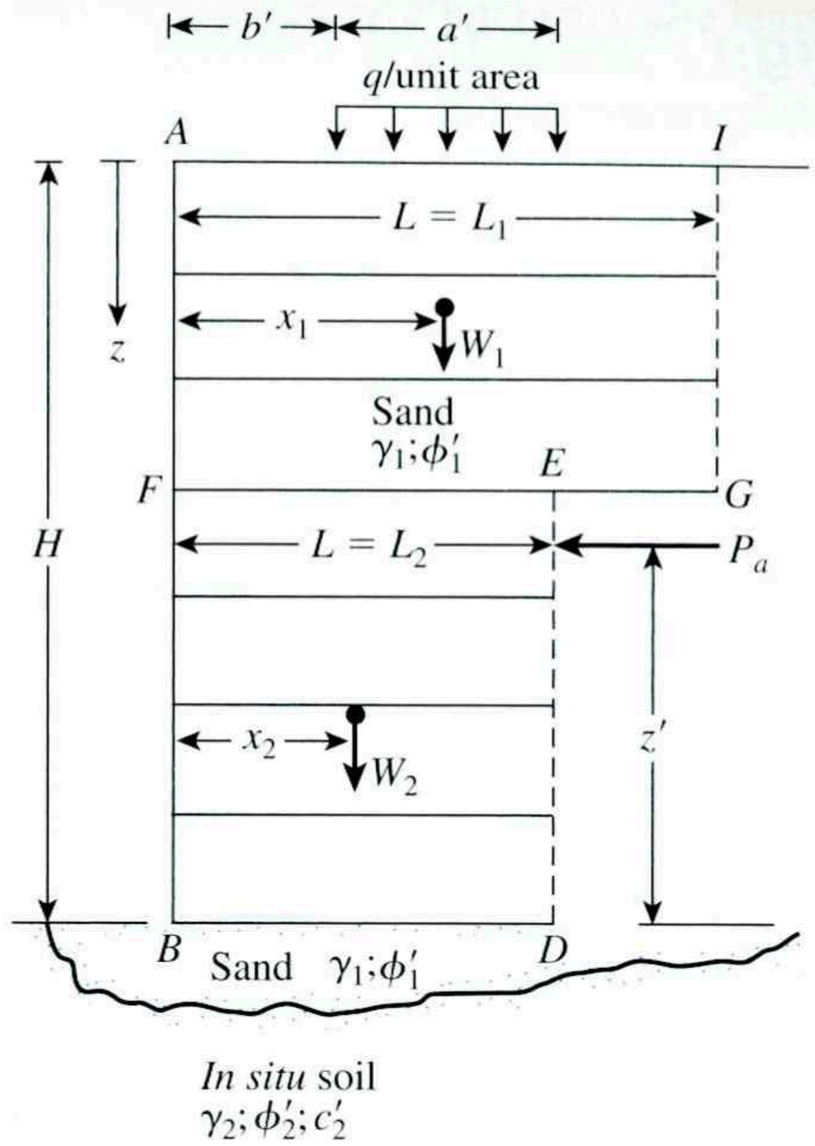

Figure 8.31 Stability check for the retaining wall

$$M_R = W_1x_1 + W_2x_2 + \cdots + qa'\left(b' + \frac{a'}{2}\right) \tag{8.49}$$

where

$$W_1 = (\text{area } AFEGI)\,(1)\,(\gamma_1)$$
$$W_2 = (\text{area } FBDE)\,(1)\,(\gamma_1)$$
$$\vdots$$

So,

$$\text{FS}_{(\text{overturning})} = \frac{M_R}{M_o} = \frac{W_1x_1 + W_2x_2 + \cdots + qa'\left(b' + \dfrac{a'}{2}\right)}{\left(\displaystyle\int_0^H \sigma'_a\,dz\right)z'} \tag{8.50}$$

Step 10. The check for *sliding* can be done by using Eq. (8.11), or

$$\text{FS}_{(\text{sliding})} = \frac{(W_1 + W_2 + \cdots + qa')[\tan(k\phi'_1)]}{P_a} \tag{8.51}$$

where $k \approx \frac{2}{3}$.

Step 11. Check for ultimate bearing capacity failure, which can be given as

$$q_u = c'_2 N_c + \tfrac{1}{2}\gamma_2 L_2 N_\gamma \tag{8.52}$$

The bearing capacity factors N_c and N_γ correspond to the soil friction angle ϕ'_2. (See Table 3.3.)

From Eq. 8.32, the vertical stress at $z = H$ is

$$\sigma'_{o(H)} = \gamma_1 H + \sigma'_{o(2)} \tag{8.53}$$

So the factor of safety against bearing capacity failure is

$$\mathrm{FS}_{(\text{bearing capacity})} = \frac{q_{\text{ult}}}{\sigma'_{o(H)}} \tag{8.54}$$

Generally, minimum values of $\mathrm{FS}_{(\text{overturning})} = 3$, $\mathrm{FS}_{(\text{sliding})} = 3$, and $\mathrm{FS}_{(\text{bearing capacity failure})} = 3$ to 5 are recommended.

Example 8.5

A 10 m high retaining wall with galvanized steel-strip reinforcement in a granular backfill has to be constructed. Referring to Figure 8.29, given:

Granular backfill: $\phi'_1 = 36°$
$\gamma_1 = 16.5\ \text{kN/m}^3$

Foundation soil: $\phi'_2 = 28°$
$\gamma_2 = 17.3\ \text{kN/m}^3$
$c'_2 = 50\ \text{kN/m}^2$

Galvanized steel reinforcement:

Width of strip, $w = 75$ mm
$S_V = 0.6$ m center-to-center
$S_H = 1$ m center-to-center
$f_y = 240{,}00\ \text{kN/m}^2$
$\phi'_\mu = 20°$

Required $\mathrm{FS}_{(B)} = 3$

Required $\mathrm{FS}_{(P)} = 3$

Check for the external and internal stability. Assume the corrosion rate of the galvanized steel to be 0.025 mm/year and the life span of the structure to be 50 years.

Solution

Internal Stability Check

Tie thickness: Maximum tie force, $T_{\max} = \sigma'_{a(\max)} S_V S_H$

$$\sigma_{a(\max)} = \gamma_1 H K_a = \gamma_1 H \tan^2\left(45 - \frac{\phi_1'}{2}\right)$$

so

$$T_{\max} = \gamma_1 H \tan^2\left(45 - \frac{\phi_1'}{2}\right) S_V S_H$$

From Eq. (8.47), for *tie break,*

$$t = \frac{(\sigma_a' S_V S_H)[\mathrm{FS}_{(B)}]}{w f_y} = \frac{\left[\gamma_1 H \tan^2\left(45 - \frac{\phi_1'}{2}\right) S_V S_H\right]\mathrm{FS}_{(B)}}{w f_y}$$

or

$$t = \frac{\left[(16.5)(10)\tan^2\left(45 - \frac{36}{2}\right)(0.6)(1)\right](3)}{(0.075\text{ m})(240{,}000\text{ kN/m}^2)} = 0.00428\text{m} = 4.28\text{ mm}$$

If the rate of corrosion is 0.025 mm/yr and the life span of the structure is 50 yr, then the actual thickness, t, of the ties will be

$$t = 4.28 + (0.025)(50) = 5.53\text{ mm}$$

So a **tie thickness of 6 m** would be enough.

Tie length: Refer to Eq. (8.46). For this case, $\sigma_a' = \gamma_1 z K_a$ and $\sigma_o' = \gamma_1 z$, so

$$L = \frac{(H - z)}{\tan\left(45 + \frac{\phi_1'}{2}\right)} + \frac{\mathrm{FS}_{(P)}\gamma_1 z K_a S_V S_H}{2w\gamma_1 z \tan\phi_\mu'}$$

Now the following table can be prepared. (Note: $\mathrm{FS}_{(P)} = 3$, $H = 10$ m, $w = 75$ mm, and $\phi_\mu' = 20°$.)

z(m)	Tie length L (m) [Eq. (8.46)]
2	12.65
4	11.63
6	10.61
8	9.59
10	8.57

So use a **tie length of L = 13 m.**

External Stability Check

Check for overturning: Refer to Figure 8.32. For this case, using Eq. (8.50)

$$\mathrm{FS}_{(\text{overturning})} = \frac{W_1 x_1}{\left[\int_0^H \sigma_a' \, dz\right] z'}$$

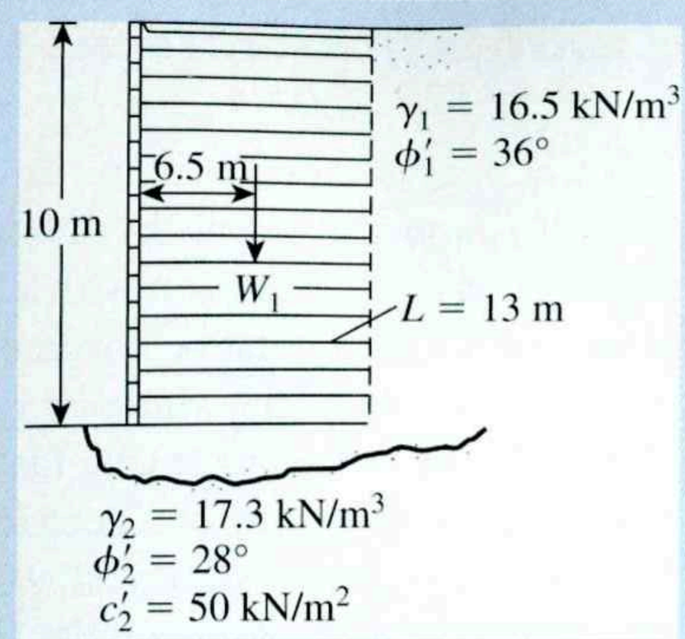

Figure 8.32 Retaining wall with galvanized steel-strip reinforcement in the backfill

$$W_1 = \gamma_1 HL = (16.5)(10)(13) = 2145 \text{ kN/m}$$

$$x_1 = 6.5 \text{ m}$$

$$P_a = \int_0^H \sigma'_a \, dz = \tfrac{1}{2}\gamma_1 K_a H^2 = (\tfrac{1}{2})(16.5)(0.26)(10)^2 = 214.5 \text{ kN/m}$$

$$z' = \frac{10}{3} = 3.33 \text{ m}$$

$$\text{FS}_{(\text{overturning})} = \frac{(2145)(6.5)}{(214.5)(3.33)} = \mathbf{19.52 > 3—OK}$$

Check for sliding: From Eq. (8.51)

$$\text{FS}_{(\text{sliding})} = \frac{W_1 \tan(k\phi'_1)}{P_a} = \frac{2145 \tan\left[\left(\frac{2}{3}\right)(36)\right]}{214.5} = \mathbf{4.45 > 3—OK}$$

Check for bearing capacity: For $\phi'_2 = 28°$, $N_c = 25.8$, $N_\gamma = 16.78$ (Table 3.3). From Eq. (8.52),

$$q_{\text{ult}} = c'_2 N_c + \tfrac{1}{2}\gamma_2 L \, N_\gamma$$

$$q_{\text{ult}} = (50)(25.8) + (\tfrac{1}{2})(17.3)(13)(16.72) = 3170.16 \text{ kN/m}^2$$

From Eq. (8.53),

$$\sigma'_{o(H)} = \gamma_1 H = (16.5)(10) = 165 \text{ kN/m}^2$$

$$\text{FS}_{(\text{bearing capacity})} = \frac{q_{\text{ult}}}{\sigma'_{o(H)}} = \frac{3170.16}{165} = \mathbf{19.2 > 5—OK}$$

8.16 Retaining Walls with Geotextile Reinforcement

Figure 8.33 shows a retaining wall in which layers of geotextile have been used as reinforcement. As in Figure 8.31, the backfill is a granular soil. In this type of retaining wall, the facing of the wall is formed by lapping the sheets as shown with a lap length of l_l. When construction is finished, the exposed face of the wall must be covered; otherwise, the geotextile will deteriorate from exposure to ultraviolet light. *Bitumen emulsion* or *Gunite* is sprayed on the wall face. A wire mesh anchored to the geotextile facing may be necessary to keep the coating on. Figure 8.34 shows the construction of a geotextile-reinforced retaining wall. Figure 8.35 shows a completed geosynthetic-reinforced soil wall. The wall is in DeBeque Canyon, Colorado. Note the versatility of the facing type. In this case, single-tier concrete block facing is integrated with a three-tier facing via rock facing.

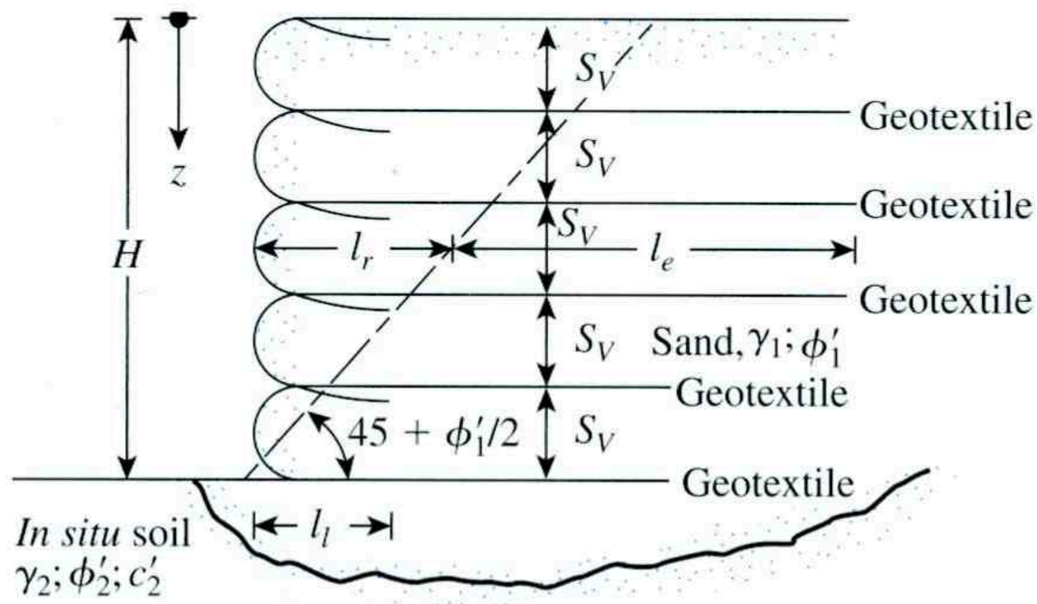

Figure 8.33 Retaining wall with geotextile reinforcement

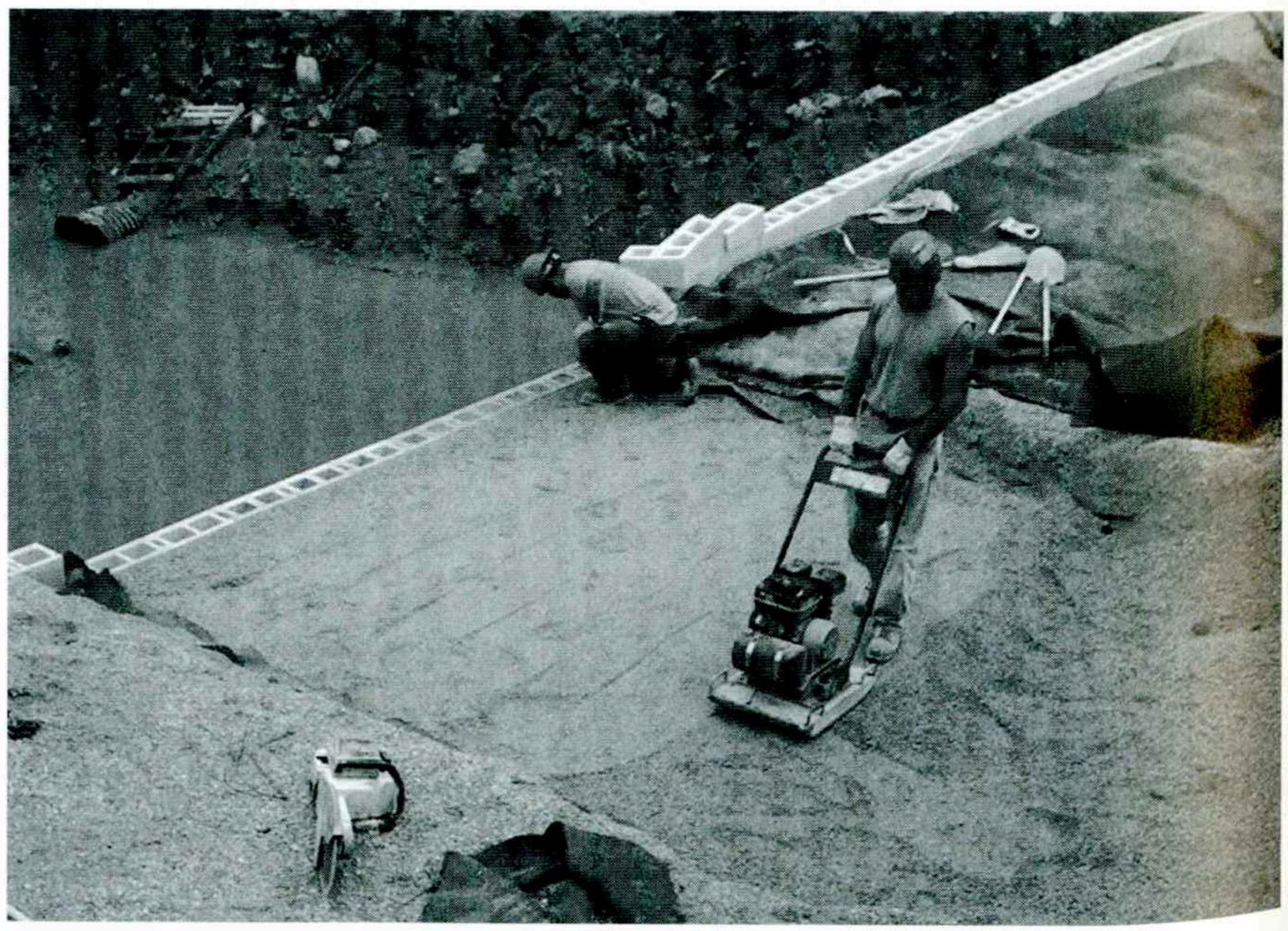

Figure 8.34 Construction of a geotextile-reinforced retaining wall (*Courtesy of Jonathan T. H. Wu, University of Colorado at Denver, Denver, Colorado*)

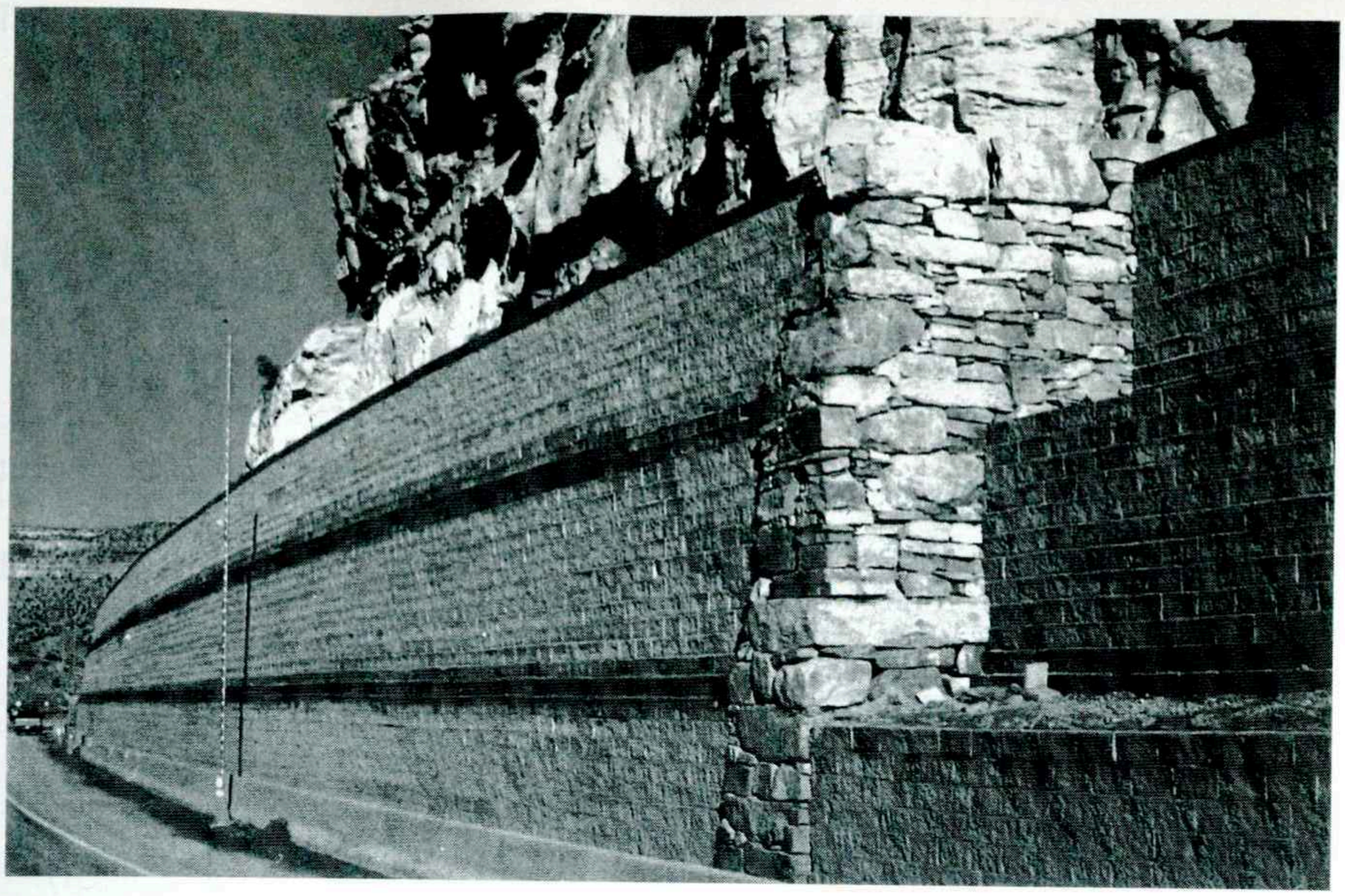

Figure 8.35 A completed geotextile-reinforced retaining wall in DeBeque Canyon, Colorado (*Courtesy of Jonathan T. H. Wu, University of Colorado at Denver, Denver, Colorado*)

The design of this type of retaining wall is similar to that presented in Section 8.15. Following is a step-by-step procedure for design based on the recommendations of Bell et al. (1975) and Koerner (2005):

Internal Stability

Step 1. Determine the active pressure distribution on the wall from the formula

$$\sigma'_a = K_a \sigma'_o = K_a \gamma_1 z \tag{8.55}$$

where

K_a = Rankine active pressure coefficient = $\tan^2(45 - \phi'_1/2)$
γ_1 = unit weight of the granular backfill
ϕ'_1 = friction angle of the granular backfill

Step 2. Select a geotextile fabric with an allowable tensile strength, T_{all} (lb/ft or kN/m).

The allowable tensile strength for retaining wall construction may be expressed as (Koerner, 2005)

$$T_{all} = \frac{T_{ult}}{RF_{id} \times RF_{cr} \times RF_{cbd}} \tag{8.56}$$

where

T_{ult} = ultimate tensile strength
RF_{id} = reduction factor for installation damage
RF_{cr} = reduction factor for creep
RF_{cbd} = reduction factor for chemical and biological degradation

The recommended values of the reduction factor are as follows (Koerner, 2005)

RF_{id}	1.1–2.0
RF_{cr}	2–4
RF_{cbd}	1–1.5

Step 3. Determine the vertical spacing of the layers at any depth z from the formula

$$S_V = \frac{T_{all}}{\sigma'_a FS_{(B)}} = \frac{T_{all}}{(\gamma_1 z K_a)[FS_{(B)}]} \tag{8.57}$$

Note that Eq. (8.57) is similar to Eq. (8.39). The magnitude of $FS_{(B)}$ is generally 1.3 to 1.5.

Step 4. Determine the length of each layer of geotextile from the formula

$$L = l_r + l_e \tag{8.58}$$

where

$$l_r = \frac{H - z}{\tan\left(45 + \frac{\phi'_1}{2}\right)} \tag{8.59}$$

and

$$l_e = \frac{S_V \sigma'_a [FS_{(P)}]}{2\sigma'_o \tan\phi'_F} \tag{8.60}$$

in which

$$\sigma'_a = \gamma_1 z K_a$$

$$\sigma'_o = \gamma_1 z$$

$$FS_{(P)} = 1.3 \text{ to } 1.5$$

ϕ'_F = friction angle at geotextile–soil interface

$\approx \frac{2}{3}\phi'_1$

Note that Eqs. (8.58), (8.59), and (8.60) are similar to Eqs. (8.43), (8.45), and (8.44), respectively.

Based on the published results, the assumption of $\phi'_F/\phi'_1 \approx \frac{2}{3}$ is reasonable and appears to be conservative. Martin et al. (1984) presented the following laboratory test results for ϕ'_F/ϕ'_1 between various types of geotextiles and sand.

Type	ϕ'_F/ϕ'_1
Woven—monofilament/concrete sand	0.87
Woven—silt film/concrete sand	0.8
Woven—silt film/rounded sand	0.86
Woven—silt film/silty sand	0.92
Nonwoven—melt-bonded/concrete sand	0.87
Nonwoven—needle-punched/concrete sand	1.0
Nonwoven—needle-punched/rounded sand	0.93
Nonwoven—needle-punched/silty sand	0.91

Step 5. Determine the lap length, l_l, from

$$l_l = \frac{S_V \sigma'_a \mathrm{FS}_{(P)}}{4\sigma'_o \tan\phi'_F} \tag{8.61}$$

The minimum lap length should be 1 m (3 ft).

External Stability

Step 6. Check the factors of safety against overturning, sliding, and bearing capacity failure as described in Section 8.15 (Steps 9, 10, and 11).

Example 8.6

A geotextile-reinforced retaining wall 5 m high is shown in Figure 8.36. For the granular backfill, $\gamma_1 = 15.7\ \mathrm{kN/m^3}$ and $\phi'_1 = 36°$. For the geotextile, $T_{\mathrm{ult}} = 52.5$ kN/m. For the design of the wall, determine S_V, L, and l_l. Use $\mathrm{RF_{id}} = 1.2$, $\mathrm{RF_{cr}} = 2.5$, and $\mathrm{RF_{cbd}} = 1.25$.

Solution

We have

$$K_a = \tan^2\left(45 - \frac{\phi'_1}{2}\right) = 0.26$$

Determination of S_V

To find S_V, we make a few trials. From Eq. (8.57),

$$S_V = \frac{T_{\mathrm{all}}}{(\gamma_1 z K_a)[\mathrm{FS}_{(B)}]}$$

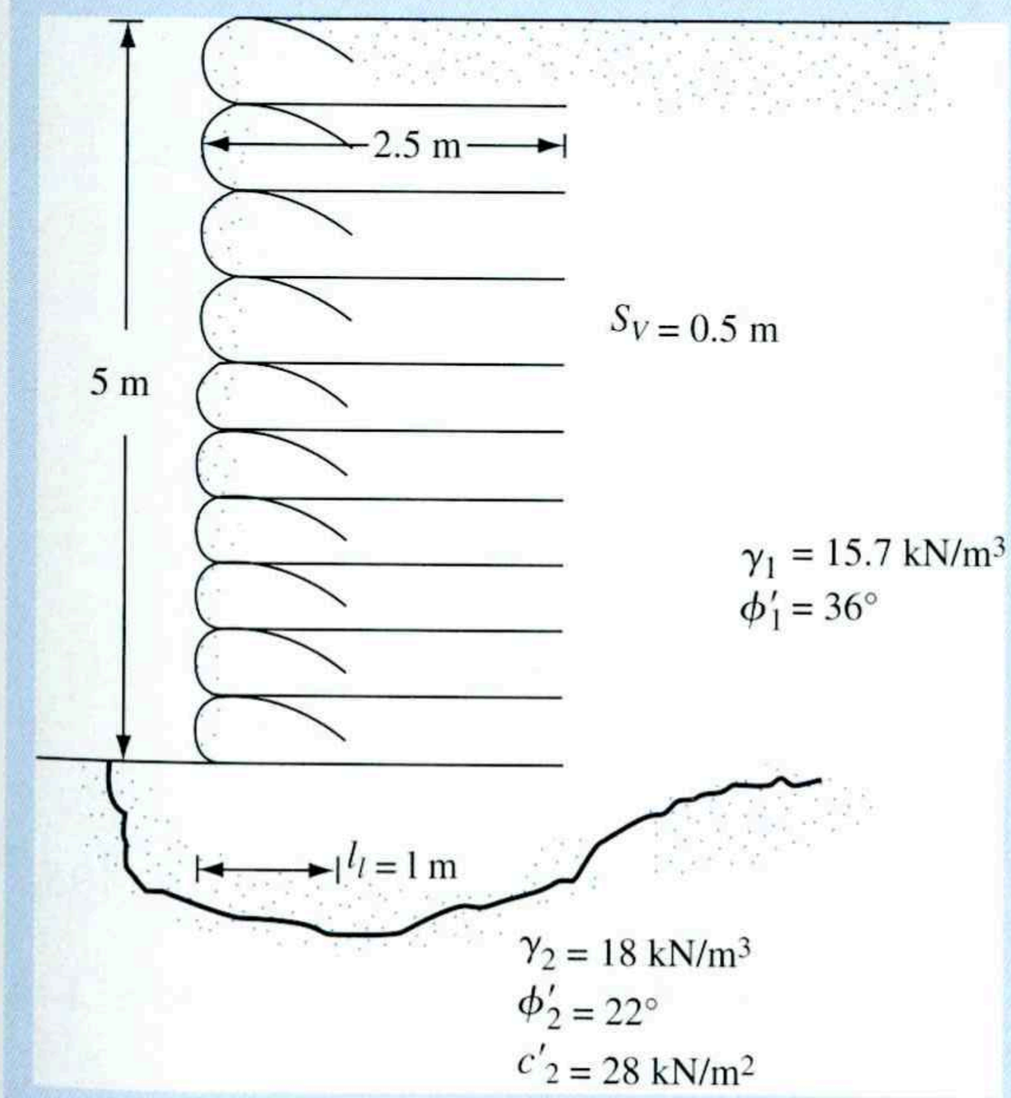

Figure 8.36 Geotextile-reinforced retaining wall

From Eq. (8.56),

$$T_{all} = \frac{T_{uef}}{RF_{id} \times RF_{cr} \times RF_{cbd}} = \frac{52.5}{1.2 \times 2.5 \times 1.25} = 14 \text{ kN/m}$$

With $FS_{(B)} = 1.5$ at $z = 2$ m,

$$S_V = \frac{14}{(15.7)\,(2)\,(0.26)\,(1.5)} = 1.14 \text{ m}$$

At $z = 4$ m,

$$S_V = \frac{14}{(15.7)\,(4)\,(0.26)\,(1.5)} = 0.57 \text{ m}$$

At $z = 5$ m,

$$S_V = \frac{14}{(15.7)\,(5)\,(0.26)\,(1.5)} = 0.46 \text{ m}$$

So, **use $S_V = 0.5$ m for $z = 0$ to $z = 5$ m** (See Figure 8.36.)

Determination of L

From Eqs. (8.58), (8.59), and (8.60),

$$L = \frac{(H - z)}{\tan\left(45 + \frac{\phi_1'}{2}\right)} + \frac{S_V K_a[FS_{(P)}]}{2 \tan \phi_F'}$$

For $FS_{(P)} = 1.5$, $\tan\phi_F' = \tan[(\frac{2}{3})\,(36)] = 0.445$, and it follows that

$$L = (0.51)\,(H - z) + 0.438 S_V$$

$H = 5$ m, $S_V = 0.5$ m

At $z = 0.5$ m: $L = (0.51)(5 - 0.5) + (0.438)(0.5) = 2.514$ m
At $z = 2.5$ m: $L = (0.51)(5 - 2.5) + (0.438)(0.5) = 1.494$ m

So, **use $L = 2.5$ m throughout**.

Determination of l_l

From Eq. (8.61),

$$l_l = \frac{S_V \sigma_a'[FS_{(P)}]}{4\sigma_o' \tan\phi_F'}$$

$\sigma_a' = \gamma_1 z K_a$, $FS_{(P)} = 1.5$; with $\sigma_o' = \gamma_1 z$, $\phi_F' = \frac{2}{3}\phi_1'$. So

$$l_l = \frac{S_V K_a[FS_{(P)}]}{4 \tan \phi_F'} = \frac{S_V (0.26)\,(1.5)}{4 \tan[(\frac{2}{3})\,(36)]} = 0.219 S_V$$

$$l_l = 0.219 S_V = (0.219)\,(0.5) = 0.11 \text{ m} \leq 1 \text{ m}$$

So, use **$l_l = 1$ m.**

Example 8.7

Consider the results of the internal stability check given in Example 8.6. For the geotextile-reinforced retaining wall, calculate the factor of safety against overturning, sliding, and bearing capacity failure.

Solution

Refer to Figure 8.37.

Factor of Safety Against Overturning

From Eq. (8.50), $\text{FS}_{(\text{overturning})} = \dfrac{W_1 x_1}{(P_a)\left(\dfrac{H}{3}\right)}$

$$W_1 = (5)(2.5)(15.7) = 196.25 \text{ kN/m}$$

$$x_1 = \frac{2.5}{2} = 1.25 \text{ m}$$

$$P_a = \frac{1}{2}\gamma H^2 K_a = \left(\frac{1}{2}\right)(15.7)(5)^2(0.26) = 51.03 \text{ kN/m}$$

Hence,

$$\text{FS}_{(\text{overturning})} = \frac{(196.25)(1.25)}{51.03(5/3)} = 2.88 < 3$$

(increase length of geotextile layers to 3 m)

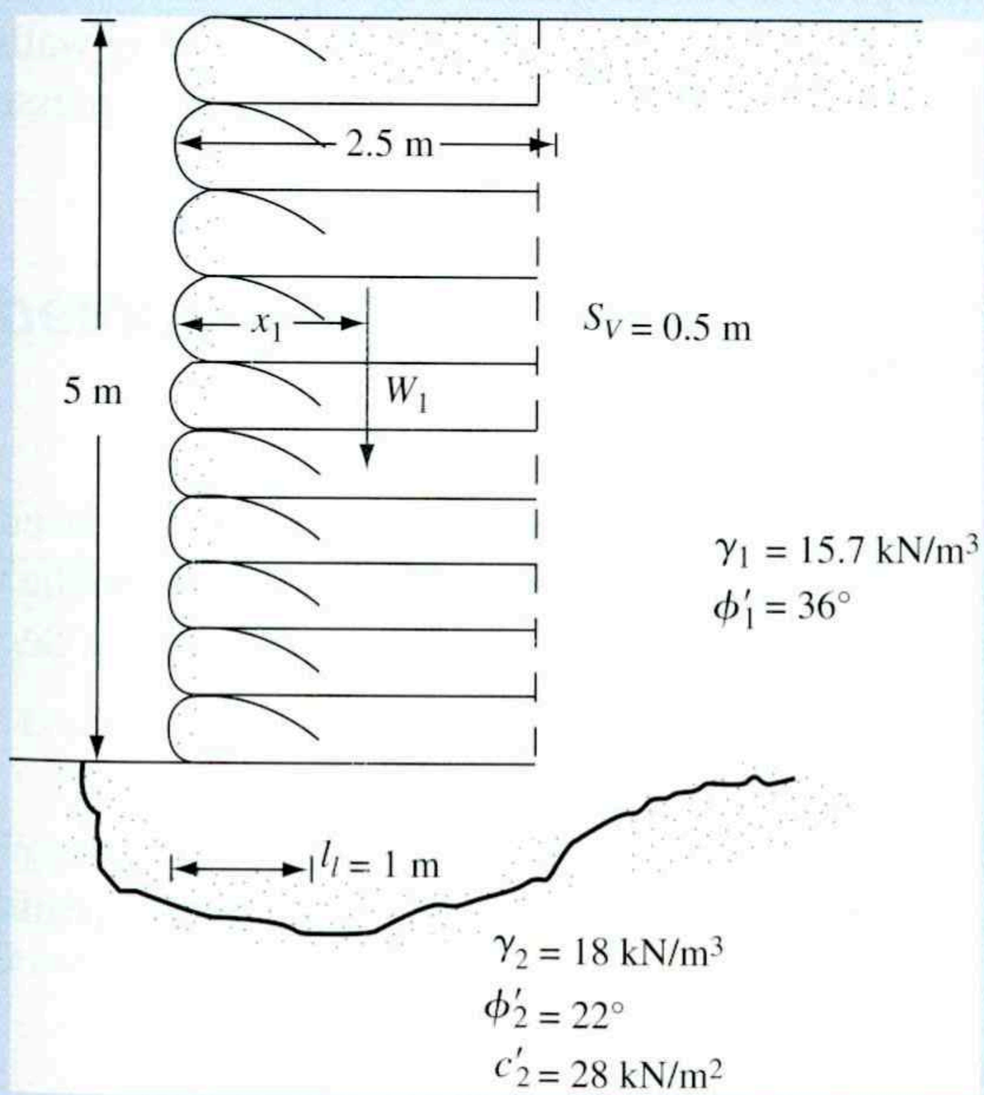

Figure 8.37 Stability check

Factor of Safety Against Sliding

From Eq. (8.51),

$$FS_{(\text{sliding})} = \frac{W_1 \tan\left(\frac{2}{3}\phi_1'\right)}{P_a} = \frac{(196.25)\left[\tan\left(\frac{2}{3} \times 36\right)\right]}{51.03} = \mathbf{1.71 > 1.5 - O.K.}$$

Factor of Safety Against Bearing Capacity Failure

From Eq. (8.52), $q_u = c_2' N_c + \frac{1}{2}\gamma_2 L_2 N_\gamma$

Given: $\gamma_2 = 18\ \text{kN/m}^3$, $L_2 = 2.5$ m, $c_2' = 28\ \text{kN/m}^2$, and $\phi_2' = 22°$. From Table 3.3, $N_c = 16.88$, and $N_\gamma = 7.13$.

$$q_u = (28)(16.88) + \left(\frac{1}{2}\right)(18)(2.5)(7.13) \approx 633\ \text{kN/m}^2$$

From Eq. (8.54),

$$FS_{(\text{bearing capacity})} = \frac{q_u}{\sigma'_{o(H)}} = \frac{633}{\gamma_1 H} = \frac{633}{(15.7)(5)} = \mathbf{8.06 > 3 - O.K.}$$

8.17 Retaining Walls with Geogrid Reinforcement—General

Geogrids can also be used as reinforcement in granular backfill for the construction of retaining walls. Figure 8.38 shows typical schematic diagrams of retaining walls with geogrid reinforcement. Figure 8.39 shows some photographs of geogrid-reinforced retaining walls in the field.

Relatively few field measurements are available for lateral earth pressure on retaining walls constructed with geogrid reinforcement. Figure 8.40 shows a comparison of measured and design lateral pressures (Berg et al., 1986) for two retaining walls constructed with precast panel facing. The figure indicates that the measured earth pressures were substantially smaller than those calculated for the Rankine active case.

8.18 Design Procedure for Geogrid-Reinforced Retaining Wall

Figure 8.41 shows a schematic diagram of a concrete panel-faced wall with a granular backfill reinforced with layers of geogrid. The design process of the wall is essentially similar to that with geotextile reinforcement of the backfill given in Section 8.16. The following is a brief step-by-step procedure.

Internal Stability

Step 1. Determine the active pressure at any depth z as [similar to Eq. (8.55)]:

$$\sigma_a' = K_a \gamma_1 z \tag{8.62}$$

where

K_a = Rankine active pressure coefficient $= \tan^2\left(45 - \frac{\phi_1'}{2}\right)$

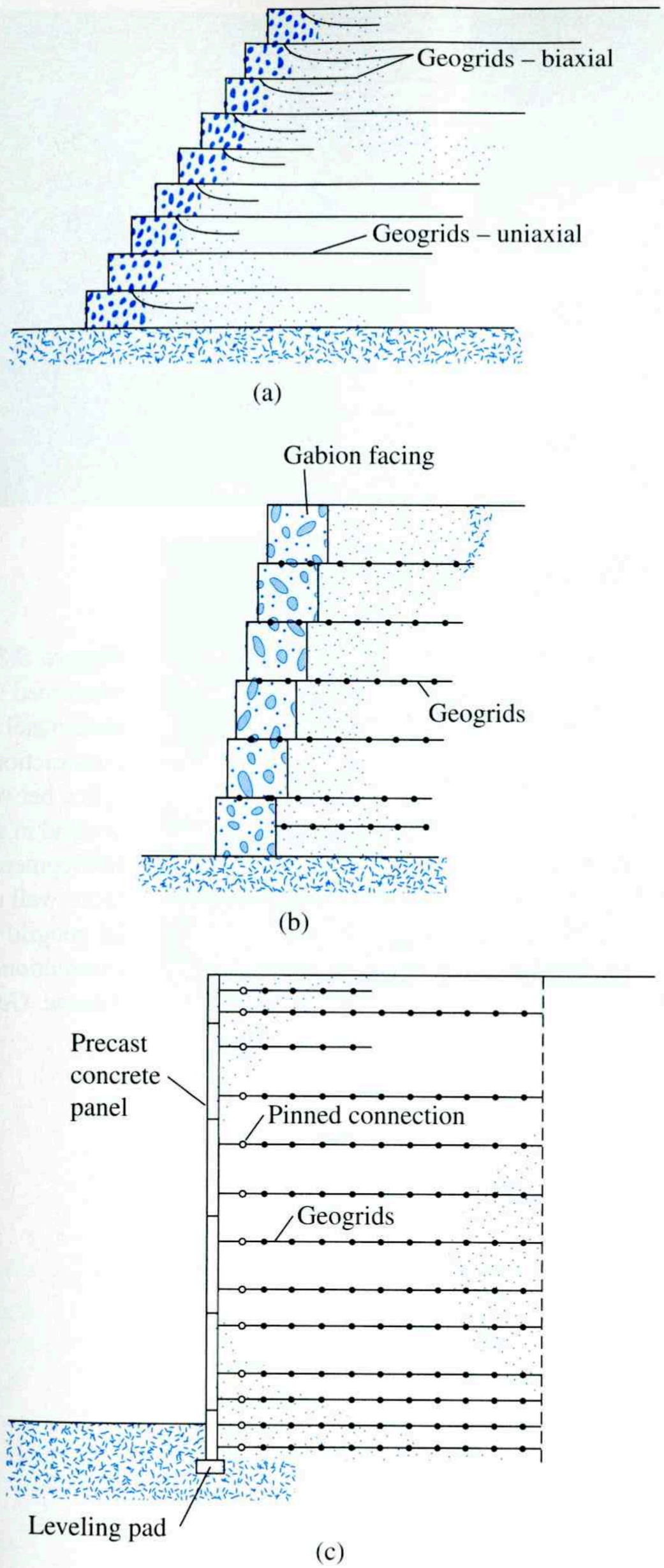

Figure 8.38 Typical schematic diagrams of retaining walls with geogrid reinforcement: (a) geogrid wraparound wall; (b) wall with gabion facing; (c) concrete panel-faced wall (After The Tensar Corporation, 1986)

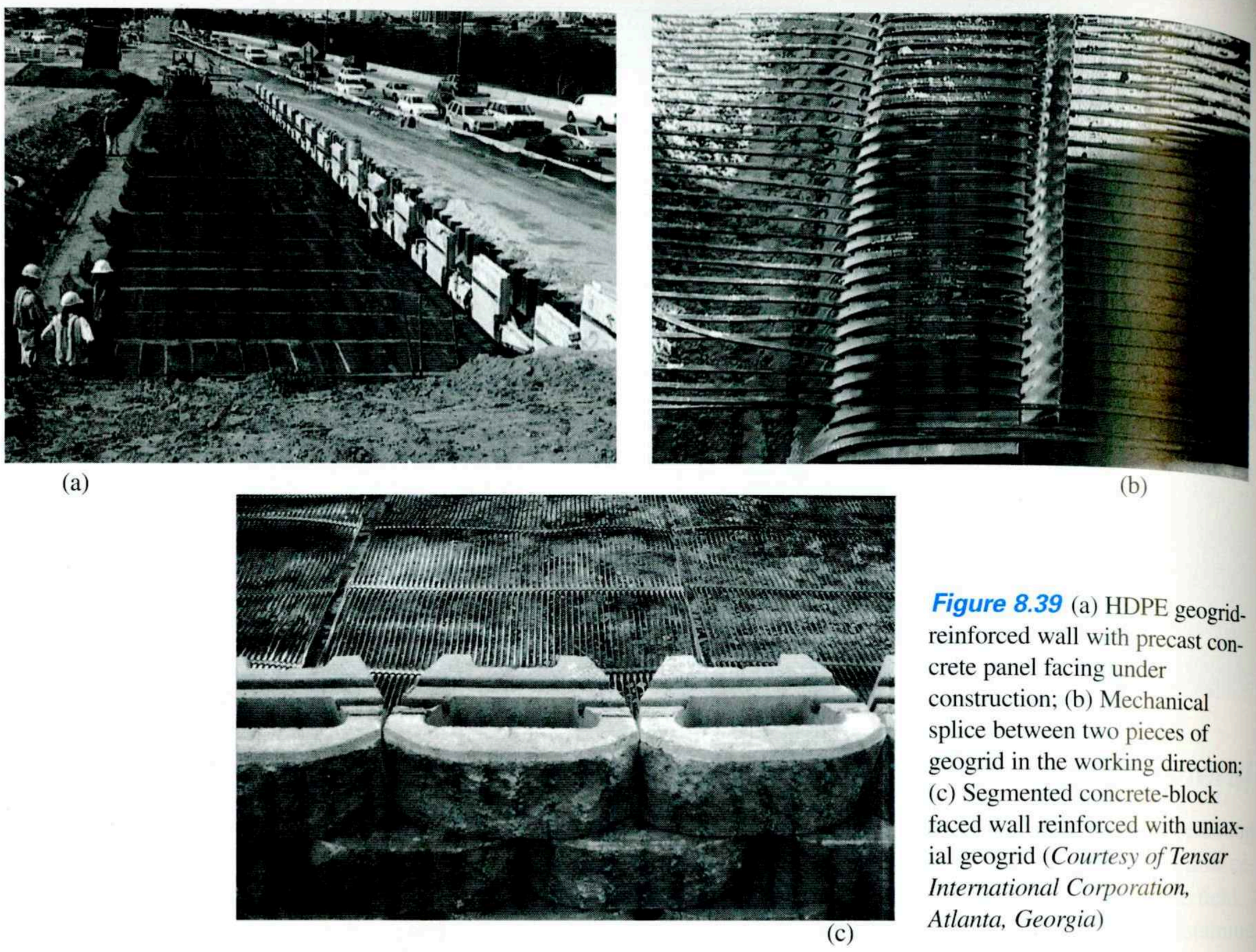

(a) (b) (c)

Figure 8.39 (a) HDPE geogrid-reinforced wall with precast concrete panel facing under construction; (b) Mechanical splice between two pieces of geogrid in the working direction; (c) Segmented concrete-block faced wall reinforced with uniaxial geogrid (*Courtesy of Tensar International Corporation, Atlanta, Georgia*)

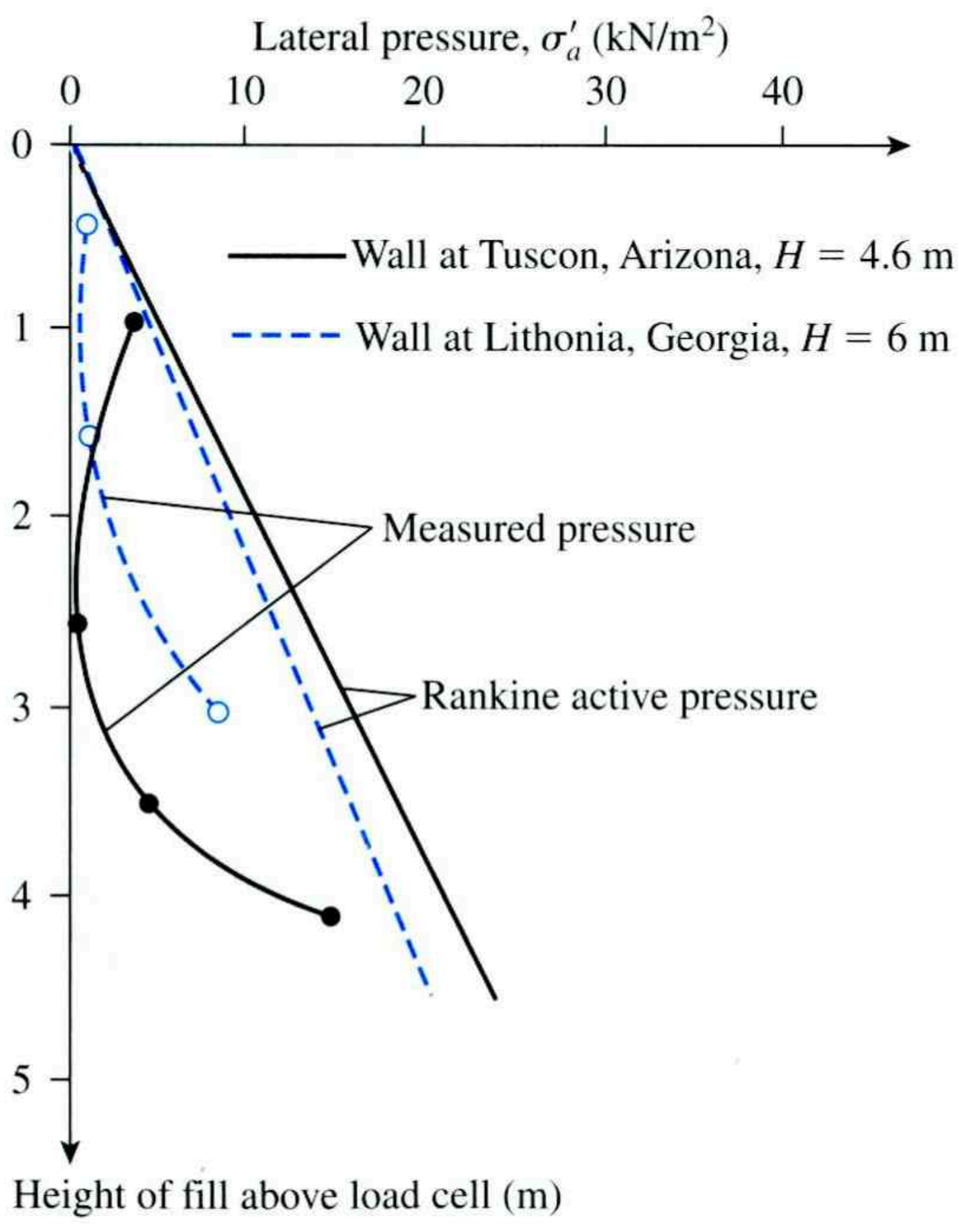

Figure 8.40 Comparison of theoretical and measured lateral pressures in geogrid reinforced retaining walls (Based on Berg et al., 1986)

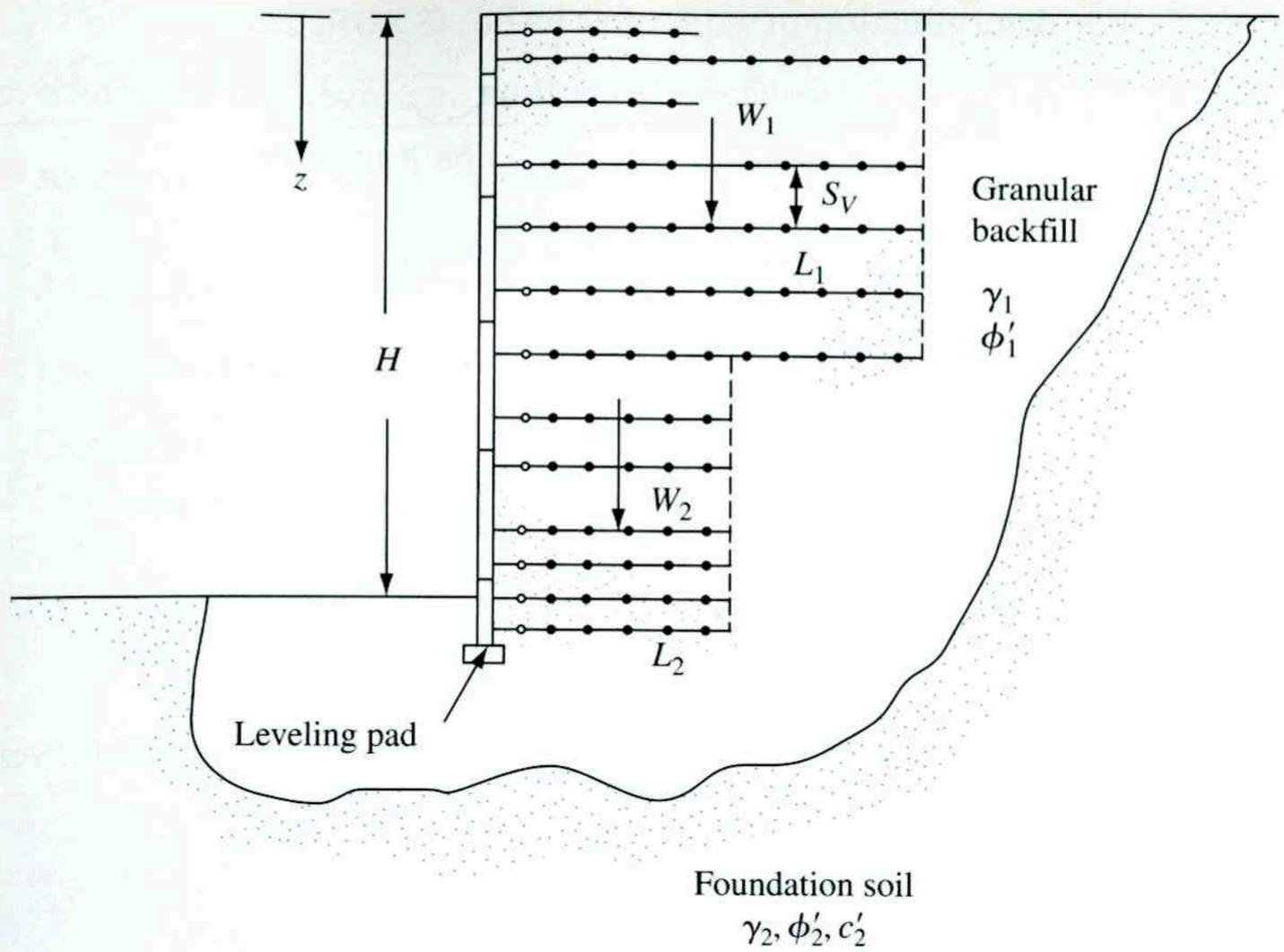

Figure 8.41 Design of geogrid-reinforced retaining wall

Step 2. Select a geogrid with allowable tensile strength, T_{all} [similar to Eq. (8.56)] (Koerner, 2005):

$$T_{all} = \frac{T_{ult}}{RF_{id} \times RF_{cr} \times RF_{cbd}} \tag{8.63}$$

where

RF_{id} = reduction factor for installation damage (1.1 to 1.4)
RF_{cr} = reduction factor for creep (2.0 to 3.0)
RF_{cbd} = reduction factor for chemical and biological degradation (1.1 to 1.5).

Step 3. Obtain the vertical spacing of the geogrid layers, S_V, as

$$S_V = \frac{T_{all} C_r}{\sigma'_a \, FS_{(B)}} \tag{8.64}$$

where C_r = coverage ratio for geogrid.

The *coverage ratio* is the fractional plan area at any particular elevation that is actually occupied by geogrid. For example, if there is a 0.3 m (1 ft) wide space between each 1.2 m (4 ft) wide piece of geogrid, the coverage ratio is

$$C_r = \frac{1.2 \text{ m}}{1.2 \text{ m} + 0.3 \text{ m}} = 0.8$$

Step 4. Calculate the length of each layer of geogrid at a depth z as [Eq. (8.58)]

$$L = l_r + l_e$$

$$l_r = \frac{H - z}{\tan^2\left(45 - \frac{\phi'_1}{2}\right)} \tag{8.65}$$

For determination of l_e [similar to Eq. (8.60)],

$$\mathrm{FS}_{(P)} = \frac{\text{resistance to pullout at a given normal effective stress}}{\text{pullout force}} \tag{8.66}$$

$$= \frac{(2)(l_e)(C_i\sigma_0' \tan\phi_1')(C_r)}{S_V\sigma_a'}$$

$$= \frac{(2)(l_e)(C_i \tan\phi_1')(C_r)}{S_V K_a}$$

where C_i = interaction coefficient or

$$l_e = \frac{S_V K_a \mathrm{FS}_{(P)}}{2C_r C_i \tan\phi_1'} \tag{8.67}$$

Thus, at a given depth z, the total length, L, of the geogrid layer is

$$L = l_r + l_e = \frac{H - z}{\tan\left(45 + \dfrac{\phi_1'}{2}\right)} + \frac{S_V K_a \mathrm{FS}_{(P)}}{2C_r C_i \tan\phi_1'} \tag{8.68}$$

The interaction coefficient, C_i, can be determined experimentally in the laboratory. The following is an approximate range for C_i for various types of backfill.

Gravel, sandy gravel	0.75–0.8
Well graded sand, gravelly sand	0.7–0.75
Fine sand, silty sand	0.55–0.6

External Stability

Check the factors of safety against overturning, sliding, and bearing capacity failure as described in Section 8.15 (Steps 9, 10, and 11).

Example 8.8

Consider a geogrid-reinforced retaining wall. Referring to Figure 8.41, given: $H = 6$ m, $\gamma_1 = 16.5$ kN/m^3, $\phi_1' = 35°$, $T_{\text{all}} = 45$ kN/m, $\mathrm{FS}_{(B)} = 1.5$, $\mathrm{FS}_{(P)} = 1.5$, $C_r = 0.8$, and $C_i = 0.75$. For the design of the wall, determine S_V and L.

Solution

$$K_a = \tan^2\left(45 - \frac{\phi_1'}{2}\right) = \tan^2\left(45 - \frac{35}{2}\right) = 0.27$$

Determination of S_V

From Eq. (8.64),

$$S_v = \frac{T_{\text{all}}C_r}{\sigma_a' \mathrm{FS}_{(B)}} = \frac{T_{\text{all}}C_r}{\gamma z K_a \mathrm{FS}_{(B)}} = \frac{(45)(0.8)}{(16.5)(z)(0.27)(1.5)} = \frac{5.39}{z}$$

At $z = 2$ m: $S_v = \dfrac{5.39}{2} = 2.7$ m

At $z = 4$ m: $S_v = \dfrac{5.39}{4} = 1.35$ m

At $z = 5$ m: $S_v = \dfrac{5.39}{5} = 1.08$ m

Use $S_V \approx$ **1 m**

Determination of L

From Eq. (8.68),

$$L = \frac{H - z}{\tan\left(45 + \dfrac{\phi_1'}{2}\right)} + \frac{S_V K_a \mathrm{FS}_{(P)}}{2C_r C_i \tan\phi_1'} = \frac{6 - z}{\tan\left(45 + \dfrac{35}{2}\right)} + \frac{(1\text{ m})(0.27)(1.5)}{(2)(0.8)(0.75)(\tan 35°)}$$

At $z = 1$ m: $L = 0.52(6 - 1) + 0.482 = 3.08 \text{ m} \approx 3.1$ m

At $z = 3$ m: $L = 0.52(6 - 3) + 0.482 = 2.04 \text{ m} \approx 2.1$ m

At $z = 5$ m: $L = 0.52(6 - 5) + 0.482 = 1.0$ m

So, use **$L = 3$ m for $z = 0$ to 6 m.** ■

Problems

In Problems 8.1 through 8.4, use $\gamma_{\text{concrete}} = 23.58$ kN/m³. Also, in Eq. (8.11), use $k_1 = k_2 = 2/3$ and $P_p = 0$.

8.1 For the cantilever retaining wall shown in Figure P8.1, let the following data be given:

Wall dimensions: $H = 8$ m, $x_1 = 0.4$ m, $x_2 = 0.6$ m, $x_3 = 1.5$ m, $x_4 = 3.5$ m, $x_5 = 0.96$ m, $D = 1.75$ m, $\alpha = 10°$

Soil properties: $\gamma_1 = 16.8$ kN/m³, $\phi_1' = 32°$, $\gamma_2 = 17.6$ kN/m³, $\phi_2' = 28°$, $c_2' = 30$ kN/m²

Calculate the factor of safety with respect to overturning, sliding, and bearing capacity.

8.2 Repeat Problem 8.1 with the following:

Wall dimensions: $H = 6.5$ m, $x_1 = 0.3$ m, $x_2 = 0.6$ m, $x_3 = 0.8$ m, $x_4 = 2$ m, $x_5 = 0.8$ m, $D = 1.5$ m, $\alpha = 0°$

Soil properties: $\gamma_1 = 18.08$ kN/m³, $\phi_1' = 36°$, $\gamma_2 = 19.65$ kN/m³, $\phi_2' = 15°$, $c_2' = 30$ kN/m²

8.3 A gravity retaining wall is shown in Figure P8.3. Calculate the factor of safety with respect to overturning and sliding, given the following data:

Wall dimensions: $H = 6$ m, $x_1 = 0.6$ m, $x_2 = 2$ m, $x_3 = 2$ m, $x_4 = 0.5$ m, $x_5 = 0.75$ m, $x_6 = 0.8$ m, $D = 1.5$ m

Soil properties: $\gamma_1 = 16.5$ kN/m³, $\phi_1' = 32°$, $\gamma_2 = 18$ kN/m³, $\phi_2' = 22°$, $c_2' = 40$ kN/m²

Use the Rankine active earth pressure in your calculation.

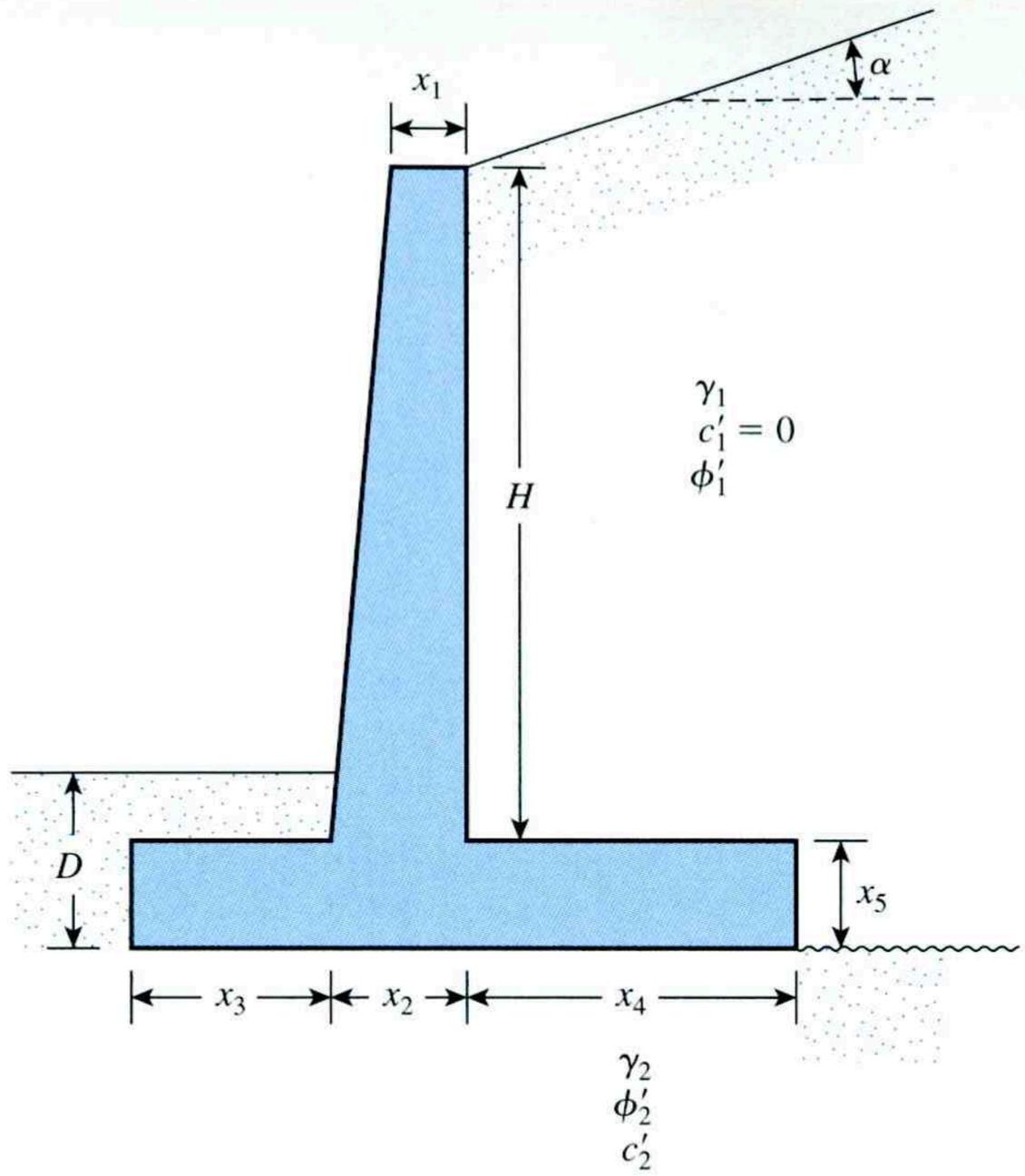

Figure P8.1

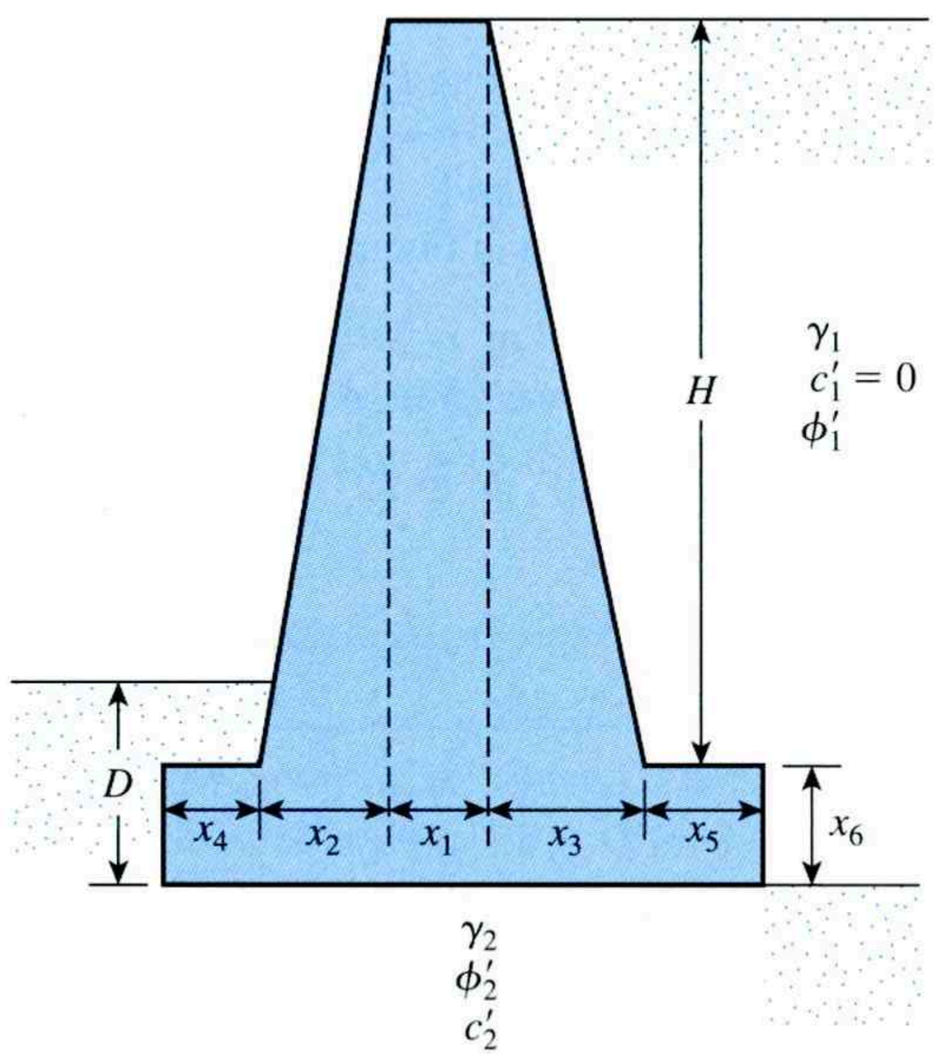

Figure P8.3

8.4 Repeat Problem 8.3 using Coulomb's active earth pressure in your calculation and letting $\delta' = 2/3\ \phi'_1$.

8.5 Refer to Figure P8.5 for the design of a gravity retaining wall for earthquake condition Given: $k_v = 0$ and $k_h = 0.3$.

a. What should be the weight of the wall for a zero displacement condition? Use a factor of safety of 2.

b. What should be the weight of the wall for an allowable displacement of 50.8 mm?

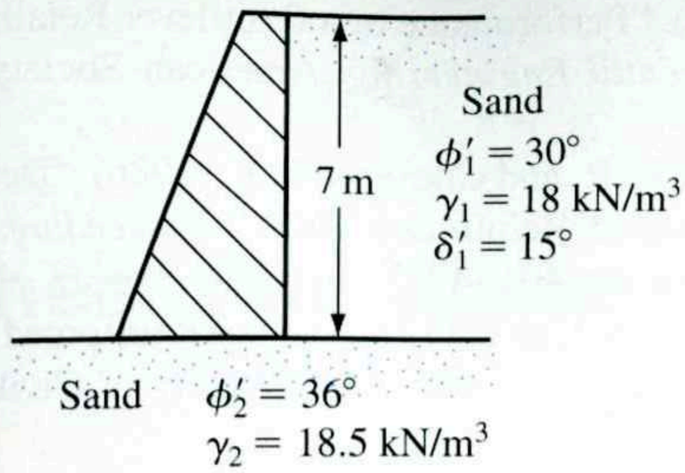

Figure P8.5

Given: $A_v = 0.15$ and $A_a = 0.25$. Use a factor of safety of 2.

8.6 In Figure 8.29a, use the following parameters:

Wall: $H = 8$ m

Soil: $\gamma_1 = 17$ kN/m³, $\phi_1' = 35°$

Reinforcement: $S_V = 1$ m and $S_H = 1.5$ m

Surcharge: $q = 70$ kN/m², $a' = 1.5$ m, and $b' = 2$ m

Calculate the vertical stress σ_o' [Eqs. (8.32), (8.33) and (8.34)] at $z = 2$ m, 4 m, 6 m and 8 m.

8.7 For the data given in Problem 8.6, calculate the lateral pressure σ_a' at $z = 2$ m, 4 m, 6 m and 8 m. Use Eqs. (8.35), (8.36) and (8.37).

8.8 A reinforced earth retaining wall (Figure 8.29) is to be 10 m. high. Here,

Backfill: unit weight, $\gamma_1 = 16$ kN/m³ and soil friction angle, $\phi_1' = 34°$

Reinforcement: vertical spacing, $S_V = 1$ m; horizontal spacing, $S_H = 1.25$ m; width of reinforcement = 120 mm., $f_y = 260$ MN/m²; $\phi_\mu = 25°$; factor of safety against tie pullout = 3; and factor of safety against tie breaking = 3

Determine:

a. The required thickness of ties

b. The required maximum length of ties

8.9 In Problem 8.8 assume that the ties at all depths are the length determined in Part b. For the *in situ* soil, $\phi_2' = 25°$, $\gamma_2 = 15.5$ kN/m³, $c_2' = 30$ kN/m². Calculate the factor of safety against (a) overturning, (b) sliding, and (c) bearing capacity failure.

8.10 A retaining wall with geotextile reinforcement is 6-m high. For the granular backfill, $\gamma_1 = 15.9$ kN/m³ and $\phi_1' = 30°$. For the geotextile, $T_{all} = 16$ kN/m. For the design of the wall, determine S_V, L, and l_l. Use $FS_{(B)} = FS_{(P)} = 1.5$.

8.11 With the S_V, L, and l_l determined in Problem 8.10, check the overall stability (i.e., factor of safety against overturning, sliding, and bearing capacity failure) of the wall. For the *in situ* soil, $\gamma_2 = 16.8$ kN/m³, $\phi_2' = 20°$, and $c_2' = 55$ kN/m².

References

APPLIED TECHNOLOGY COUNCIL (1978). "Tentative Provisions for the Development of Seismic Regulations for Buildings," *Publication ATC 3-06*, Palo Alto, California.

BELL, J. R., STILLEY, A. N., and VANDRE, B. (1975). "Fabric Retaining Earth Walls," *Proceedings, Thirteenth Engineering Geology and Soils Engineering Symposium*, Moscow, ID.

9 Sheet Pile Walls

9.1 Introduction

Connected or semiconnected sheet piles are often used to build continuous walls for waterfront structures that range from small waterfront pleasure boat launching facilities to large dock facilities. (See Figure 9.1.) In contrast to the construction of other types of retaining wall, the building of sheet pile walls does not usually require dewatering of the site. Sheet piles are also used for some temporary structures, such as braced cuts. (See Chapter 10.) The principles of sheet-pile wall design are discussed in the current chapter.

Several types of sheet pile are commonly used in construction: (a) wooden sheet piles, (b) precast concrete sheet piles, and (c) steel sheet piles. Aluminum sheet piles are also marketed.

Wooden sheet piles are used only for temporary, light structures that are above the water table. The most common types are ordinary wooden planks and *Wakefield piles.* The wooden planks are about 50 mm × 300 mm (2 in. × 12 in.) in cross section and are driven edge to edge (Figure 9.2a). Wakefield piles are made by nailing three planks together, with the middle plank offset by 50 to 75 mm (2 to 3 in.) (Figure 9.2b). Wooden planks can also be milled to form *tongue-and-groove piles,* as shown in Figure 9.2c. Figure 9.2d shows another type of wooden sheet pile that has precut grooves. Metal *splines* are driven into the grooves of the adjacent sheetings to hold them together after they are sunk into the ground.

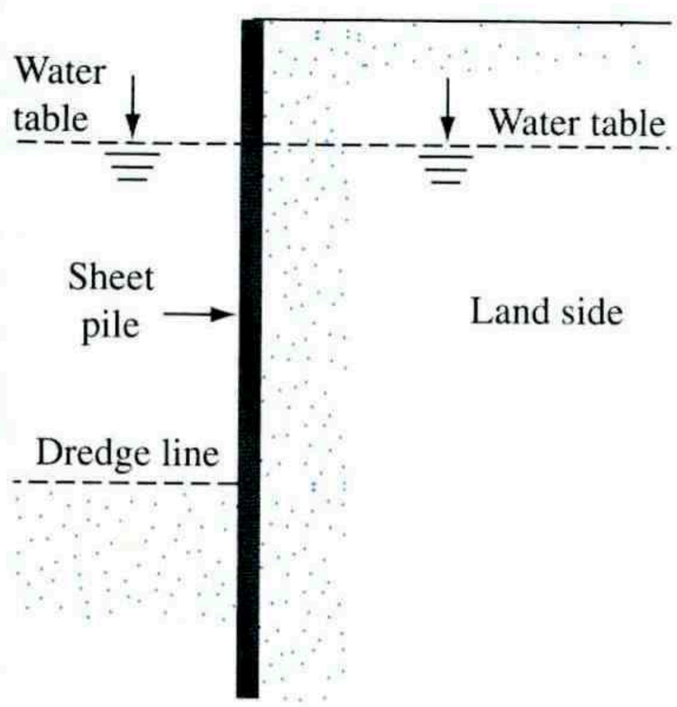

Figure 9.1 Example of waterfront sheet-pile wall

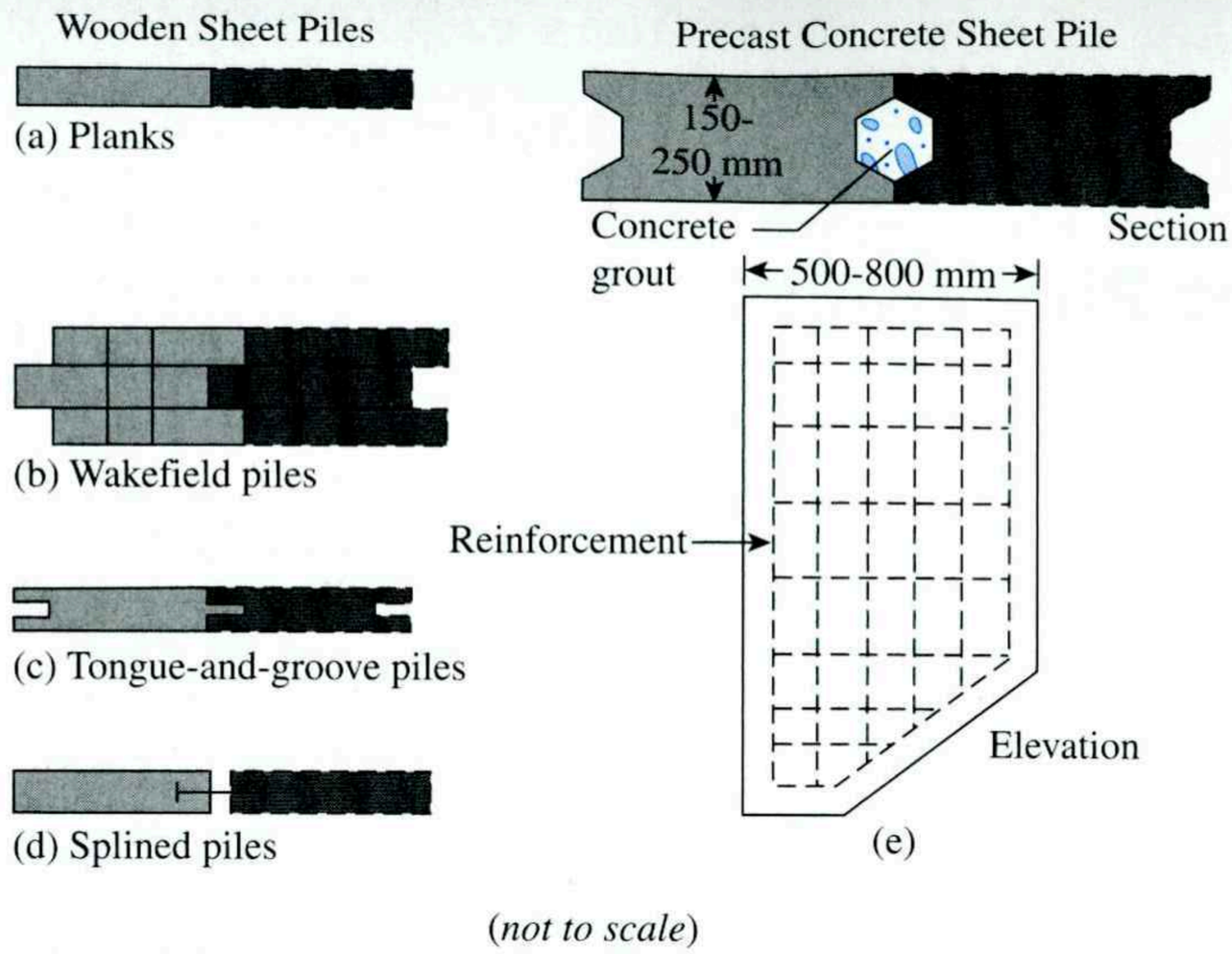

Figure 9.2 Various types of wooden and concrete sheet pile

Precast concrete sheet piles are heavy and are designed with reinforcements to withstand the permanent stresses to which the structure will be subjected after construction and also to handle the stresses produced during construction. In cross section, these piles are about 500 to 800 mm (20 to 32 in.) wide and 150 to 250 mm (6 to 10 in.) thick. Figure 9.2e is a schematic diagram of the elevation and the cross section of a reinforced concrete sheet pile.

Steel sheet piles in the United States are about 10 to 13 mm (0.4 to 0.5 in.) thick. European sections may be thinner and wider. Sheet-pile sections may be *Z, deep arch, low arch,* or *straight web* sections. The interlocks of the sheet-pile sections are shaped like a *thumb-and-finger* or *ball-and-socket* joint for watertight connections. Figure 9.3a is a schematic diagram of the thumb-and-finger type of interlocking for straight web sections. The ball-and-socket type of interlocking for *Z* section piles is shown in Figure 9.3b. Figure 9.4 shows a sheet pile wall. Table 9.1 lists the properties of the steel sheet pile sections produced by the Bethlehem Steel Corporation. The allowable design flexural stress for the steel sheet piles is as follows:

Type of steel	Allowable stress	
ASTM A-328	170 MN/m^2	(25,000 lb/in^2)
ASTM A-572	210 MN/m^2	(30,000 lb/in^2)
ASTM A-690	210 MN/m^2	(30,000 lb/in^2)

Steel sheet piles are convenient to use because of their resistance to the high driving stress that is developed when they are being driven into hard soils. Steel sheet piles are also lightweight and reusable.

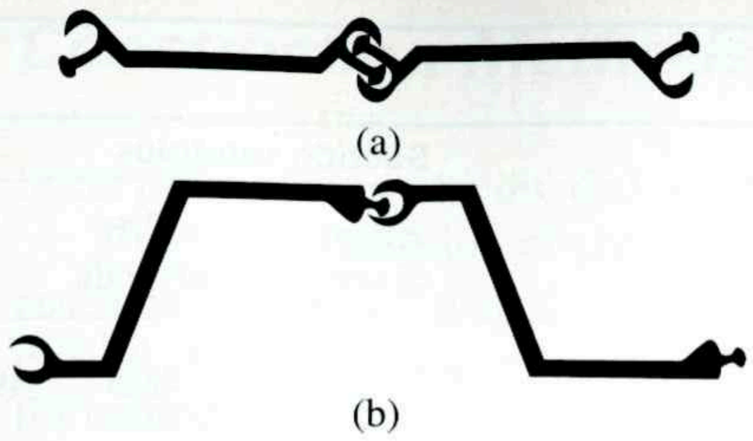

Figure 9.3 (a) Thumb-and-finger type sheet pile connection; (b) ball-and-socket type sheet-pile connection

Figure 9.4 A steel sheet pile wall (*Courtesy of N. Sivakugan, James Cook University, Australia*)

Table 9.1 Properties of Some Sheet-Pile Sections Produced by Bethlehem Steel Corporation

Section designation	Sketch of section	Section modulus		Moment of inertia	
		m^3/m of wall	in^3/ft of wall	m^4/m of wall	in^4/ft of wall
PZ-40	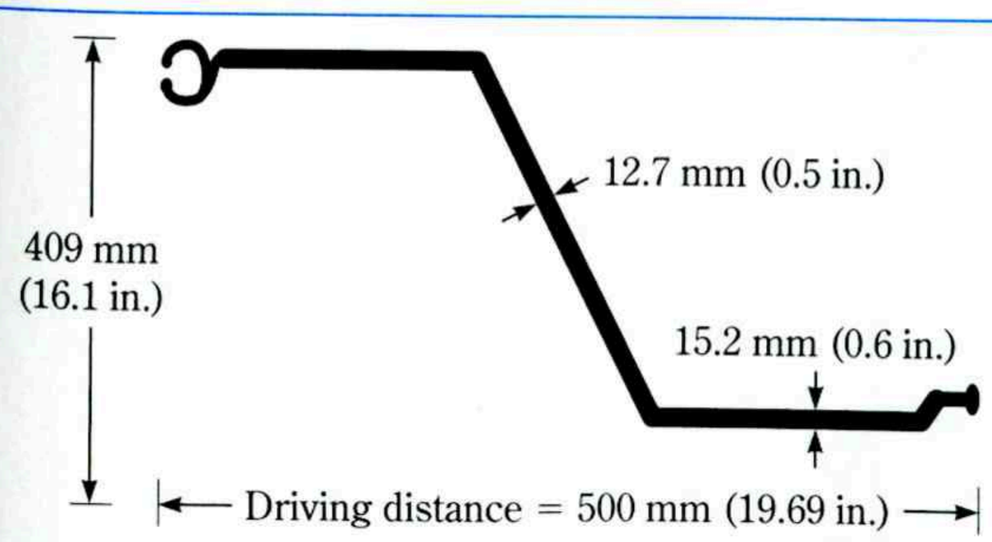	326.4×10^{-5}	60.7	670.5×10^{-6}	490.8

(Continued)

Table 9.1 (*Continued*)

Section designation	Sketch of section	Section modulus m^3/m of wall	Section modulus in^3/ft of wall	Moment of inertia m^4/m of wall	Moment of inertia in^4/ft of wall
PZ-35	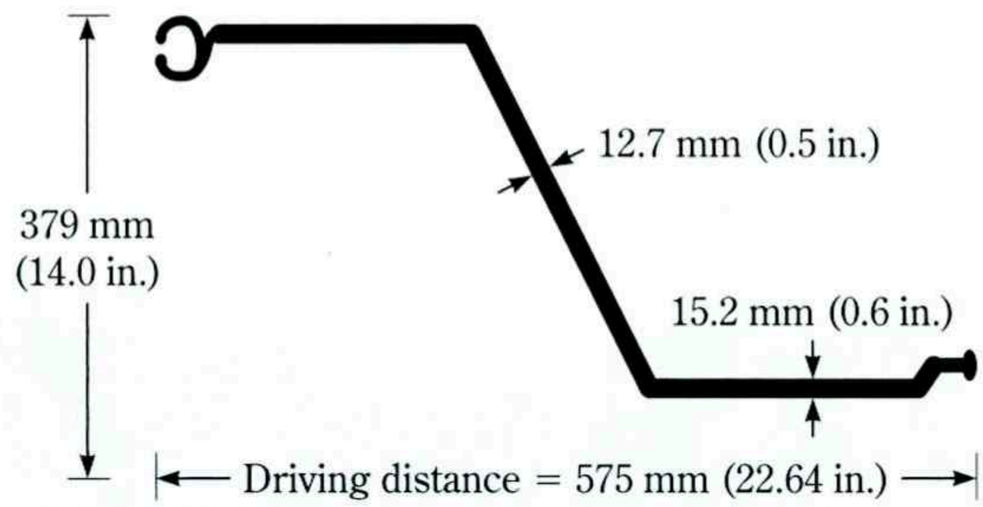	260.5×10^{-5}	48.5	493.4×10^{-6}	361.2
PZ-27	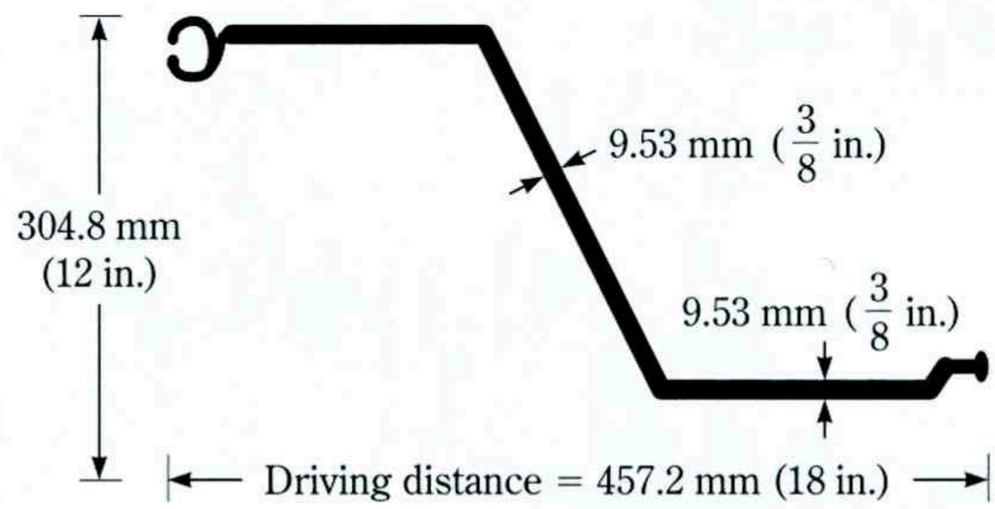	162.3×10^{-5}	30.2	251.5×10^{-6}	184.2
PZ-22	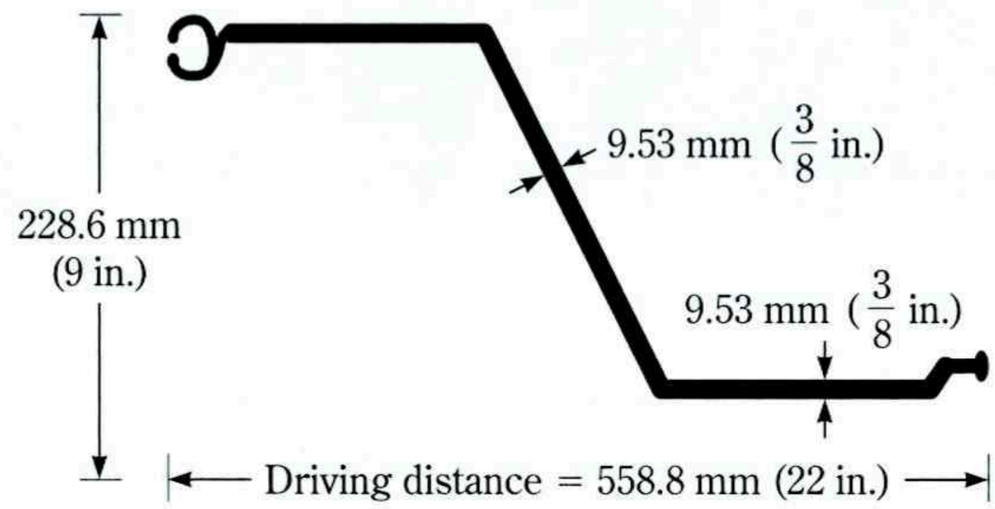	97×10^{-5}	18.1	115.2×10^{-6}	84.4
PSA-31	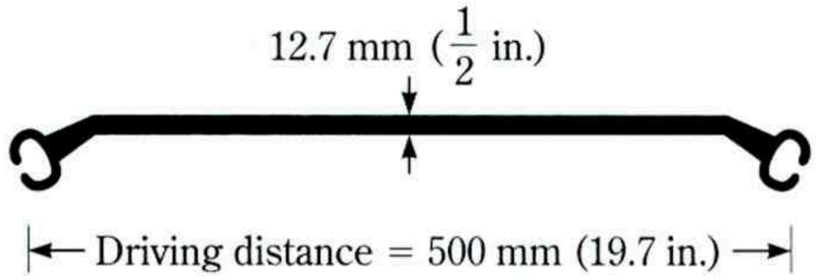	10.8×10^{-5}	2.01	4.41×10^{-6}	3.23
PSA-23	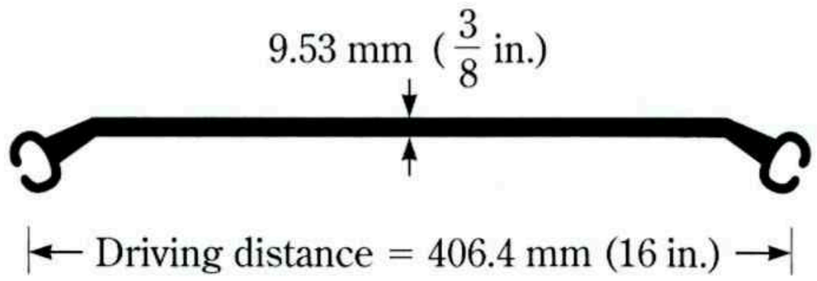	12.8×10^{-5}	2.4	5.63×10^{-6}	4.13

9.2 Construction Methods

Sheet pile walls may be divided into two basic categories: (a) cantilever and (b) anchored.

In the construction of sheet pile walls, the sheet pile may be driven into the ground and then the backfill placed on the land side, or the sheet pile may first be driven into the ground and the soil in front of the sheet pile dredged. In either case, the soil used for backfill behind the sheet pile wall is usually granular. The soil below the dredge line may be sandy or clayey. The surface of soil on the water side is referred to as the *mud line* or *dredge line.*

Thus, construction methods generally can be divided into two categories (Tsinker, 1983):

1. Backfilled structure
2. Dredged structure

The sequence of construction for a *backfilled structure* is as follows (see Figure 9.5):

Step 1. Dredge the *in situ* soil in front and back of the proposed structure.
Step 2. Drive the sheet piles.
Step 3. Backfill up to the level of the anchor, and place the anchor system.
Step 4. Backfill up to the top of the wall.

For a cantilever type of wall, only Steps 1, 2, and 4 apply. The sequence of construction for a *dredged structure* is as follows (see Figure 9.6):

Step 1. Drive the sheet piles.
Step 2. Backfill up to the anchor level, and place the anchor system.
Step 3. Backfill up to the top of the wall.
Step 4. Dredge the front side of the wall.

With cantilever sheet pile walls, Step 2 is not required.

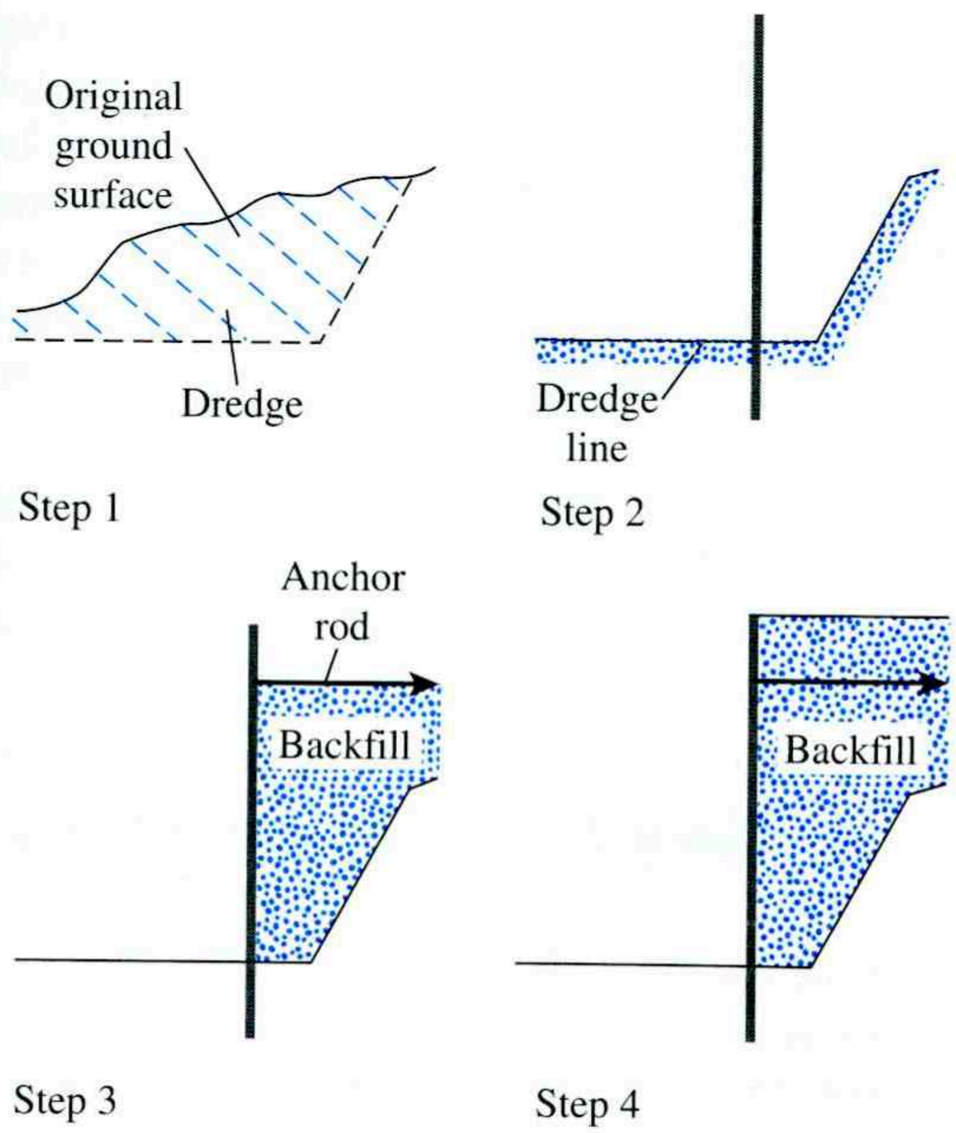

Figure 9.5 Sequence of construction for a backfilled structure

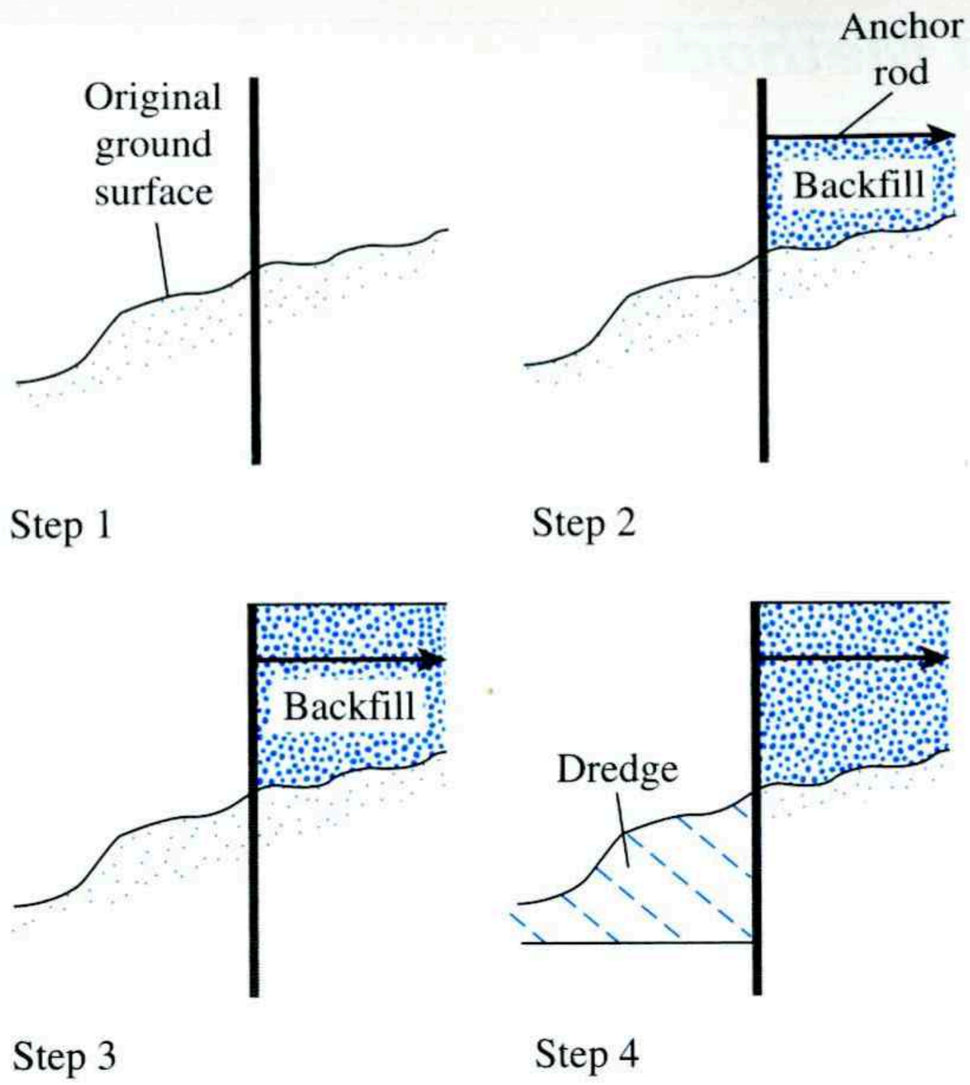

Figure 9.6 Sequence of construction for a dredged structure

9.3 Cantilever Sheet Pile Walls

Cantilever sheet pile walls are usually recommended for walls of moderate height—about 6 m (≈20 ft) or less, measured above the dredge line. In such walls, the sheet piles act as a wide cantilever beam above the dredge line. The basic principles for estimating net lateral pressure distribution on a cantilever sheet-pile wall can be explained with the aid of Figure 9.7. The figure shows the nature of lateral yielding of a cantilever wall penetrating a sand layer below the dredge line. The wall rotates about point O (Figure 9.7a). Because the hydrostatic pressures at any depth from both sides of the wall will cancel each other, we consider only the effective lateral soil pressures. In zone A, the lateral pressure is just the active pressure from the land side. In zone B, because of the nature of yielding of the wall, there will be active pressure from the land side and passive pressure from the water side. The condition is reversed in zone C—that is, below the point of rotation, O. The net actual pressure distribution on the wall is like that shown in Figure 9.7b. However, for design purposes, Figure 9.7c shows a simplified version.

Sections 9.4 through 9.7 present the mathematical formulation of the analysis of cantilever sheet pile walls. Note that, in some waterfront structures, the water level may fluctuate as the result of tidal effects. Care should be taken in determining the water level that will affect the net pressure diagram.

9.4 Cantilever Sheet Piling Penetrating Sandy Soils

To develop the relationships for the proper depth of embedment of sheet piles driven into a granular soil, examine Figure 9.8a. The soil retained by the sheet piling above the dredge line also is sand. The water table is at a depth L_1 below the top of the wall.

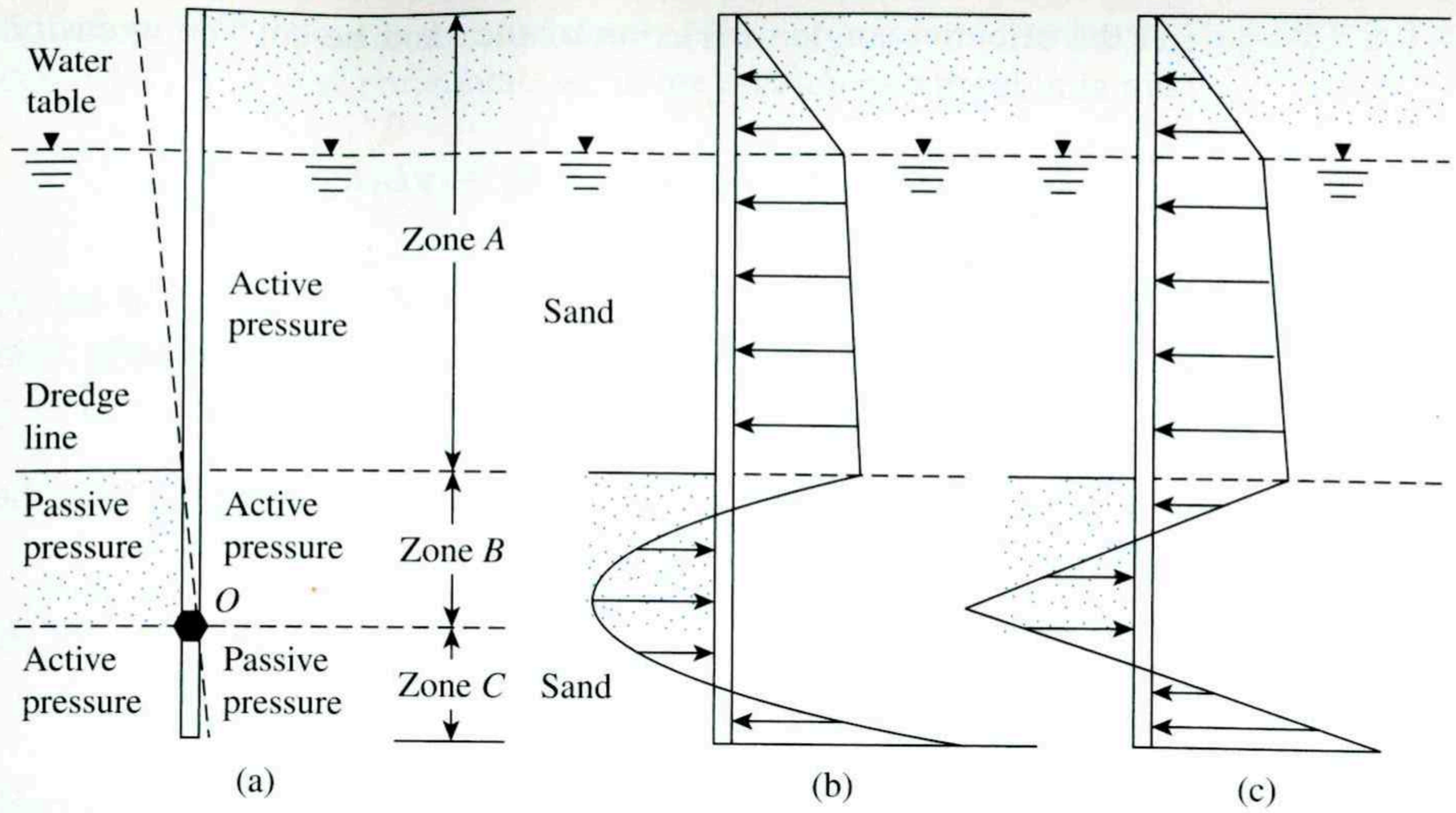

Figure 9.7 Cantilever sheet pile penetrating sand

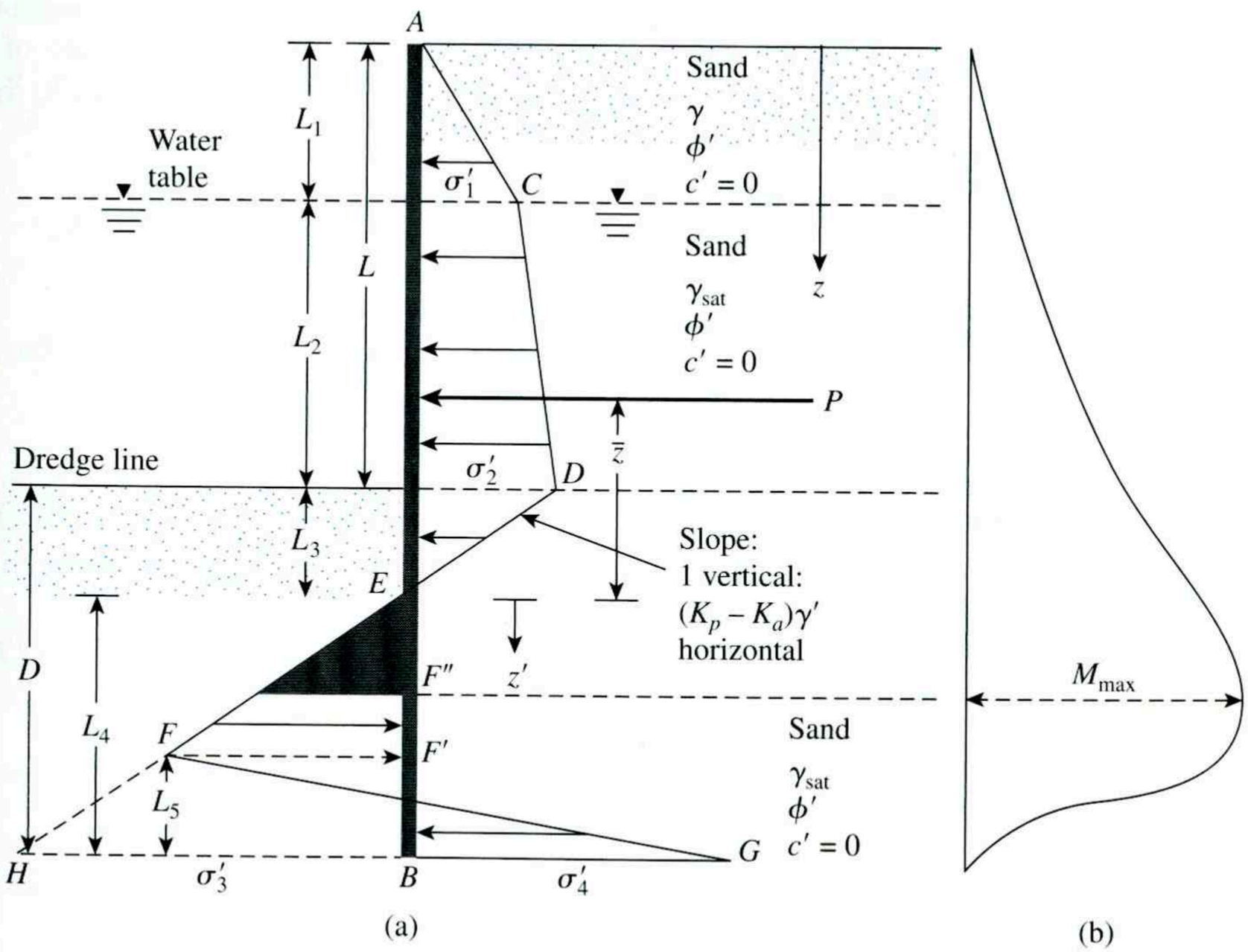

Figure 9.8 Cantilever sheet pile penetrating sand: (a) variation of net pressure diagram; (b) variation of moment

Let the effective angle of friction of the sand be ϕ'. The intensity of the active pressure at a depth $z = L_1$ is

$$\sigma'_1 = \gamma L_1 K_a \tag{9.1}$$

where

K_a = Rankine active pressure coefficient = $\tan^2(45 - \phi'/2)$
γ = unit weight of soil above the water table

Similarly, the active pressure at a depth $z = L_1 + L_2$ (i.e., at the level of the dredge line) is

$$\sigma'_2 = (\gamma L_1 + \gamma' L_2) K_a \tag{9.2}$$

where γ' = effective unit weight of soil = $\gamma_{sat} - \gamma_w$.

Note that, at the level of the dredge line, the hydrostatic pressures from both sides of the wall are the same magnitude and cancel each other.

To determine the net lateral pressure below the dredge line up to the point of rotation, O, as shown in Figure 9.7a, an engineer has to consider the passive pressure acting from the left side (the water side) toward the right side (the land side) of the wall and also the active pressure acting from the right side toward the left side of the wall. For such cases, ignoring the hydrostatic pressure from both sides of the wall, the active pressure at depth z is

$$\sigma'_a = [\gamma L_1 + \gamma' L_2 + \gamma'(z - L_1 - L_2)] K_a \tag{9.3}$$

Also, the passive pressure at depth z is

$$\sigma'_p = \gamma'(z - L_1 - L_2) K_p \tag{9.4}$$

where K_p = Rankine passive pressure coefficient = $\tan^2(45 + \phi'/2)$.

Combining Eqs. (9.3) and (9.4) yields the net lateral pressure, namely,

$$\begin{aligned} \sigma' &= \sigma'_a - \sigma'_p = (\gamma L_1 + \gamma' L_2) K_a - \gamma'(z - L_1 - L_2)(K_p - K_a) \\ &= \sigma'_2 - \gamma'(z - L)(K_p - K_a) \end{aligned} \tag{9.5}$$

where $L = L_1 + L_2$.

The net pressure, σ' equals zero at a depth L_3 below the dredge line, so

$$\sigma'_2 - \gamma'(z - L)(K_p - K_a) = 0$$

or

$$(z - L) = L_3 = \frac{\sigma'_2}{\gamma'(K_p - K_a)} \tag{9.6}$$

Equation (9.6) indicates that the slope of the net pressure distribution line *DEF* is 1 vertical to $(K_p - K_a)\gamma'$ horizontal, so, in the pressure diagram,

$$\overline{HB} = \sigma'_3 = L_4(K_p - K_a)\gamma' \tag{9.7}$$

At the bottom of the sheet pile, passive pressure, σ'_p, acts from the right toward the left side, and active pressure acts from the left toward the right side of the sheet pile, so, at $z = L + D$,

$$\sigma'_p = (\gamma L_1 + \gamma' L_2 + \gamma' D)K_p \tag{9.8}$$

At the same depth,

$$\sigma'_a = \gamma' D K_a \tag{9.9}$$

Hence, the net lateral pressure at the bottom of the sheet pile is

$$\begin{aligned}\sigma'_p - \sigma'_a = \sigma'_4 &= (\gamma L_1 + \gamma' L_2)K_p + \gamma' D(K_p - K_a)\\ &= (\gamma L_1 + \gamma' L_2)K_p + \gamma' L_3(K_p - K_a) + \gamma' L_4(K_p - K_a)\\ &= \sigma'_5 + \gamma' L_4(K_p - K_a)\end{aligned} \tag{9.10}$$

where

$$\sigma'_5 = (\gamma L_1 + \gamma' L_2)K_p + \gamma' L_3(K_p - K_a) \tag{9.11}$$

$$D = L_3 + L_4 \tag{9.12}$$

For the stability of the wall, the principles of statics can now be applied:

$$\Sigma \text{ horizontal forces per unit length of wall} = 0$$

and

$$\Sigma \text{ moment of the forces per unit length of wall about point } B = 0$$

For the summation of the horizontal forces, we have

$$\text{Area of the pressure diagram } ACDE - \text{area of } EFHB + \text{area of } FHBG = 0$$

or

$$P - \tfrac{1}{2}\sigma'_3 L_4 + \tfrac{1}{2}L_5(\sigma'_3 + \sigma'_4) = 0 \tag{9.13}$$

where P = area of the pressure diagram *ACDE*.

Summing the moment of all the forces about point *B* yields

$$P(L_4 + \bar{z}) - \left(\frac{1}{2}L_4\sigma'_3\right)\left(\frac{L_4}{3}\right) + \frac{1}{2}L_5(\sigma'_3 + \sigma'_4)\left(\frac{L_5}{3}\right) = 0 \tag{9.14}$$

From Eq. (9.13),

$$L_5 = \frac{\sigma'_3 L_4 - 2P}{\sigma'_3 + \sigma'_4} \tag{9.15}$$

Combining Eqs. (9.7), (9.10), (9.14), and (9.15) and simplifying them further, we obtain the following fourth-degree equation in terms of L_4:

$$L_4^4 + A_1 L_4^3 - A_2 L_4^2 - A_3 L_4 - A_4 = 0 \tag{9.16}$$

In this equation,

$$A_1 = \frac{\sigma'_5}{\gamma'(K_p - K_a)} \tag{9.17}$$

$$A_2 = \frac{8P}{\gamma'(K_p - K_a)} \tag{9.18}$$

$$A_3 = \frac{6P[2\bar{z}\gamma'(K_p - K_a) + \sigma'_5]}{\gamma'^2(K_p - K_a)^2} \tag{9.19}$$

$$A_4 = \frac{P(6\bar{z}\sigma'_5 + 4P)}{\gamma'^2(K_p - K_a)^2} \tag{9.20}$$

Step-by-Step Procedure for Obtaining the Pressure Diagram

Based on the preceding theory, a step-by-step procedure for obtaining the pressure diagram for a cantilever sheet pile wall penetrating a granular soil is as follows:

Step 1. Calculate K_a and K_p.
Step 2. Calculate σ'_1 [Eq. (9.1)] and σ'_2 [Eq. (9.2)]. (*Note:* L_1 and L_2 will be given.)
Step 3. Calculate L_3 [Eq. (9.6)].
Step 4. Calculate P.
Step 5. Calculate $\bar{z}$ (i.e., the center of pressure for the area *ACDE*) by taking the moment about *E*.
Step 6. Calculate σ'_5 [Eq. (9.11)].
Step 7. Calculate A_1, A_2, A_3, and A_4 [Eqs. (9.17) through (9.20)].
Step 8. Solve Eq. (9.16) by trial and error to determine L_4.
Step 9. Calculate σ'_4 [Eq. (9.10)].
Step 10. Calculate σ'_3 [Eq. (9.7)].
Step 11. Obtain L_5 from Eq. (9.15).
Step 12. Draw a pressure distribution diagram like the one shown in Figure 9.8a.
Step 13. Obtain the theoretical depth [see Eq. (9.12)] of penetration as $L_3 + L_4$. The actual depth of penetration is increased by about 20 to 30%.

Note that some designers prefer to use a factor of safety on the passive earth pressure coefficient at the beginning. In that case, in Step 1,

$$K_{p(\text{design})} = \frac{K_p}{\text{FS}}$$

where FS = factor of safety (usually between 1.5 and 2).

For this type of analysis, follow Steps 1 through 12 with the value of $K_a = \tan^2(45 - \phi'/2)$ and $K_{p(\text{design})}$ (instead of K_p). The actual depth of penetration can now be determined by adding L_3, obtained from Step 3, and L_4, obtained from Step 8.

Calculation of Maximum Bending Moment

The nature of the variation of the moment diagram for a cantilever sheet pile wall is shown in Figure 9.8b. The maximum moment will occur between points E and F'. Obtaining the maximum moment ($M_{\max}$) per unit length of the wall requires determining the point of zero shear. For a new axis z' (with origin at point E) for zero shear,

$$P = \tfrac{1}{2}(z')^2(K_p - K_a)\gamma'$$

or

$$z' = \sqrt{\frac{2P}{(K_p - K_a)\gamma'}} \tag{9.21}$$

Once the point of zero shear force is determined (point F'' in Figure 9.8a), the magnitude of the maximum moment can be obtained as

$$M_{\max} = P(\bar{z} + z') - [\tfrac{1}{2}\gamma' z'^2(K_p - K_a)](\tfrac{1}{3})z' \tag{9.22}$$

The necessary profile of the sheet piling is then sized according to the allowable flexural stress of the sheet pile material, or

$$S = \frac{M_{\max}}{\sigma_{\text{all}}} \tag{9.23}$$

where

S = section modulus of the sheet pile required per unit length of the structure
σ_{all} = allowable flexural stress of the sheet pile

Example 9.1

Figure 9.9 shows a cantilever sheet pile wall penetrating a granular soil. Here, $L_1 = 2$ m, $L_2 = 3$ m, $\gamma = 15.9$ kN/m^3, $\gamma_{\text{sat}} = 19.33$ kN/m^3, and $\phi' = 32°$.

a. What is the theoretical depth of embedment, D?
b. For a 30% increase in D, what should be the total length of the sheet piles?
c. What should be the minimum section modulus of the sheet piles? Use $\sigma_{\text{all}} = 172$ MN/m^2.

Solution

Part a

Using Figure 9.8a for the pressure distribution diagram, one can now prepare the following table for a step-by-step calculation.

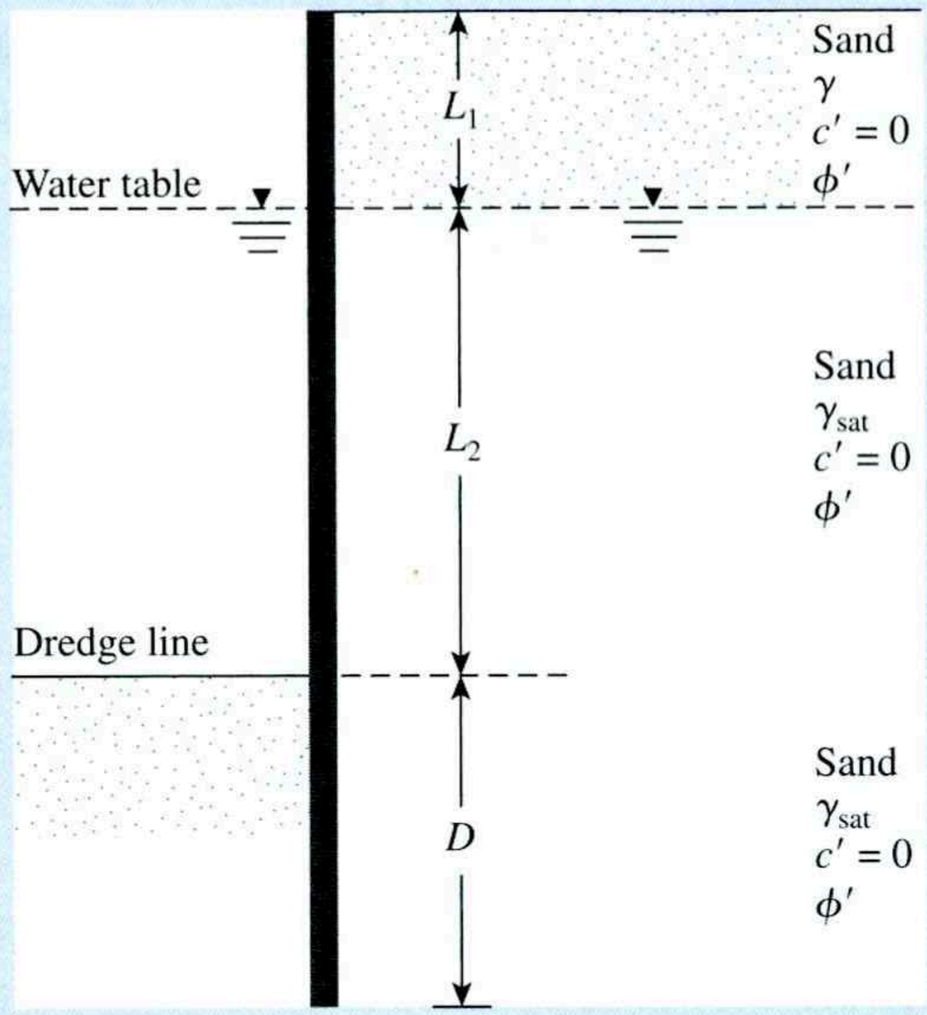

Figure 9.9 Cantilever sheet-pile wall

Quantity required	Eq. no.	Equation and calculation
K_a	—	$\tan^2\left(45 - \frac{\phi'}{2}\right) = \tan^2\left(45 - \frac{32}{2}\right) = 0.307$
K_p	—	$\tan^2\left(45 + \frac{\phi'}{2}\right) = \tan^2\left(45 + \frac{32}{2}\right) = 3.25$
σ_1'	9.1	$\gamma L_1 K_a = (15.9)(2)(0.307) = 9.763\ \text{kN/m}^2$
σ_2'	9.2	$(\gamma L_1 + \gamma' L_2)K_a = [(15.9)(2) + (19.33 - 9.81)(3)](0.307) = 18.53\ \text{kN/m}^2$
L_3	9.6	$\frac{\sigma_2'}{\gamma'(K_p - K_a)} = \frac{18.53}{(19.33 - 9.81)(3.25 - 0.307)} = 0.66\ \text{m}$
P	—	$\frac{1}{2}\sigma_1' L_1 + \sigma_1' L_2 + \frac{1}{2}(\sigma_2' - \sigma_1')L_2 + \frac{1}{2}\sigma_2' L_3$ $= (\frac{1}{2})(9.763)(2) + (9.763)(3) + (\frac{1}{2})(18.53 - 9.763)(3) + (\frac{1}{2})(18.53)(0.66)$ $= 9.763 + 29.289 + 13.151 + 6.115 = 58.32\ \text{kN/m}$
$\bar{z}$	—	$\frac{\Sigma M_E}{P} = \frac{1}{58.32}\left[\begin{array}{l} 9.763(0.66 + 3 + \frac{2}{3}) + 29.289(0.66 + \frac{3}{2}) \\ + 13.151(0.66 + \frac{3}{3}) + 6.115(0.66 \times \frac{2}{3}) \end{array}\right] = 2.23\ \text{m}$
σ_5'	9.11	$(\gamma L_1 + \gamma' L_2)K_p + \gamma' L_3(K_p - K_a) = [(15.9)(2) + (19.33 - 9.81)(3)](3.25) + (19.33 - 9.81)(0.66)(3.25 - 0.307) = 214.66\ \text{kN/m}^2$
A_1	9.17	$\frac{\sigma_5'}{\gamma'(K_p - K_a)} = \frac{214.66}{(19.33 - 9.81)(3.25 - 0.307)} = 7.66$
A_2	9.18	$\frac{8P}{\gamma'(K_p - K_a)} = \frac{(8)(58.32)}{(19.33 - 9.81)(3.25 - 0.307)} = 16.65$

A_3	9.19	$\dfrac{6P[2\bar{z}\gamma'(K_p - K_a) + \sigma'_5]}{\gamma'^2(K_p - K_a)^2}$
		$= \dfrac{(6)(58.32)[(2)(2.23)(19.33 - 9.81)(3.25 - 0.307) + 214.66]}{(19.33 - 9.81)^2(3.25 - 0.307)^2}$
		$= 151.93$
A_4	9.20	$\dfrac{P(6\bar{z}\sigma'_5 + 4P)}{\gamma'^2(K_p - K_a)^2} = \dfrac{58.32[(6)(2.23)(214.66) + (4)(58.32)]}{(19.33 - 9.81)^2(3.25 - 0.307)^2}$
		$= 230.72$
L_4	9.16	$L_4^4 + A_1L_4^3 - A_2L_4^2 - A_3L_4 - A_4 = 0$
		$L_4^4 + 7.66L_4^3 - 16.65L_4^2 - 151.93L_4 - 230.72 = 0;\ L_4 \approx 4.8$ m

Thus,

$$D_{\text{theory}} = L_3 + L_4 = 0.66 + 4.8 = \mathbf{5.46\ m}$$

Part b

The total length of the sheet piles is

$$L_1 + L_2 + 1.3(L_3 + L_4) = 2 + 3 + 1.3(5.46) = \mathbf{12.1\ m}$$

Part c

Finally, we have the following table.

Quantity required	Eq. no.	Equation and calculation
z'	9.21	$\sqrt{\dfrac{2P}{(K_p - K_a)\gamma'}} = \sqrt{\dfrac{(2)(58.32)}{(3.25 - 0.307)(19.33 - 9.81)}} = 2.04$ m
$M_{\max}$	9.22	$P(\bar{z} + z') - \left[\dfrac{1}{2}\gamma' z'^2(K_p - K_a)\right]\dfrac{z'}{3} = (58.32)(2.23 + 2.04)$
		$-\left[\left(\dfrac{1}{2}\right)(19.33 - 9.81)(2.04)^2(3.25 - 0.307)\right]\dfrac{2.04}{3}$
		$= 209.39$ kN·m/m
S	9.29	$\dfrac{M_{\max}}{\sigma_{\text{all}}} = \dfrac{209.39\ \text{kN}\cdot\text{m}}{172 \times 10^3\ \text{kN/m}^2} = \mathbf{1.217 \times 10^{-3}\ m^3/m\ of\ wall}$ ■

9.5 Special Cases for Cantilever Walls Penetrating a Sandy Soil

Sheet Pile Wall with the Absence of Water Table

In the absence of the water table, the net pressure diagram on the cantilever sheet-pile wall will be as shown in Figure 9.10, which is a modified version of Figure 9.8. In this case,

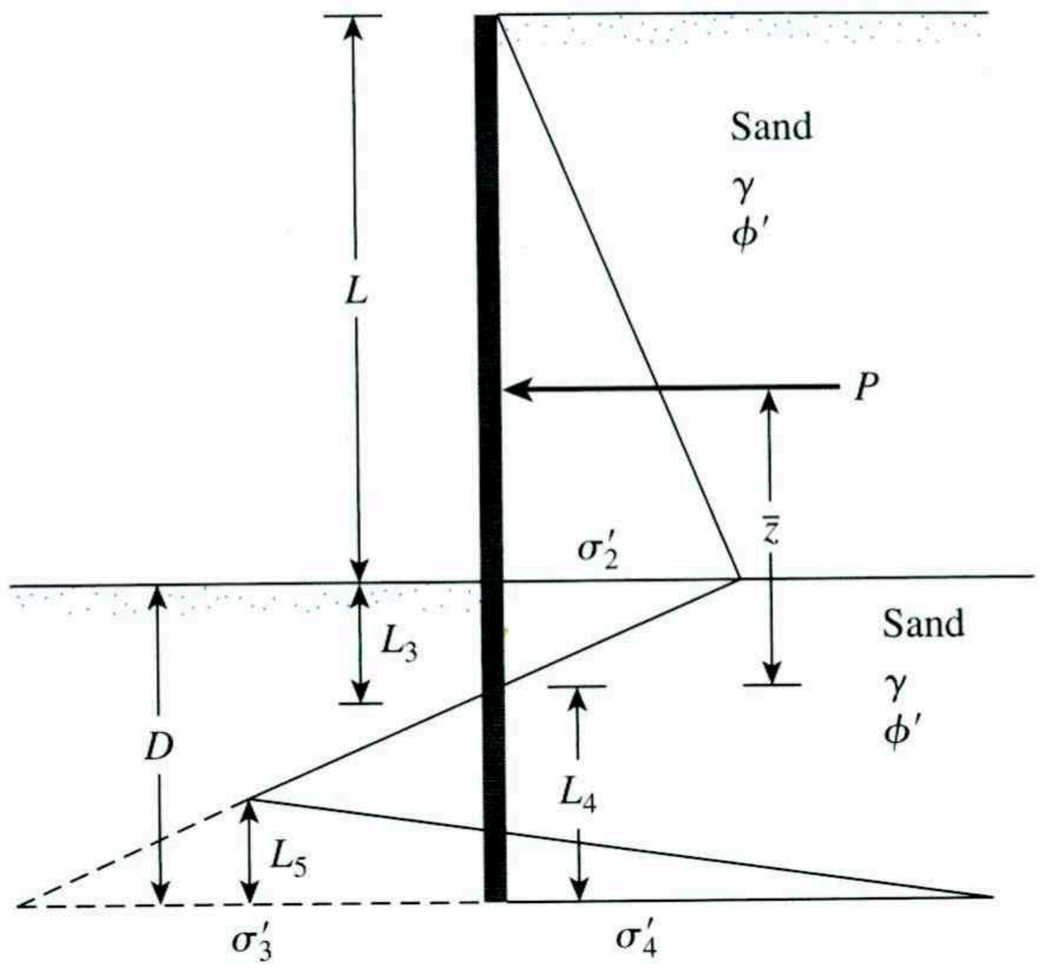

Figure 9.10 Sheet piling penetrating a sandy soil in the absence of the water table

$$\sigma'_2 = \gamma L K_a \tag{9.24}$$

$$\sigma'_3 = L_4(K_p - K_a)\gamma \tag{9.25}$$

$$\sigma'_4 = \sigma'_5 + \gamma L_4(K_p - K_a) \tag{9.26}$$

$$\sigma'_5 = \gamma L K_p + \gamma L_3(K_p - K_a) \tag{9.27}$$

$$L_3 = \frac{\sigma'_2}{\gamma(K_p - K_a)} = \frac{LK_a}{(K_p - K_a)} \tag{9.28}$$

$$P = \tfrac{1}{2}\sigma'_2 L + \tfrac{1}{2}\sigma'_2 L_3 \tag{9.29}$$

$$\bar{z} = L_3 + \frac{L}{3} = \frac{LK_a}{K_p - K_a} + \frac{L}{3} = \frac{L(2K_a + K_p)}{3(K_p - K_a)} \tag{9.30}$$

and Eq. (9.16) transforms to

$$L_4^4 + A'_1 L_4^3 - A'_2 L_4^2 - A'_3 L_4 - A'_4 = 0 \tag{9.31}$$

where

$$A'_1 = \frac{\sigma'_5}{\gamma(K_p - K_a)} \tag{9.32}$$

$$A'_2 = \frac{8P}{\gamma(K_p - K_a)} \tag{9.33}$$

$$A'_3 = \frac{6P[2\bar{z}\gamma(K_p - K_a) + \sigma'_5]}{\gamma^2(K_p - K_a)^2} \tag{9.34}$$

$$A'_4 = \frac{P(6\bar{z}\sigma'_5 + 4P)}{\gamma^2(K_p - K_a)^2} \tag{9.35}$$

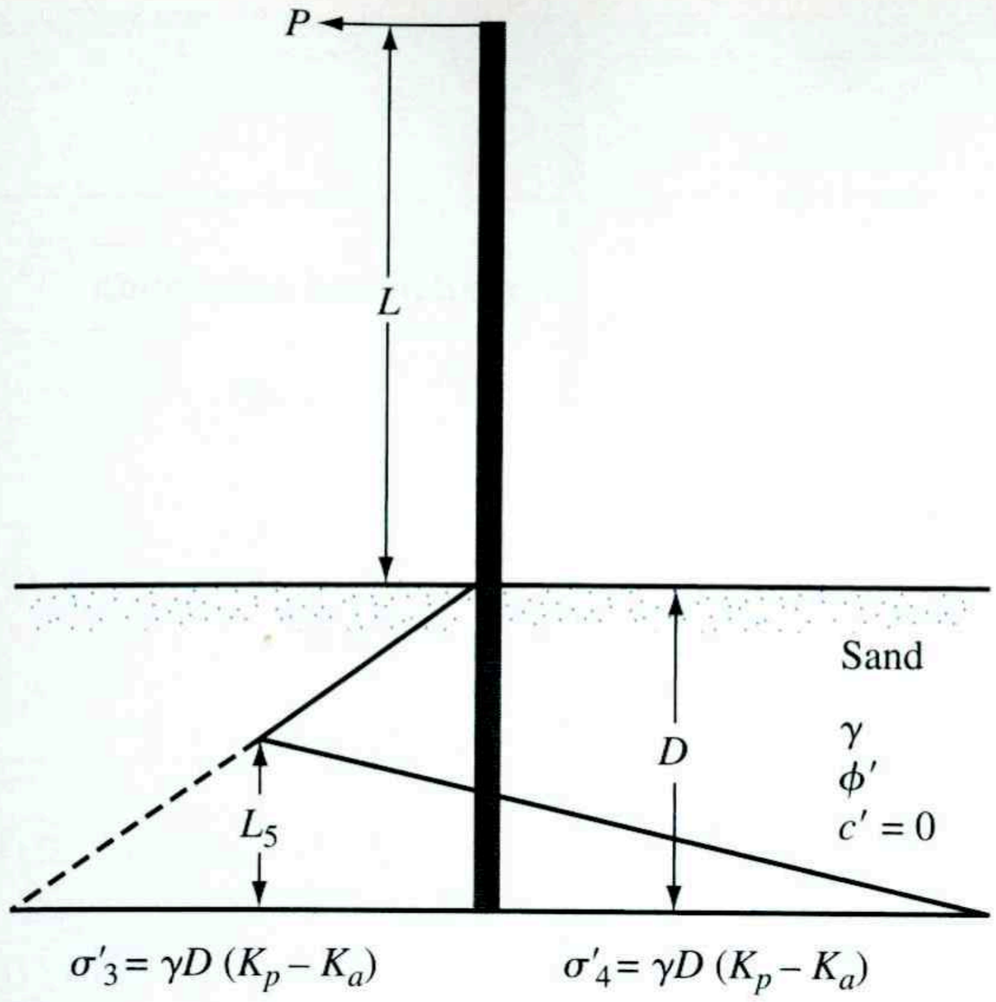

Figure 9.11 Free cantilever sheet piling penetrating a layer of sand

Free Cantilever Sheet Piling

Figure 9.11 shows a free cantilever sheet-pile wall penetrating a sandy soil and subjected to a line load of P per unit length of the wall. For this case,

$$D^4 - \left[\frac{8P}{\gamma(K_p - K_a)}\right]D^2 - \left[\frac{12PL}{\gamma(K_p - K_a)}\right]D - \left[\frac{2P}{\gamma(K_p - K_a)}\right]^2 = 0 \tag{9.36}$$

$$L_5 = \frac{\gamma(K_p - K_a)D^2 - 2P}{2D(K_p - K_a)\gamma} \tag{9.37}$$

$$M_{\max} = P(L + z') - \frac{\gamma z'^3(K_p - K_a)}{6} \tag{9.38}$$

and

$$z' = \sqrt{\frac{2P}{\gamma'(K_p - K_a)}} \tag{9.39}$$

Example 9.2

Redo parts a and b of Example 9.1, assuming the absence of the water table. Use $\gamma = 15.9\ \text{kN/m}^3$ and $\phi' = 32°$. *Note*: $L = 5$ m.

Solution

Part a

Quantity required	Eq. no.	Equation and calculation
K_a	—	$\tan^2\left(45 - \frac{\phi'}{2}\right) = \tan^2\left(45 - \frac{32}{2}\right) = 0.307$
K_p	—	$\tan^2\left(45 + \frac{\phi'}{2}\right) = \tan^2\left(45 + \frac{32}{2}\right) = 3.25$
σ_2'	9.24	$\gamma L K_a = (15.9)(5)(0.307) = 24.41\ \text{kN/m}^2$
L_3	9.28	$\frac{LK_a}{K_p - K_a} = \frac{(5)(0.307)}{3.25 - 0.307} = 0.521\ \text{m}$
σ_5'	9.27	$\gamma L K_p + \gamma L_3(K_p - K_a) = (15.9)(5)(3.25) + (15.9)(0.521)(3.25 - 0.307) = 282.76\ \text{kN/m}^2$
P	9.29	$\frac{1}{2}\sigma_2' L + \frac{1}{2}\sigma_2' L_3 = \frac{1}{2}\sigma_2'(L + L_3) = (\frac{1}{2})(24.41)(5 + 0.521) = 67.38\ \text{kN/m}$
$\bar{z}$	9.30	$\frac{L(2K_a - K_p)}{3(K_p - K_a)} = \frac{5[(2)(0.307) + 3.25]}{3(3.25 - 0.307)} = 2.188\ \text{m}$
A_1'	9.32	$\frac{\sigma_5'}{\gamma(K_p - K_a)} = \frac{282.76}{(15.9)(3.25 - 0.307)} = 6.04$
A_2'	9.33	$\frac{8P}{\gamma(K_p - K_a)} = \frac{(8)(67.38)}{(15.9)(3.25 - 0.307)} = 11.52$
A_3'	9.34	$\frac{6P[2\bar{z}\gamma(K_p - K_a) + \sigma_5']}{\gamma^2(K_p - K_a)^2} = \frac{(6)(67.38)[(2)(2.188)(15.9)(3.25 - 0.307) + 282.76]}{(15.9)^2(3.25 - 0.307)^2} = 90.01$
A_4'	9.35	$\frac{P(6\bar{z}\sigma_5' + 4P)}{\gamma^2(K_p - K_a)^2} = \frac{(67.38)[(6)(2.188)(282.76) + (4)(67.38)]}{(15.9)^2(3.25 - 0.307)^2} = 122.52$
L_4	9.31	$L_4^4 + A_1'L_4^3 - A_2'L_4^2 - A_3'L_4 - A_4' = 0$ $L_4^4 + 6.04L_4^3 - 11.52L_4^2 - 90.01L_4 - 122.52 = 0;\ L_4 \approx 4.1\ \text{m}$

$$D_{\text{theory}} = L_3 + L_4 = 0.521 + 4.1 \approx \mathbf{4.7\ m}$$

Part b

Total length, $L + 1.3(D_{\text{theory}}) = 5 + 1.3(4.7) = \mathbf{11.11\ m}$ ■

9.6 Cantilever Sheet Piling Penetrating Clay

At times, cantilever sheet piles must be driven into a clay layer possessing an undrained cohesion $c(\phi = 0)$. The net pressure diagram will be somewhat different from that shown in Figure 9.8a. Figure 9.12 shows a cantilever sheet-pile wall driven into clay with a backfill of granular soil above the level of the dredge line. The water table is at

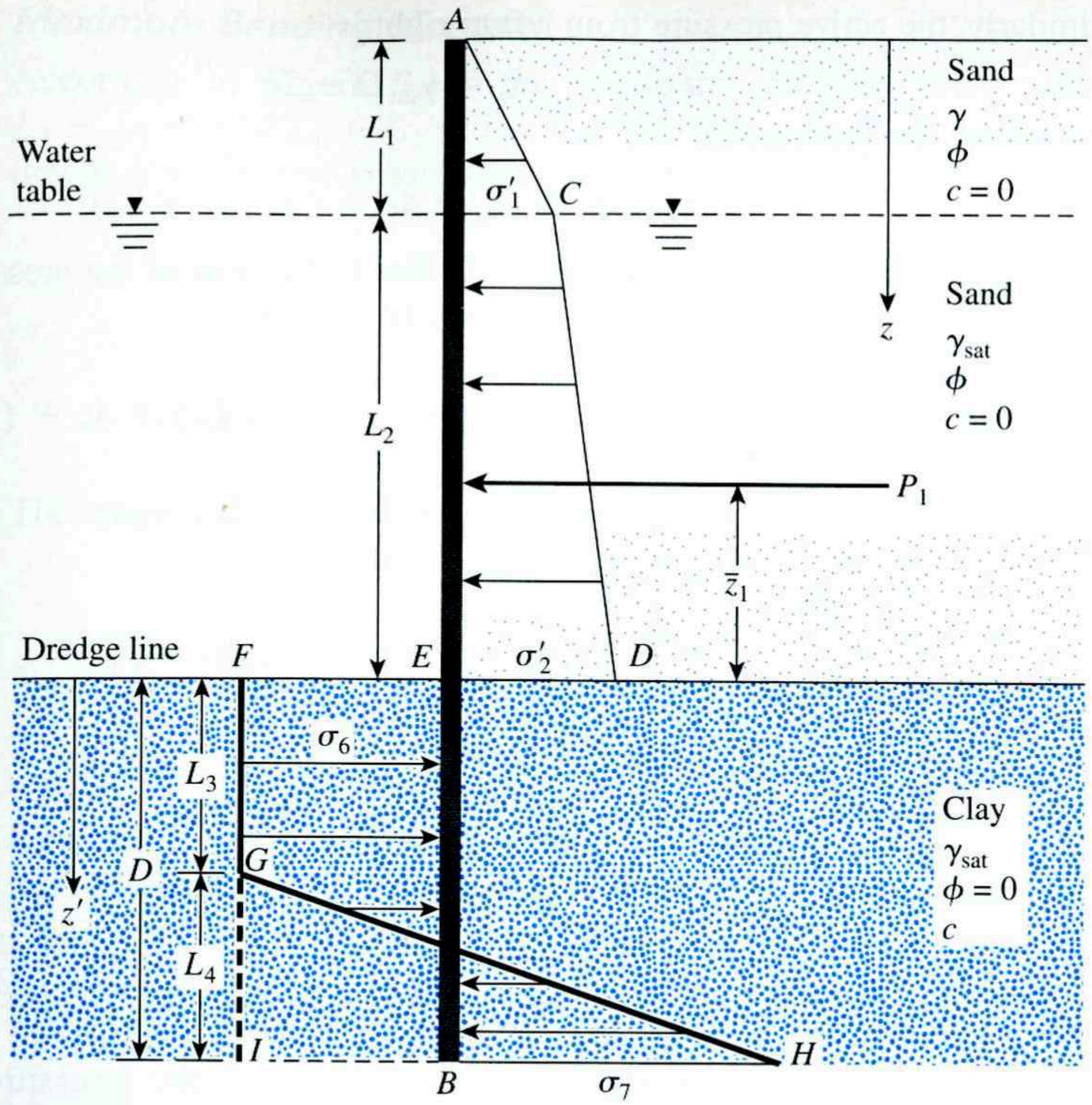

Figure 9.12 Cantilever sheet pile penetrating clay

a depth L_1 below the top of the wall. As before, Eqs. (9.1) and (9.2) give the intensity of the net pressures σ'_1 and σ'_2, and the diagram for pressure distribution above the level of the dredge line can be drawn. The diagram for net pressure distribution below the dredge line can now be determined as follows.

At any depth greater than $L_1 + L_2$, for $\phi = 0$, the Rankine active earth-pressure coefficient $K_a = 1$. Similarly, for $\phi = 0$, the Rankine passive earth-pressure coefficient $K_p = 1$. Thus, above the point of rotation (point O in Figure 9.7a), the active pressure, from right to left is

$$\sigma_a = [\gamma L_1 + \gamma' L_2 + \gamma_{sat}(z - L_1 - L_2)] - 2c \tag{9.40}$$

Similarly, the passive pressure from left to right may be expressed as

$$\sigma_p = \gamma_{sat}(z - L_1 - L_2) + 2c \tag{9.41}$$

Thus, the net pressure is

$$\begin{aligned}\sigma_6 = \sigma_p - \sigma_a &= [\gamma_{sat}(z - L_1 - L_2) + 2c] \\ &\quad - [\gamma L_1 + \gamma' L_2 + \gamma_{sat}(z - L_1 - L_2)] + 2c \\ &= 4c - (\gamma L_1 + \gamma' L_2)\end{aligned} \tag{9.42}$$

At the bottom of the sheet pile, the passive pressure from right to left is

$$\sigma_p = (\gamma L_1 + \gamma' L_2 + \gamma_{sat} D) + 2c \tag{9.43}$$

Similarly, the active pressure from left to right is

$$\sigma_a = \gamma_{\text{sat}} D - 2c \tag{9.44}$$

Hence, the net pressure is

$$\sigma_7 = \sigma_p - \sigma_a = 4c + (\gamma L_1 + \gamma' L_2) \tag{9.45}$$

For equilibrium analysis, $\Sigma F_H = 0$; that is, the area of the pressure diagram *ACDE* minus the area of *EFIB* plus the area of $GIH = 0$, or

$$P_1 - [4c - (\gamma L_1 + \gamma' L_2)]D + \tfrac{1}{2}L_4[4c - (\gamma L_1 + \gamma' L_2) + 4c + (\gamma L_1 + \gamma' L_2)] = 0$$

where P_1 = area of the pressure diagram *ACDE*.

Simplifying the preceding equation produces

$$L_4 = \frac{D[4c - (\gamma L_1 + \gamma' L_2)] - P_1}{4c} \tag{9.46}$$

Now, taking the moment about point B ($\Sigma M_B = 0$) yields

$$P_1(D + \bar{z}_1) - [4c - (\gamma L_1 + \gamma' L_2)]\frac{D^2}{2} + \frac{1}{2}L_4(8c)\left(\frac{L_4}{3}\right) = 0 \tag{9.47}$$

where $\bar{z}_1$ = distance of the center of pressure of the pressure diagram *ACDE*, measured from the level of the dredge line.

Combining Eqs. (9.46) and (9.47) yields

$$D^2[4c - (\gamma L_1 + \gamma' L_2)] - 2DP_1 - \frac{P_1(P_1 + 12c\bar{z}_1)}{(\gamma L_1 + \gamma' L_2) + 2c} = 0 \tag{9.48}$$

Equation (9.48) may be solved to obtain D, the theoretical depth of penetration of the clay layer by the sheet pile.

Step-by-Step Procedure for Obtaining the Pressure Diagram

Step 1. Calculate $K_a = \tan^2(45 - \phi'/2)$ for the granular soil (backfill).
Step 2. Obtain σ_1' and σ_2'. [See Eqs. (9.1) and (9.2).]
Step 3. Calculate P_1 and $\bar{z}_1$.
Step 4. Use Eq. (9.48) to obtain the theoretical value of D.
Step 5. Using Eq. (9.46), calculate L_4.
Step 6. Calculate σ_6 and σ_7. [See Eqs. (9.42) and (9.45).]
Step 7. Draw the pressure distribution diagram as shown in Figure 9.12.
Step 8. The actual depth of penetration is

$$D_{\text{actual}} = 1.4 \text{ to } 1.6(D_{\text{theoretical}})$$

Maximum Bending Moment

According to Figure 9.12, the maximum moment (zero shear) will be between $L_1 + L_2 < z < L_1 + L_2 + L_3$. Using a new coordinate system z' (with $z' = 0$ at the dredge line) for zero shear gives

$$P_1 - \sigma_6 z' = 0$$

or

$$z' = \frac{P_1}{\sigma_6} \tag{9.49}$$

The magnitude of the maximum moment may now be obtained:

$$M_{max} = P_1(z' + \bar{z}_1) - \frac{\sigma_6 z'^2}{2} \tag{9.50}$$

Knowing the maximum bending moment, we determine the section modulus of the sheet pile section from Eq. (9.23).

Example 9.3

In Figure 9.13, for the sheet pile wall, determine

a. The theoretical and actual depth of penetration. Use $D_{actual} = 1.5D_{theory}$.
b. The minimum size of sheet pile section necessary. Use $\sigma_{all} = 172.5\ \text{MN/m}^2$.

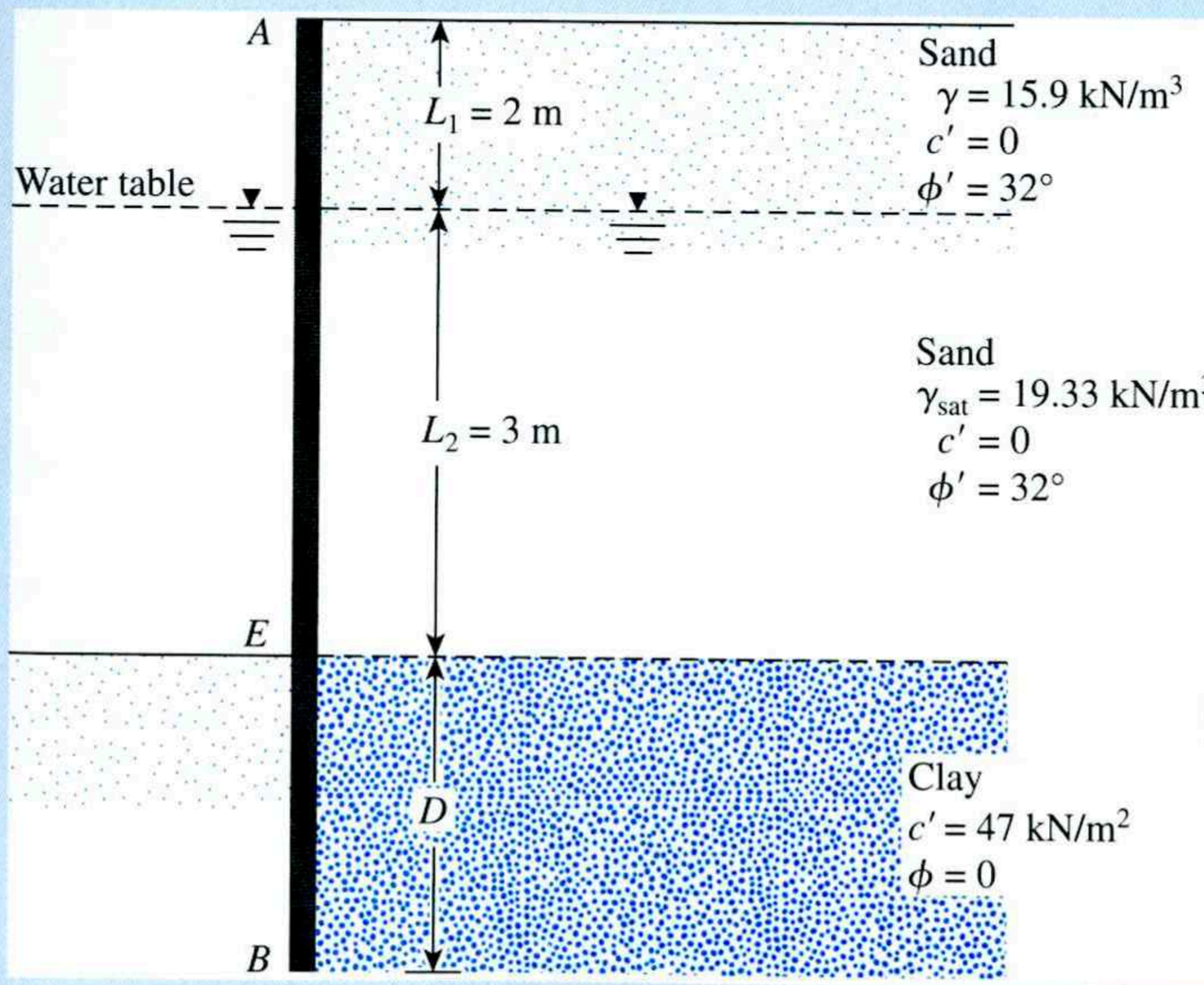

Figure 9.13 Cantilever sheet pile penetrating into saturated clay

Solution

We will follow the step-by-step procedure given in Section 9.6:

Step 1.

$$K_a = \tan^2\left(45 - \frac{\phi'}{2}\right) = \tan^2\left(45 - \frac{32}{2}\right) = 0.307$$

Step 2.

$$\sigma_1' = \gamma L_1 K_a = (15.9)(2)(0.307) = 9.763 \text{ kN/m}^2$$

$$\sigma_2' = (\gamma L_1 + \gamma' L_2)K_a = [(15.9)(2) + (19.33 - 9.81)3]0.307$$

$$= 18.53 \text{ kN/m}^2$$

Step 3. From the net pressure distribution diagram given in Figure 9.12, we have

$$P_1 = \frac{1}{2}\sigma_1' L_1 + \sigma_1' L_2 + \frac{1}{2}(\sigma_2' - \sigma_1')L_2$$

$$= 9.763 + 29.289 + 13.151 = 52.2 \text{ kN/m}$$

and

$$\bar{z}_1 = \frac{1}{52.2}\left[9.763\left(3 + \frac{2}{3}\right) + 29.289\left(\frac{3}{2}\right) + 13.151\left(\frac{3}{3}\right)\right]$$

$$= 1.78 \text{ m}$$

Step 4. From Eq. (9.48),

$$D^2[4c - (\gamma L_1 + \gamma' L_2)] - 2DP_1 - \frac{P_1(P_1 + 12c\bar{z}_1)}{(\gamma L_1 + \gamma' L_2) + 2c} = 0$$

Substituting proper values yields

$$D^2\{(4)(47) - [(2)(15.9) + (19.33 - 9.81)3]\} - 2D(52.2)$$

$$- \frac{52.2[52.2 + (12)(47)(1.78)]}{[(15.9)(2) + (19.33 - 9.81)3] + (2)(47)} = 0$$

or

$$127.64D^2 - 104.4D - 357.15 = 0$$

Solving the preceding equation, we obtain $D = 2.13$ m.

Step 5. From Eq. (9.46),

$$L_4 = \frac{D[4c - (\gamma L_1 + \gamma' L_2)] - P_1}{4c}$$

and

$$4c - (\gamma L_1 + \gamma' L_2) = (4)(47) - [(15.9)(2) + (19.33 - 9.81)3]$$

$$= 127.64 \text{ kN/m}^2$$

So,

$$L_4 = \frac{2.13(127.64) - 52.2}{(4)(47)} = 1.17 \text{ m}$$

Step 6.

$$\sigma_6 = 4c - (\gamma L_1 + \gamma' L_2) = 127.64 \text{ kN/m}^2$$

$$\sigma_7 = 4c + (\gamma L_1 + \gamma' L_2) = 248.36 \text{ kN/m}^2$$

Step 7. The net pressure distribution diagram can now be drawn, as shown in Figure 9.12.

Step 8. $D_{\text{actual}} \approx 1.5 D_{\text{theoretical}} = 1.5(2.13) \approx \mathbf{3.2\ m}$

Maximum-Moment Calculation

From Eq. (9.49),

$$z' = \frac{P_1}{\sigma_6} = \frac{52.2}{127.64} \approx 0.41 \text{ m}$$

Again, from Eq. (9.49),

$$M_{\max} = P_1(z' + \bar{z}_1) - \frac{\sigma_6 z'^2}{2}$$

So

$$M_{\max} = 52.2(0.41 + 1.78) - \frac{127.64(0.41)^2}{2}$$

$$= 114.32 - 10.73 = 103.59 \text{ kN-m/m}$$

The minimum required section modulus (assuming that $\sigma_{\text{all}} = 172.5 \text{ MN/m}^2$) is

$$S = \frac{103.59 \text{ kN-m/m}}{172.5 \times 10^3 \text{ kN/m}^2} = \mathbf{0.6 \times 10^{-3}\ m^3/m\ of\ the\ wall}$$

9.7 Special Cases for Cantilever Walls Penetrating Clay

Sheet Pile Wall in the Absence of Water Table

As in Section 9.5, relationships for special cases for cantilever walls penetrating clay may also be derived. Referring to Figure 9.14, we can write

$$\sigma_2' = \gamma L K_a \tag{9.51}$$

$$\sigma_6 = 4c - \gamma L \tag{9.52}$$

$$\sigma_7 = 4c + \gamma L \tag{9.53}$$

$$P_1 = \tfrac{1}{2} L \sigma_2' = \tfrac{1}{2} \gamma L^2 K_a \tag{9.54}$$

and

$$L_4 = \frac{D(4c - \gamma L) - \frac{1}{2}\gamma L^2 K_a}{4c} \tag{9.55}$$

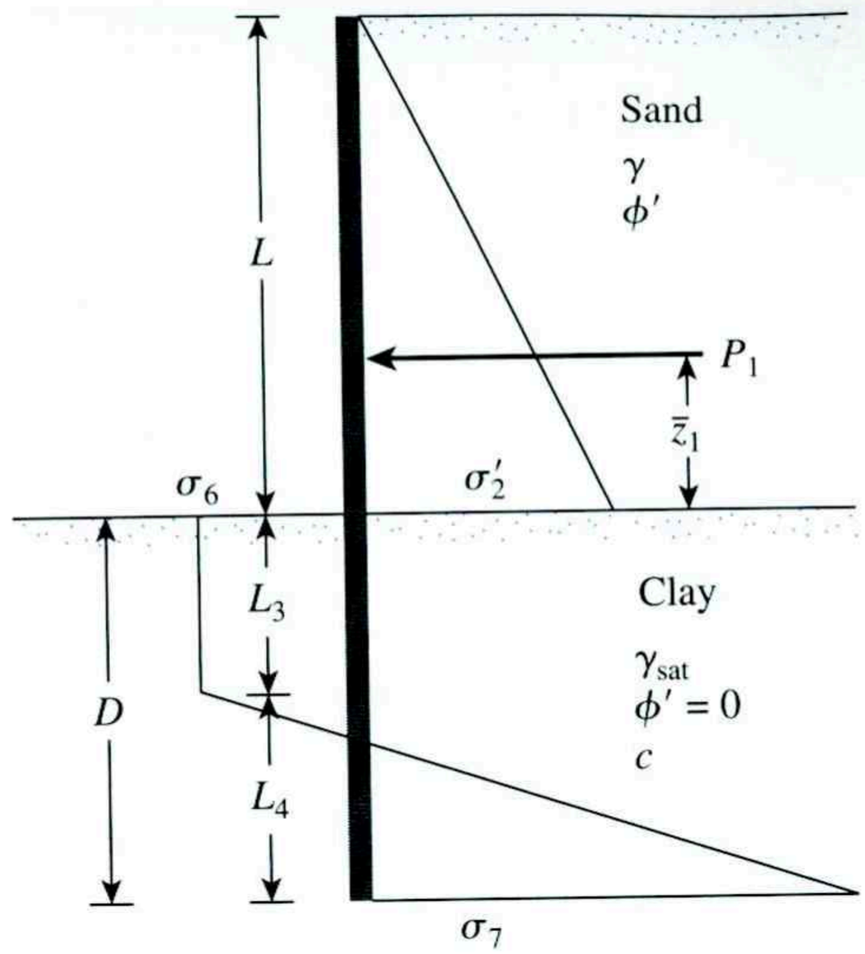

Figure 9.14 Sheet-pile wall penetrating clay

The theoretical depth of penetration, D, can be calculated [in a manner similar to the calculation of Eq. (9.48)] as

$$D^2(4c - \gamma L) - 2DP_1 - \frac{P_1(P_1 + 12c\bar{z}_1)}{\gamma L + 2c} = 0 \tag{9.56}$$

where $\bar{z}_1 = \dfrac{L}{3}$. (9.57)

The magnitude of the maximum moment in the wall is

$$M_{max} = P_1(z' + \bar{z}_1) - \frac{\sigma_6 z'^2}{2} \tag{9.58}$$

where $z' = \dfrac{P_1}{\sigma_6} = \dfrac{\frac{1}{2}\gamma L^2 K_a}{4c - \gamma L}$. (9.59)

Free Cantilever Sheet-Pile Wall Penetrating Clay

Figure 9.15 shows a free cantilever sheet-pile wall penetrating a clay layer. The wall is being subjected to a line load of P per unit length. For this case,

$$\sigma_6 = \sigma_7 = 4c \tag{9.60}$$

The depth of penetration, D, may be obtained from the relation

$$4D^2c - 2PD - \frac{P(P + 12cL)}{2c} = 0 \tag{9.61}$$

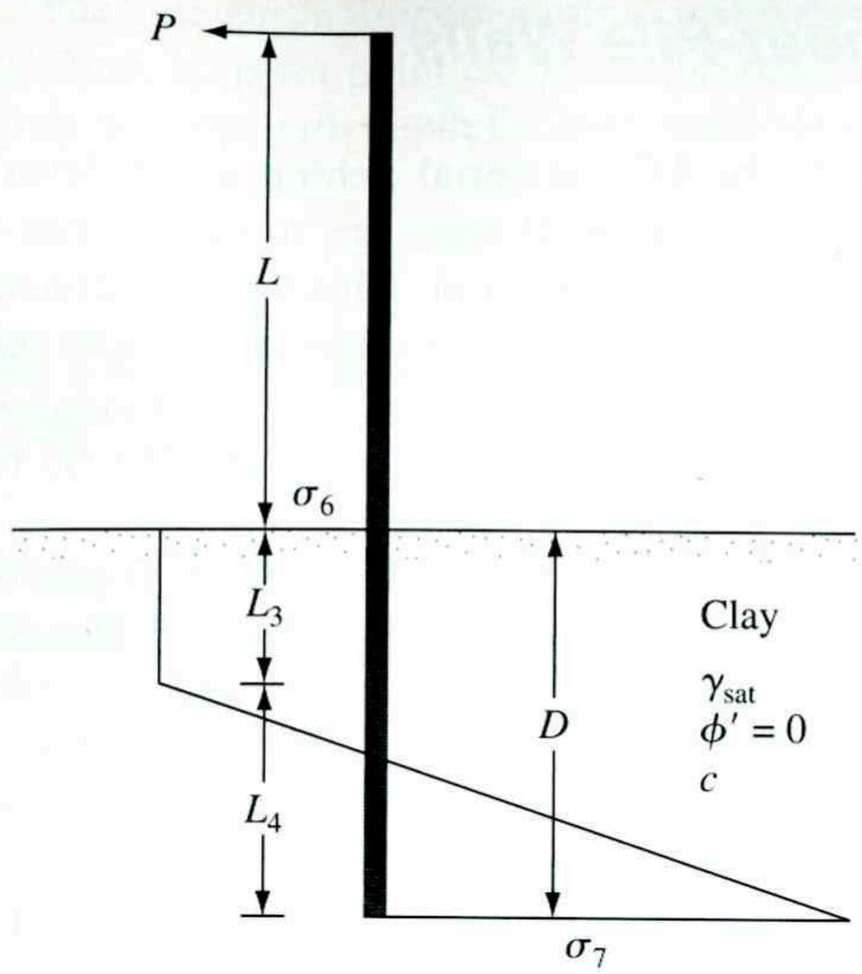

Figure 9.15 Free cantilever sheet piling penetrating clay

Also, note that, for a construction of the pressure diagram,

$$L_4 = \frac{4cD - P}{4c} \tag{9.62}$$

The maximum moment in the wall is

$$M_{max} = P(L + z') - \frac{4cz'^2}{2} \tag{9.63}$$

where $z' = \dfrac{P}{4c}$ (9.64)

Example 9.4

Refer to the free cantilever sheet-pile wall shown in Figure 9.15, for which $P = 32$ kN/m, $L = 3.5$ m, and $c = 12$ kN/m^2. Calculate the theoretical depth of penetration.

Solution

From Eq. (9.61),

$$4D^2c - 2PD - \frac{P(P + 12cL)}{2c} = 0$$

$$(4)(D^2)(12) - (2)(32)(D) - \frac{32[32 + (12)(12)(3.5)]}{(2)(12)} = 0$$

$$48D^2 - 64D - 714.7 = 0$$

Hence $D \approx$ **4.6 m**. ■

9.8 Anchored Sheet-Pile Walls

When the height of the backfill material behind a cantilever sheet-pile wall exceeds about 6 m (≈20 ft), tying the wall near the top to anchor plates, anchor walls, or anchor piles becomes more economical. This type of construction is referred to as *anchored sheet-pile wall* or an *anchored bulkhead.* Anchors minimize the depth of penetration required by the sheet piles and also reduce the cross-sectional area and weight of the sheet piles needed for construction. However, the tie rods and anchors must be carefully designed.

The two basic methods of designing anchored sheet-pile walls are (a) the *free earth support* method and (b) the *fixed earth support* method. Figure 9.16 shows the assumed nature of deflection of the sheet piles for the two methods.

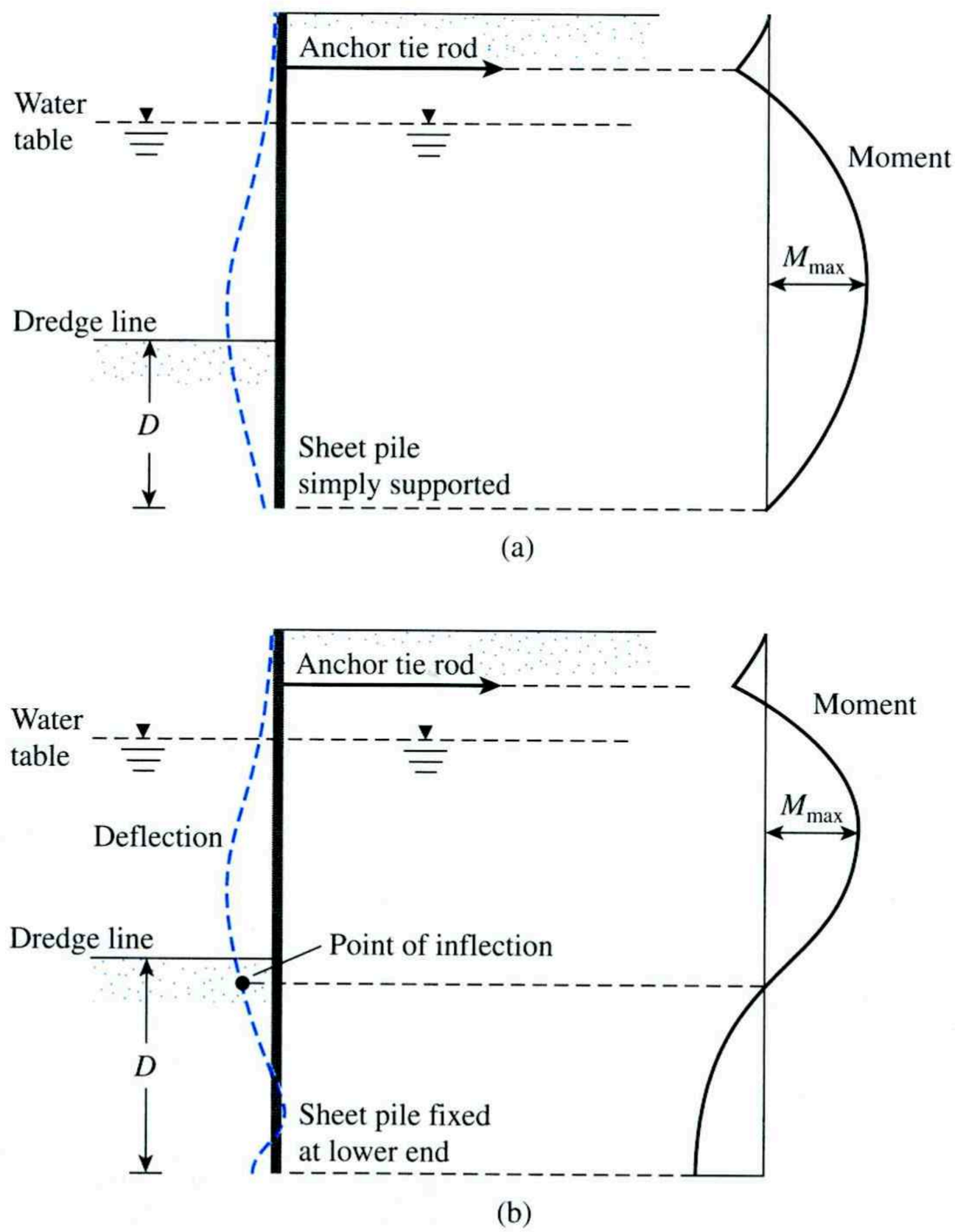

Figure 9.16 Nature of variation of deflection and moment for anchored sheet piles: (a) free earth support method; (b) fixed earth support method

The free earth support method involves a minimum penetration depth. Below the dredge line, no pivot point exists for the static system. The nature of the variation of the bending moment with depth for both methods is also shown in Figure 9.16. Note that

$$D_{\text{free earth}} < D_{\text{fixed earth}}$$

9.9 Free Earth Support Method for Penetration of Sandy Soil

Figure 9.17 shows an anchor sheet-pile wall with a granular soil backfill; the wall has been driven into a granular soil. The tie rod connecting the sheet pile and the anchor is located at a depth l_1 below the top of the sheet-pile wall.

The diagram of the net pressure distribution above the dredge line is similar to that shown in Figure 9.8. At depth $z = L_1, \sigma'_1 = \gamma L_1 K_a$, and at $z = L_1 + L_2, \sigma'_2 = (\gamma L_1 + \gamma' L_2) K_a$. Below the dredge line, the net pressure will be zero at $z = L_1 + L_2 + L_3$. The relation for L_3 is given by Eq. (9.6), or

$$L_3 = \frac{\sigma'_2}{\gamma'(K_p - K_a)}$$

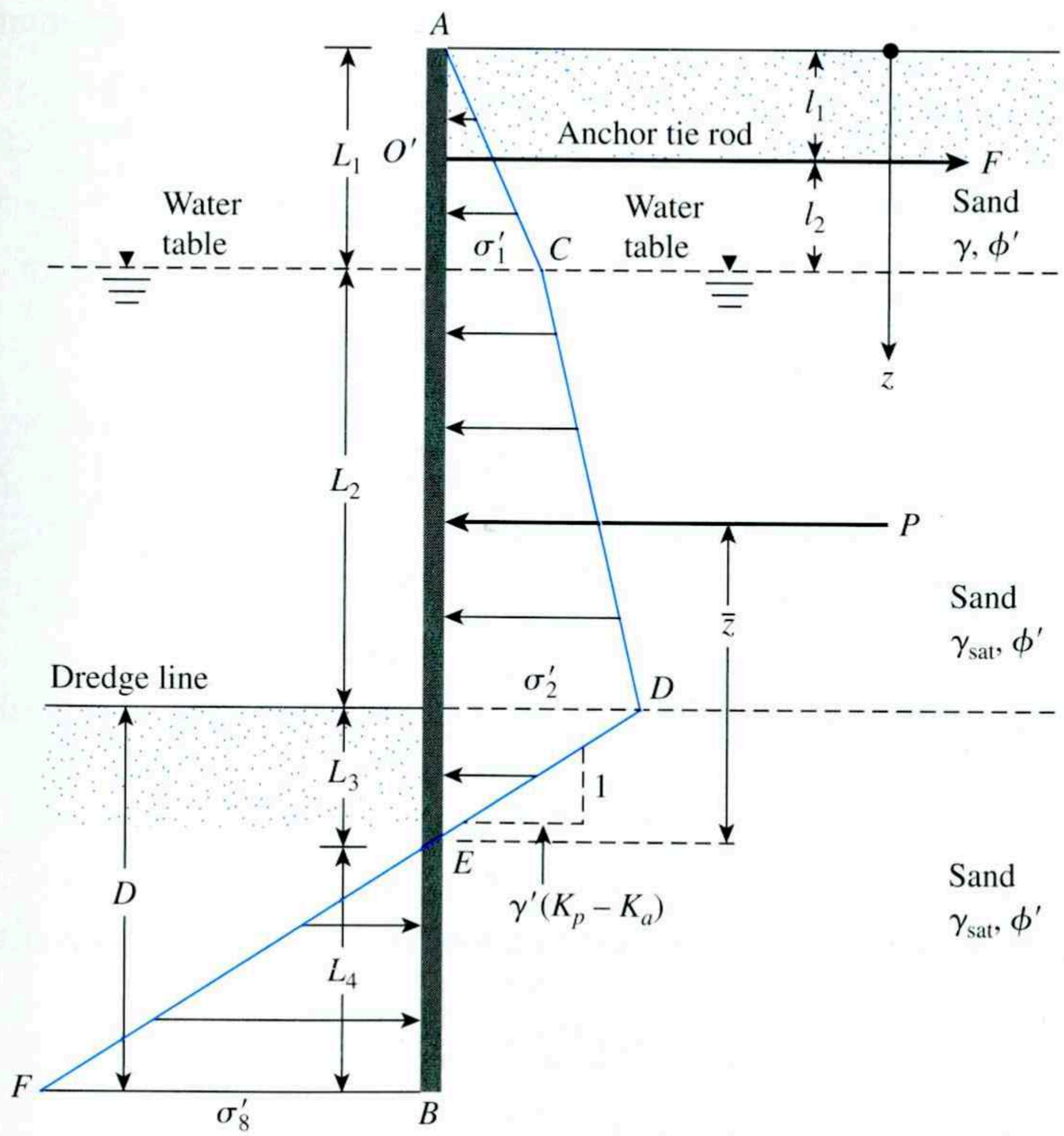

Figure 9.17 Anchored sheet-pile wall penetrating sand

At $z = L_1 + L_2 + L_3 + L_4$, the net pressure is given by

$$\sigma'_8 = \gamma'(K_p - K_a)L_4 \tag{9.65}$$

Note that the slope of the line DEF is 1 vertical to $\gamma'(K_p - K_a)$ horizontal.

For equilibrium of the sheet pile, Σ horizontal forces $= 0$, and Σ moment about $O' = 0$. (*Note:* Point O' is located at the level of the tie rod.)

Summing the forces in the horizontal direction (per unit length of the wall) gives

$$\text{Area of the pressure diagram } ACDE - \text{area of } EBF - F = 0$$

where F = tension in the tie rod/unit length of the wall, or

$$P - \tfrac{1}{2}\sigma'_8 L_4 - F = 0$$

or

$$F = P - \tfrac{1}{2}[\gamma'(K_p - K_a)]L_4^2 \tag{9.66}$$

where P = area of the pressure diagram $ACDE$. Now, taking the moment about point O' gives

$$-P[(L_1 + L_2 + L_3) - (\bar{z} + l_1)] + \tfrac{1}{2}[\gamma'(K_p - K_a)]L_4^2(l_2 + L_2 + L_3 + \tfrac{2}{3}L_4) = 0$$

or

$$L_4^3 + 1.5L_4^2(l_2 + L_2 + L_3) - \frac{3P[(L_1 + L_2 + L_3) - (\bar{z} + l_1)]}{\gamma'(K_p - K_a)} = 0 \tag{9.67}$$

Equation (9.67) may be solved by trial and error to determine the theoretical depth, L_4:

$$D_{\text{theoretical}} = L_3 + L_4$$

The theoretical depth is increased by about 30 to 40% for actual construction, or

$$D_{\text{actual}} = 1.3 \text{ to } 1.4 D_{\text{theoretical}} \tag{9.68}$$

The step-by-step procedure in Section 9.4 indicated that a factor of safety can be applied to K_p at the beginning [i.e., $K_{p(\text{design})} = K_p/\text{FS}$]. If that is done, there is no need to increase the theoretical depth by 30 to 40%. This approach is often more conservative.

The maximum theoretical moment to which the sheet pile will be subjected occurs at a depth between $z = L_1$ and $z = L_1 + L_2$. The depth z for zero shear and hence maximum moment may be evaluated from

$$\tfrac{1}{2}\sigma_1' L_1 - F + \sigma_1'(z - L_1) + \tfrac{1}{2}K_a\gamma'(z - L_1)^2 = 0 \tag{9.69}$$

Once the value of z is determined, the magnitude of the maximum moment is easily obtained.

Example 9.5

Let $L_1 = 3.05$ m, $L_2 = 6.1$ m, $l_1 = 1.53$ m, $l_2 = 1.52$ m, $c' = 0$, $\phi' = 30°$, $\gamma = 16$ kN/m^3, $\gamma_{sat} = 19.5$ kN/m^3, and $E = 207 \times 10^3$ MN/m^2 in Figure 9.17.

a. Determine the theoretical and actual depths of penetration. (*Note*: $D_{actual} = 1.3D_{theory}$.)
b. Find the anchor force per unit length of the wall.
c. Determine the maximum moment, M_{max}.

Solution

Part a

We use the following table.

Quantity required	Eq. no.	Equation and calculation
K_a	—	$\tan^2\left(45 - \frac{\phi'}{2}\right) = \tan^2\left(45 - \frac{30}{2}\right) = \frac{1}{3}$
K_P	—	$\tan^2\left(45 + \frac{\phi'}{2}\right) = \tan^2\left(45 + \frac{30}{2}\right) = 3$
$K_p - K_a$	—	$3 - 0.333 = 2.667$
γ'	—	$\gamma_{sat} - \gamma_w = 19.5 - 9.81 = 9.69$ kN/m^3
σ_1'	9.1	$\gamma L_1 K_a = (16)(3.05)(\frac{1}{3}) = 16.27$ kN/m^2
σ_2'	9.2	$(\gamma L_1 + \gamma' L_2)K_a = [(16)(3.05) + (9.69)(6.1)]\frac{1}{3} = 35.97$ kN/m^2
L_3	9.6	$\frac{\sigma_2'}{\gamma'(K_p - K_a)} = \frac{35.97}{(9.69)(2.667)} = 1.39$ m
P	—	$\frac{1}{2}\sigma_1' L_1 + \sigma_2' L_2 + \frac{1}{2}(\sigma_2' - \sigma_1')L_2 + \frac{1}{2}\sigma_2' L_3 = (\frac{1}{2})(16.27)(3.05) + (16.27)(6.1) + (\frac{1}{2})(35.97 - 16.27)(6.1) + (\frac{1}{2})(35.97)(1.39) = 24.81 + 99.25 + 60.01 + 25.0 = 209.07$ kN/m
$\bar{z}$	—	$\frac{\Sigma M_E}{P} = \left[(24.81)\left(1.39 + 6.1 + \frac{3.05}{3}\right) + (99.25)\left(1.39 + \frac{6.1}{2}\right) + (60.01)\left(1.39 + \frac{6.1}{3}\right) + (25.0)\left(\frac{2 \times 1.39}{3}\right)\right]\frac{1}{209.07} = 4.21$ m

L_4	9.67	$L_4^3 + 1.5L_4^2(l_2 + L_2 + L_3) - \dfrac{3P[(L_1 + L_2 + L_3) - (\bar{z} + l_1)]}{\gamma'(K_p - K_a)} = 0$
		$L_4^3 + 1.5L_4^2(1.52 + 6.1 + 1.39) - \dfrac{(3)(209.07)[(3.05 + 6.1 + 1.39) - (4.21 + 1.53)]}{(9.69)(2.667)} = 0$
		$L_4 = 2.7$ m
D_{theory}	—	$L_3 + L_4 = 1.39 + 2.7 = 4.09 \approx$ **4.1 m**
D_{actual}	—	$1.3D_{\text{theory}} = (1.3)(4.1) =$ **5.33 m**

Part b

The anchor force per unit length of the wall is

$$F = P - \tfrac{1}{2}\gamma'(K_p - K_a)L_4^2$$
$$= 209.07 - \left(\tfrac{1}{2}\right)(9.69)(2.667)(2.7)^2 = 114.87 \text{ kN/m} \approx \mathbf{115\ kN/m}$$

Part c

From Eq. (9.69), for zero shear,

$$\tfrac{1}{2}\sigma_1' L_1 - F + \sigma_1'(z - L_1) + \tfrac{1}{2}K_a\gamma'(z - L_1)^2 = 0$$

Let $z - L_1 = x$, so that

$$\tfrac{1}{2}\sigma_1' l_1 - F + \sigma_1' x + \tfrac{1}{2}K_a\gamma' x^2 = 0$$

or

$$\left(\tfrac{1}{2}\right)(16.27)(3.05) - 115 + (16.27)(x) + \left(\tfrac{1}{2}\right)\left(\tfrac{1}{3}\right)(9.69)x^2 = 0$$

giving $\quad x^2 + 10.07x - 55.84 = 0$

Now, $x = 4$ m and $z = x + L_1 = 4 + 3.05 = 7.05$ m. Taking the moment about the point of zero shear, we obtain

$$M_{\max} = -\frac{1}{2}\sigma_1' L_1\left(x + \frac{3.05}{3}\right) + F(x + 1.52) - \sigma_1'\frac{x^2}{2} - \frac{1}{2}K_a\gamma' x^2\left(\frac{x}{3}\right)$$

or

$$M_{\max} = -\left(\frac{1}{2}\right)(16.27)(3.05)\left(4 + \frac{3.05}{3}\right) + (115)(4 + 1.52) - (16.27)\left(\frac{4^2}{2}\right)$$
$$-\left(\frac{1}{2}\right)\left(\frac{1}{3}\right)(9.69)(4)^2\left(\frac{4}{3}\right) = \mathbf{344.9\ kN \cdot m/m}$$

9.10 Design Charts for Free Earth Support Method (Penetration into Sandy Soil)

Using the free earth support method, Hagerty and Nofal (1992) provided simplified design charts for quick estimation of the depth of penetration, D, anchor force, F, and maximum moment, M_{max}, for anchored sheet-pile walls penetrating into sandy soil, as shown in Figure 9.17. They made the following assumptions for their analysis.

a. The soil friction angle, ϕ', above and below the dredge line is the same.
b. The angle of friction between the sheet-pile wall and the soil is $\phi'/2$.
c. The passive earth pressure below the dredge line has a logarithmic spiral failure surface.
d. For active earth-pressure calculation, Coulomb's theory is valid.

The magnitudes of D, F, and M_{max} may be calculated from the following relationships:

$$\frac{D}{L_1 + L_2} = (GD)(CDL_1) \tag{9.70}$$

$$\frac{F}{\gamma_a(L_1 + L_2)^2} = (GF)(CFL_1) \tag{9.71}$$

$$\frac{M_{max}}{\gamma_a(L_1 + L_2)^3} = (GM)(CML_1) \tag{9.72}$$

where

$$\gamma_a = \text{average unit weight of soil} = \frac{\gamma L_1^2 + (\gamma_{sat} - \gamma_w)L_2^2 + 2\gamma L_1 L_2}{(L_1 + L_2)^2} \tag{9.73}$$

GD = generalized nondimensional embedment

$$= \frac{D}{L_1 + L_2} \quad (\text{for } L_1 = 0 \text{ and } L_2 = L_1 + L_2)$$

GF = generalized nondimensional anchor force

$$= \frac{F}{\gamma_a(L_1 + L_2)^2} \quad (\text{for } L_1 = 0 \text{ and } L_2 = L_1 + L_2)$$

GM = generalized nondimensional moment

$$= \frac{M_{max}}{\gamma_a (L_1 + L_2)^3} \quad (\text{for } L_1 = 0 \text{ and } L_2 = L_1 + L_2)$$

CDL_1, CFL_1, CML_1 = correction factors for $L_1 \neq 0$

The variations of GD, GF, GM, CDL_1, CFL_1, and CML_1 are shown in Figures 9.18, 9.19, 9.20, 9.21, 9.22, and 9.23, respectively.

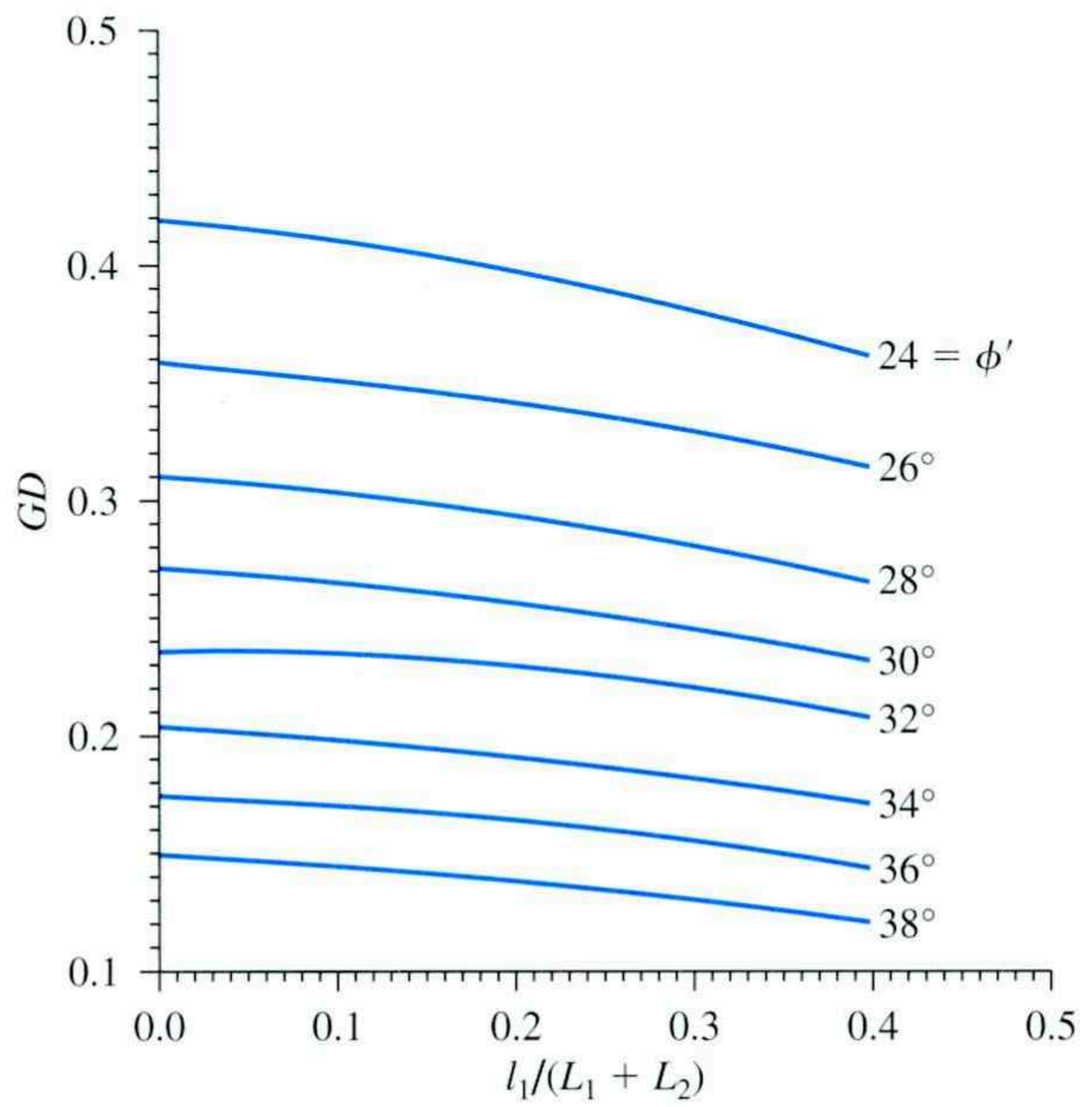

Figure 9.18 Variation of GD with $l_1/(L_1 + L_2)$ and ϕ' (Hagerty, D. J., and Nofal, M. M. (1992). "Design Aids: Anchored Bulkheads in Sand," *Canadian Geotechnical Journal*, Vol. 29, No. 5, pp. 789–795. © 2008 NRC Canada or its licensors. Reproduced with permission.)

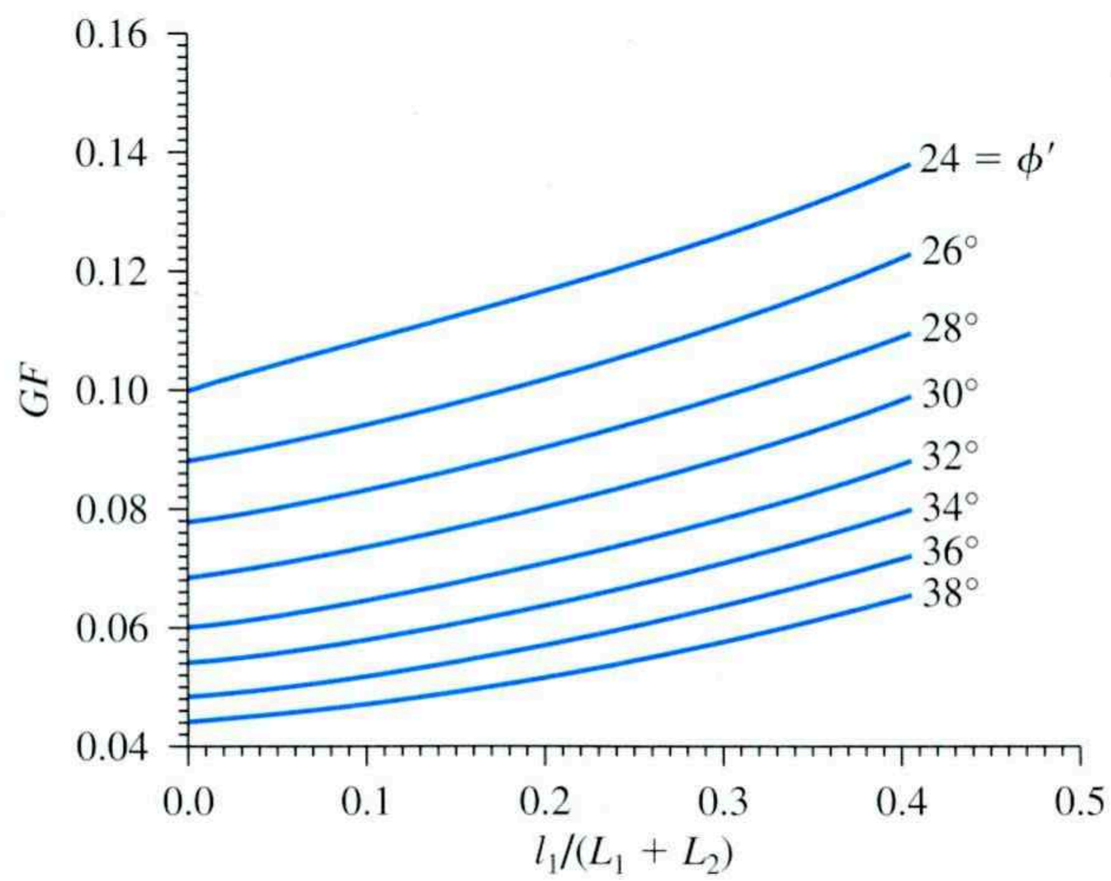

Figure 9.19 Variation of GF with $l_1/(L_1 + L_2)$ and ϕ' (After Hagerty and Nofal, 1992) (Hagerty, D. J., and Nofal, M. M. (1992). "Design Aids: Anchored Bulkheads in Sand," *Canadian Geotechnical Journal*, Vol. 29, No. 5, pp. 789-795. © 2008 NRC Canada or its licensors. Reproduced with permission.

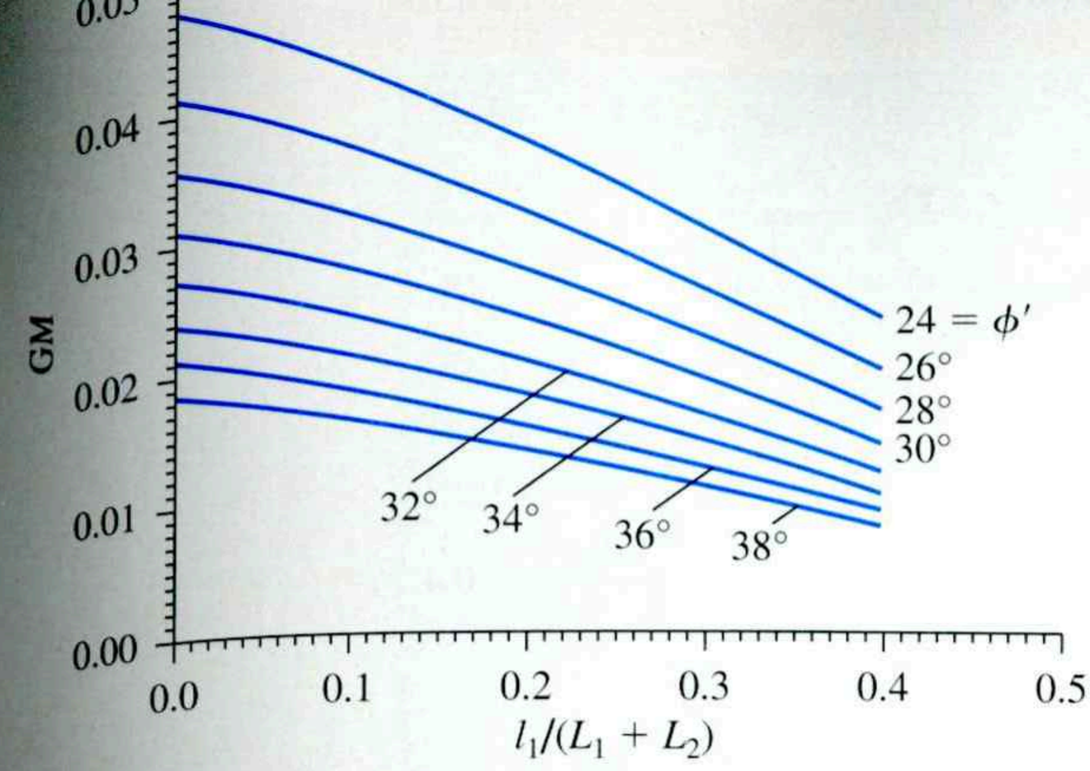

Figure 9.20 Variation of GM with $l_1/(L_1 + L_2)$ and ϕ' (Hagerty, D. J., and Nofal, M. M. (1992). "Design Aids: Anchored Bulkheads in Sand," *Canadian Geotechnical Journal*, Vol. 29, No. 5, pp. 789–795. © 2008 NRC Canada or its licensors. Reproduced with permission.)

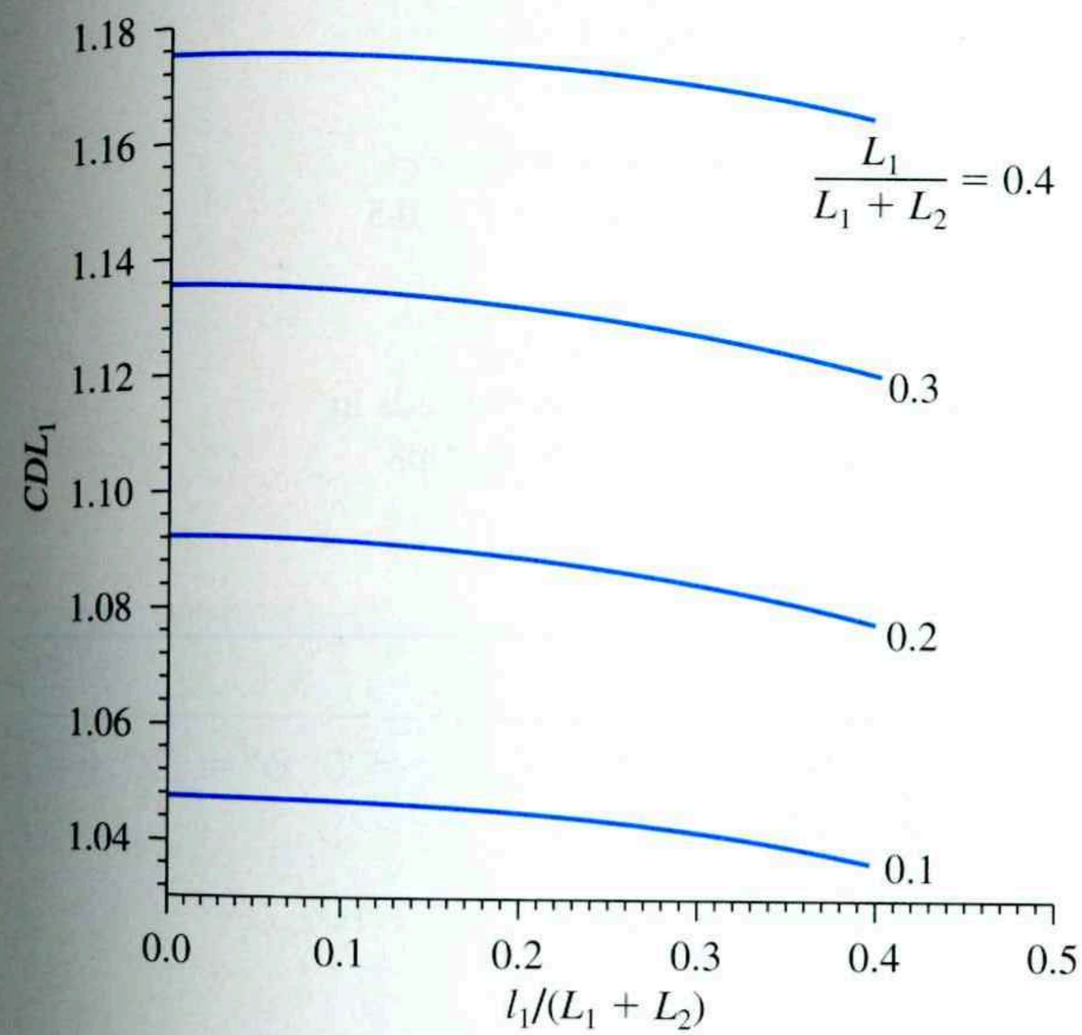

Figure 9.21 Variation of CDL_1 with $L_1/(L_1 + L_2)$ and $l_1/(L_1 + L_2)$ (Hagerty, D. J., and Nofal, M. M. (1992). "Design Aids: Anchored Bulkheads in Sand," *Canadian Geotechnical Journal*, Vol. 29, No. 5, pp. 789–795. © 2008 NRC Canada or its licensors. Reproduced with permission.)

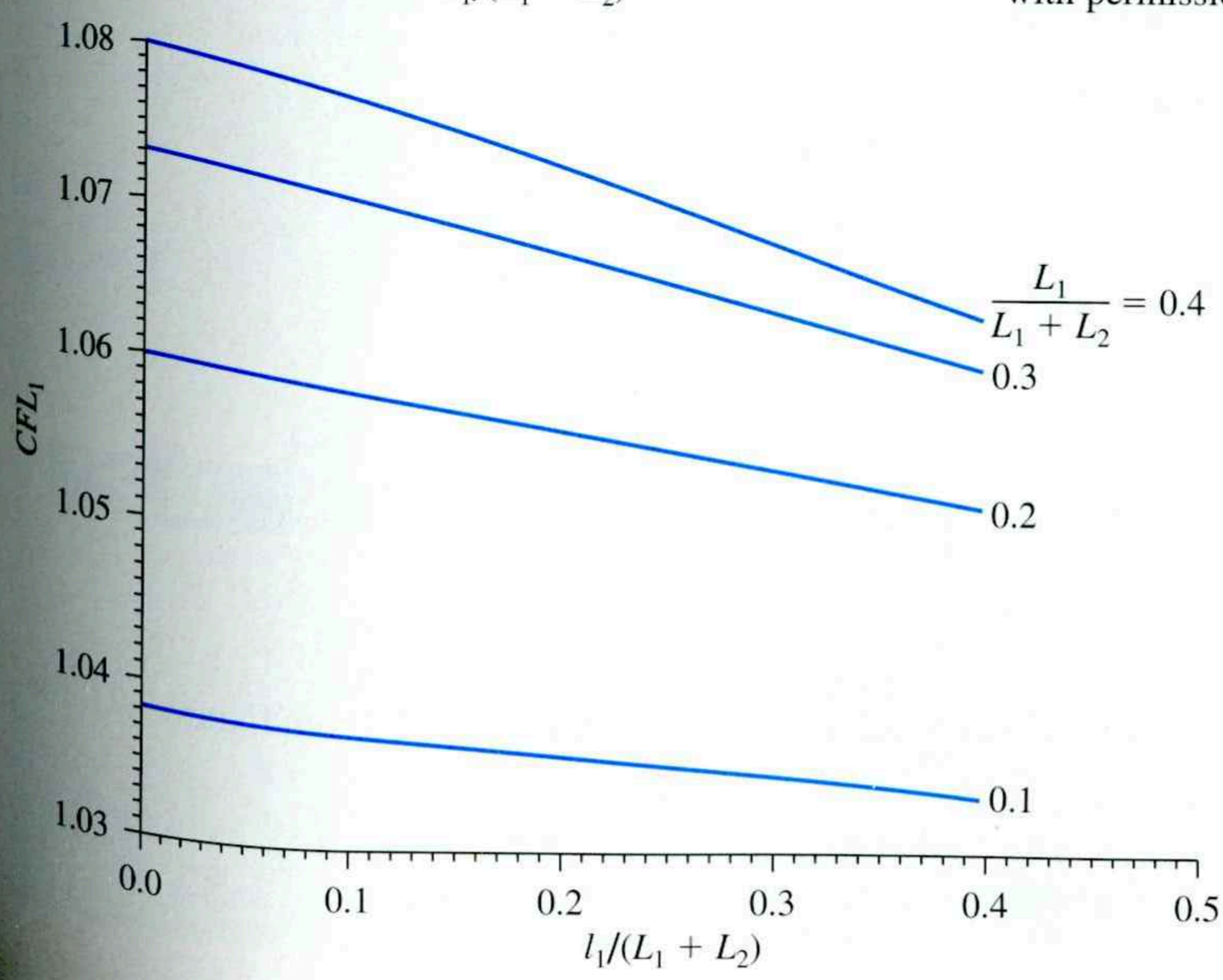

Figure 9.22 Variation of CFL_1 with $L_1/(L_1 + L_2)$ and $l_1/(L_1 + L_2)$ (Hagerty, D. J., and Nofal, M. M. (1992). "Design Aids: Anchored Bulkheads in Sand," *Canadian Geotechnical Journal*, Vol. 29, No. 5, pp. 789–795. © 2008 NRC Canada or its licensors. Reproduced with permission.)

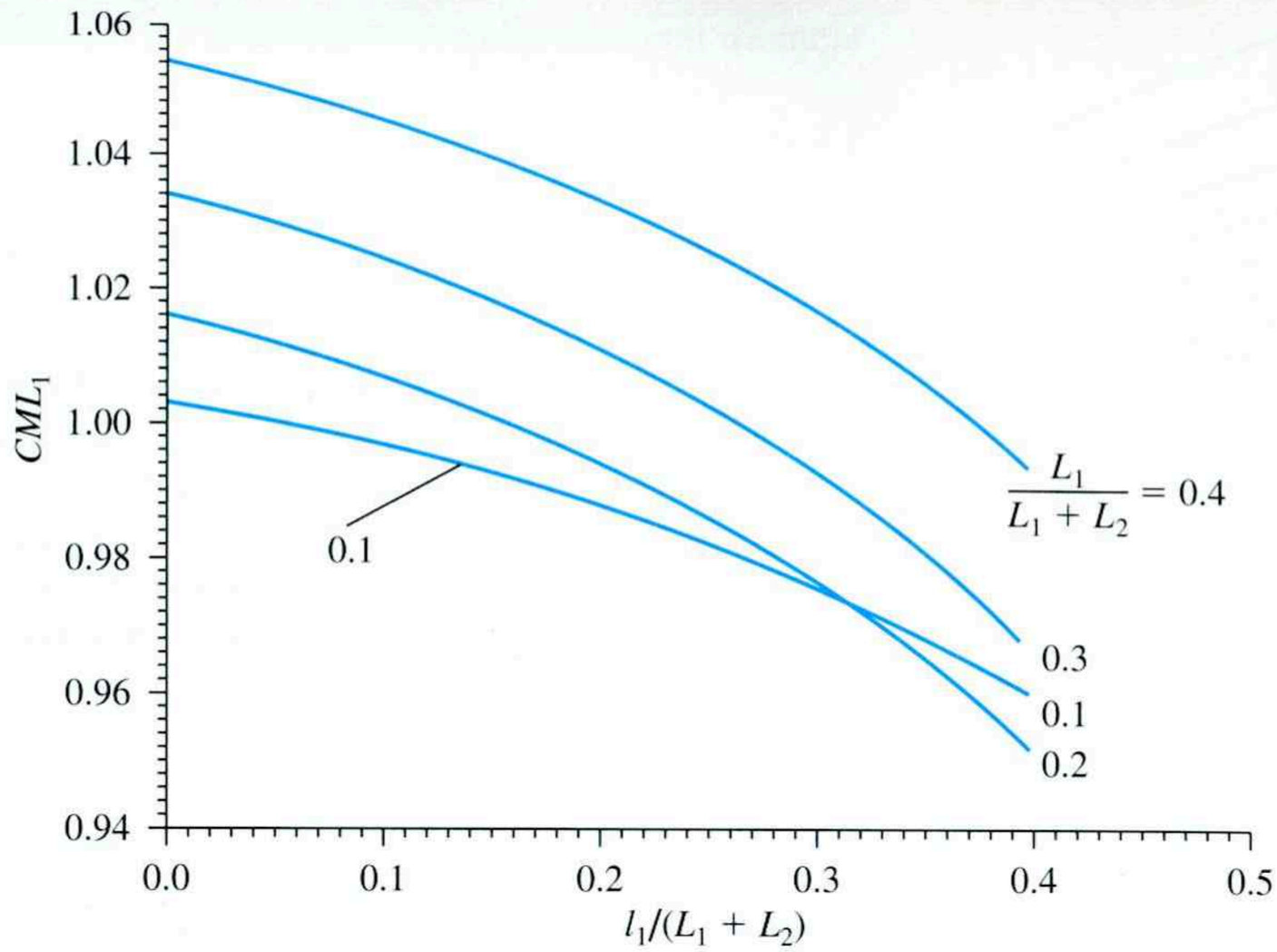

Figure 9.23 Variation of CML_1 with $L_1/(L_1 + L_2)$ and $l_1/(L_1 + L_2)$ (Hagerty, D. J., and Nofal, M. M. (1992). "Design Aids: Anchored Bulkheads in Sand," *Canadian Geotechnical Journal*, Vol. 29, No. 5, pp. 789–795. © 2008 NRC Canada or its licensors. Reproduced with permission.)

Example 9.6

Refer to Figure 9.17. Given: $L_1 = 2$ m, $L_2 = 3$ m, $l_1 = l_2 = 1$ m, $c = 0$, $\phi' = 32°$ $\gamma = 15.9$ kN/m^3, and $\gamma_{sat} = 19.33$ kN/m^3. Determine:

a. Theoretical and actual depth of penetration. *Note*: $D_{actual} = 1.4D_{theory}$.
b. Anchor force per unit length of wall.
c. Maximum moment, M_{max}.

Use the charts presented in Section 9.10.

Solution

Part a
From Eq. (9.70),

$$\frac{D}{L_1 + L_2} = (GD)(CDL_1)$$

$$\frac{l_1}{L_1 + L_2} = \frac{1}{2 + 3} = 0.2$$

From Figure 9.18 for $l_1/(L_1 + L_2) = 0.2$ and $\phi' = 32°$, $GD = 0.22$. From Figure 9.21, for

$$\frac{L_1}{L_1 + L_2} = \frac{2}{2 + 3} = 0.4 \qquad \text{and} \qquad \frac{l_1}{L_1 + L_2} = 0.2$$

$CDL_1 \approx 1.172$. So

$$D_{\text{theory}} = (L_1 + L_2)(GD)(CDL_1) = (5)(0.22)(1.172) \approx 1.3$$

$$D_{\text{actual}} \approx (1.4)(1.3) = 1.82 \approx \mathbf{2\ m}$$

Part b

From Figure 9.19 for $l_1/(L_1 + L_2) = 0.2$ and $\phi' = 32°$, $GF \approx 0.074$. Also, from Figure 9.22, for

$$\frac{L_1}{L_1 + L_2} = \frac{2}{2 + 3} = 0.4, \quad \frac{l_1}{L_1 + L_2} = 0.2, \quad \text{and} \quad \phi' = 32°$$

$CFL_1 = 1.073$. From Eq. (9.73),

$$\gamma_a = \frac{\gamma L_1^2 + \gamma' L_2^2 + 2\gamma L_1 L_2}{(L_1 + L_2)^2}$$

$$= \frac{(15.9)(2)^2 + (19.33 - 9.81)(3)^2 + (2)(15.9)(2)(3)}{(2 + 3)^2} = 13.6\ \text{kN/m}^3$$

Using Eq. (9.71) yields

$$F = \gamma_a(L_1 + L_2)^2(GF)(CFL_1) = (13.6)(5)^2(0.074)(1.073) \approx \mathbf{27\ kN/m}$$

Part c

From Figure 9.20, for $l_1/(L_1 + L_2) = 0.2$ and $\phi = 32°$, $GM = 0.021$. Also, from Figure 9.23, for

$$\frac{L_1}{L_1 + L_2} = \frac{2}{2 + 3} = 0.4, \quad \frac{l_1}{L_1 + L_2} = 0.2, \quad \text{and} \quad \phi' = 32°$$

$CML_1 = 1.036$. Hence from Eq. (9.72),

$$M_{\max} = \gamma_a(L_1 + L_2)^3(GM)(CML_1) = (13.6)(5)^3(0.021)(1.036) = \mathbf{36.99\ kN \cdot m/m}$$ ■

9.11 Moment Reduction for Anchored Sheet-Pile Walls

Sheet piles are flexible, and hence sheet-pile walls yield (i.e., become displaced laterally), which redistributes the lateral earth pressure. This change tends to reduce the maximum bending moment, $M_{\max}$, as calculated by the procedure outlined in Section 9.9. For that reason, Rowe (1952, 1957) suggested a procedure for reducing the maximum design moment on the sheet pile walls *obtained from the free earth support method.* This section discusses the procedure of moment reduction for sheet piles *penetrating into sand.*

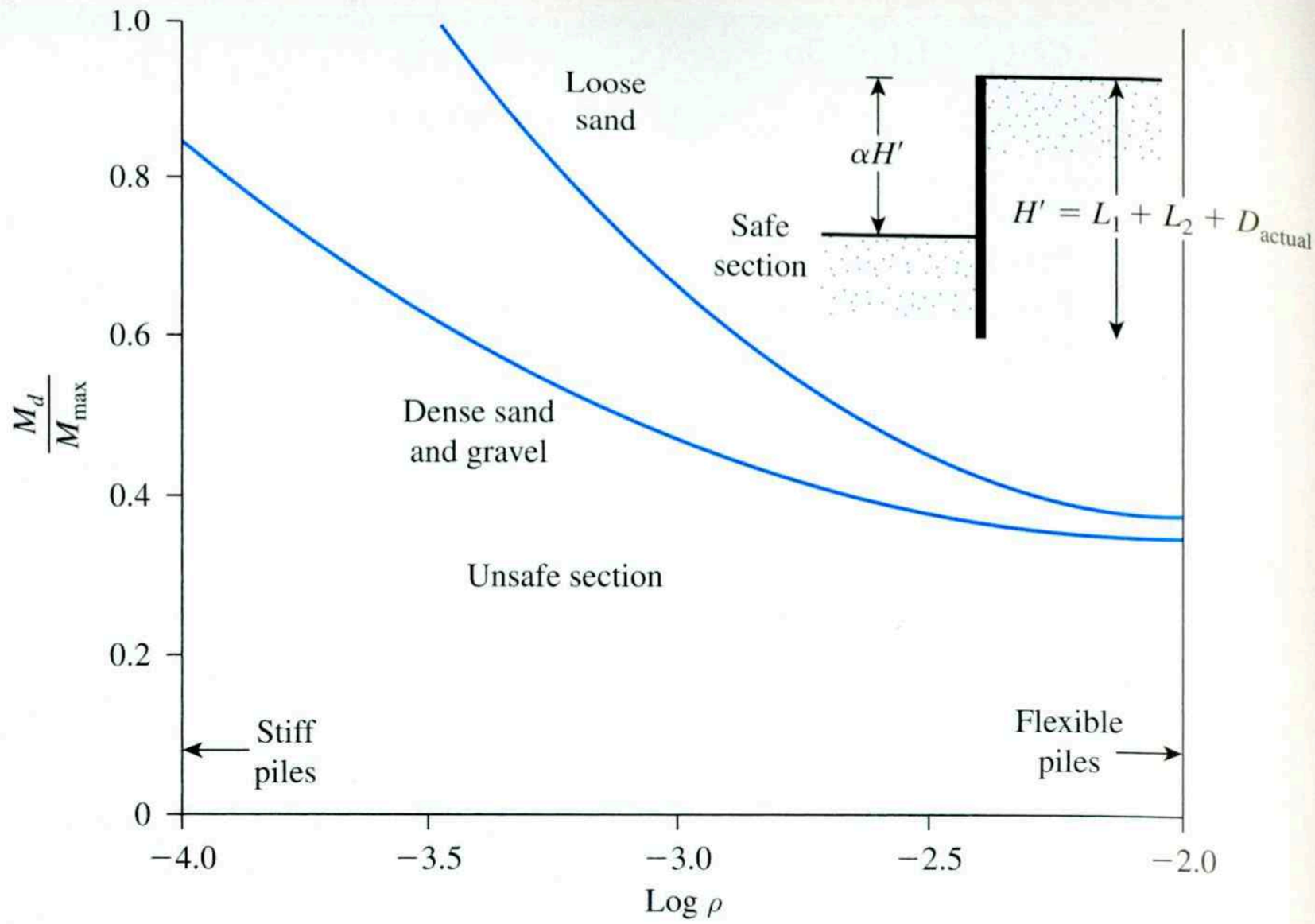

Figure 9.24 Plot of log ρ against M_d/M_{max} for sheet-pile walls penetrating sand (From Rowe, P. W. (1952). "Anchored Sheet Pile Walls," Proceedings, Institute of Civil Engineers, Vol. 1, Part 1, pp. 27–70.)

In Figure 9.24, which is valid for the case of a sheet pile penetrating sand, the following notation is used:

1. H' = total height of pile driven (i.e., $L_1 + L_2 + D_{actual}$)
2. Relative flexibility of pile $= \rho = 10.91 \times 10^{-7}\left(\frac{H'^4}{EI}\right)$ (9.74a)

   where

   H' is in meters
   E = modulus of elasticity of the pile material (MN/m^2)
   I = moment of inertia of the pile section per meter of the wall (m^4/m of wall)
3. M_d = design moment
4. M_{max} = maximum theoretical moment

In English units, Eq. (9.74a) takes the form

$$\rho = \frac{H'^4}{EI} \tag{9.74b}$$

where H' is in ft, E is in lb/in^2, and I is in in^4/ft of the wall.

The procedure for the use of the moment reduction diagram (see Figure 9.24) is as follows:

Step 1. Choose a sheet pile section (e.g., from among those given in Table 9.1).

Step 2. Find the modulus S of the selected section (Step 1) per unit length of the wall.

Step 3. Determine the moment of inertia of the section (Step 1) per unit length of the wall.

Step 4. Obtain H' and calculate ρ [see Eq. (9.74a) or Eq. (9.74b)].

Step 5. Find $\log \rho$.

Step 6. Find the moment capacity of the pile section chosen in Step 1 as $M_d = \sigma_{\text{all}} S$.

Step 7. Determine $M_d/M_{\max}$. Note that $M_{\max}$ is the maximum theoretical moment determined before.

Step 8. Plot $\log \rho$ (Step 5) and $M_d/M_{\max}$ in Figure 9.24.

Step 9. Repeat Steps 1 through 8 for several sections. The points that fall above the curve (in loose sand or dense sand, as the case may be) are *safe sections.*

The points that fall below the curve are *unsafe sections.* The cheapest section may now be chosen from those points which fall above the proper curve. Note that the section chosen will have an $M_d < M_{\max}$.

Example 9.7

Refer to Example 9.5. Use Rowe's moment reduction diagram (Figure 9.24) to find an appropriate sheet pile section. For the sheet pile, use $E = 207 \times 10^3\ \text{MN/m}^2$ and $\sigma_{\text{all}} = 172{,}500\ \text{kN/m}^2$.

Solution

$$H' = L_1 + L_2 + D_{\text{actual}} = 3.05 + 6.1 + 5.33 = 14.48\ \text{m}$$

$M_{\max} = 344.9\ \text{kN} \cdot \text{m/m}$. Now the following table can be prepared.

Section	$I(\text{m}^4/\text{m})$	$H'(\text{m})$	$\rho = 10.91 \times 10^{-7}\left(\frac{H'^4}{EI}\right)$	$\log \rho$	$S(\text{m}^3/\text{m})$	$M_d = S\sigma_{\text{all}}$ $(\text{kN} \cdot \text{m/m})$	$\frac{M_d}{M_{\max}}$
PZ-22	115.2×10^{-6}	14.48	20.11×10^{-4}	-2.7	97×10^{-5}	167.33	0.485
PZ-27	251.5×10^{-6}	14.48	9.21×10^{-4}	-3.04	162.3×10^{-5}	284.84	0.826

Figure 9.25 gives a plot of $M_d/M_{\max}$ versus ρ. It can be seen that **PZ-27** will be sufficient.

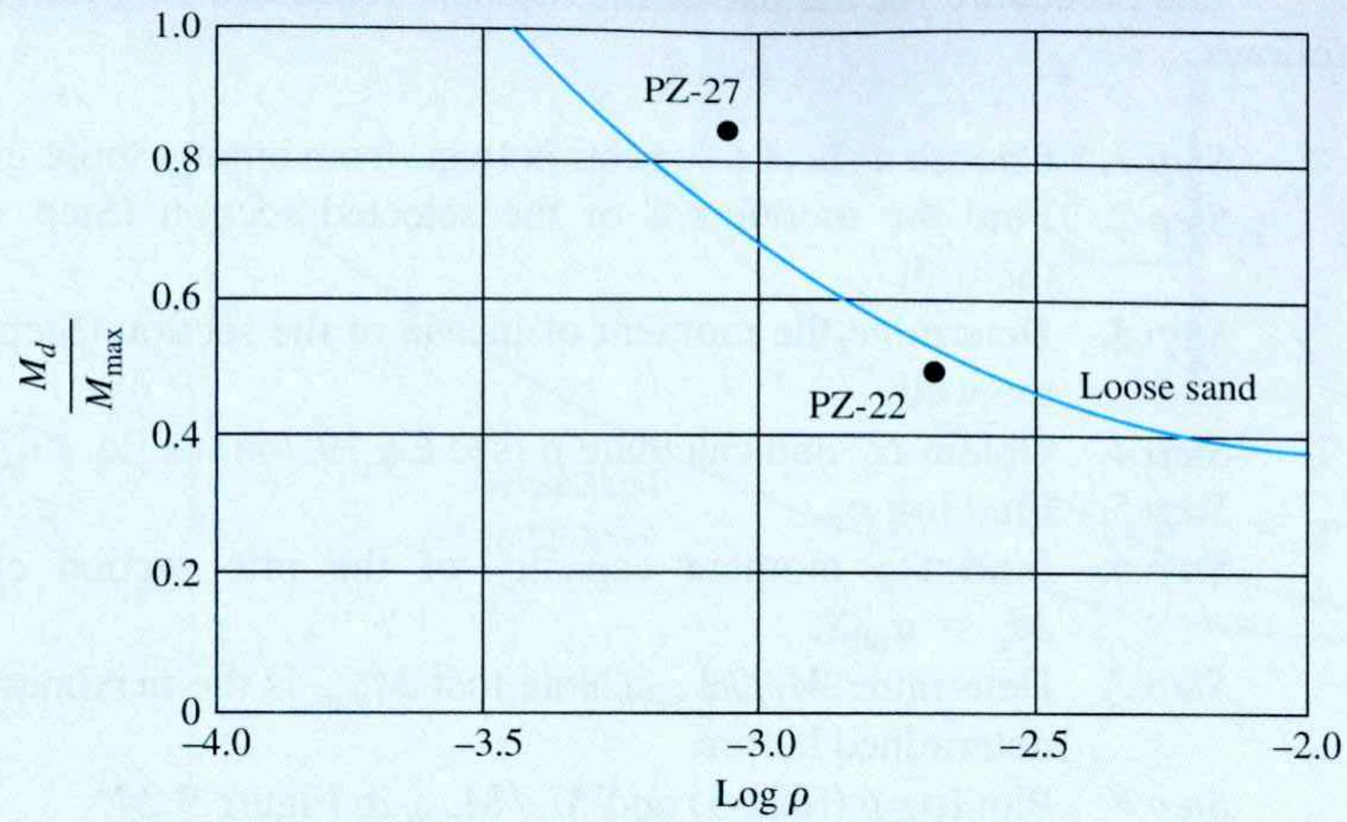

Figure 9.25 Plot of M_d/M_{max} versus log ρ

9.12 Computational Pressure Diagram Method for Penetration into Sandy Soil

The computational pressure diagram (CPD) method for sheet pile penetrating a sandy soil is a simplified method of design and an alternative to the free earth method described in Sections 9.9 and 9.11 (Nataraj and Hoadley, 1984). In this method, the net pressure diagram shown in Figure 9.17 is replaced by rectangular pressure diagrams, as in Figure 9.26. Note that $\overline{\sigma}'_a$ is the width of the net active pressure diagram above the dredge line and $\overline{\sigma}'_p$ is the width of the net passive pressure diagram below the dredge line. The magnitudes of $\overline{\sigma}'_a$ and $\overline{\sigma}'_p$ may respectively be expressed as

$$\overline{\sigma}'_a = CK_a\gamma'_{av}L \tag{9.75}$$

and

$$\overline{\sigma}'_p = RCK_a\gamma'_{av}L = R\overline{\sigma}'_a \tag{9.76}$$

where

$$\gamma'_{av} = \text{average effective unit weight of sand} \approx \frac{\gamma L_1 + \gamma' L_2}{L_1 + L_2} \tag{9.77}$$

C = coefficient

$$R = \text{coefficient} = \frac{L(L - 2l_1)}{D(2L + D - 2l_1)} \tag{9.78}$$

The range of values for C and R is given in Table 9.2.

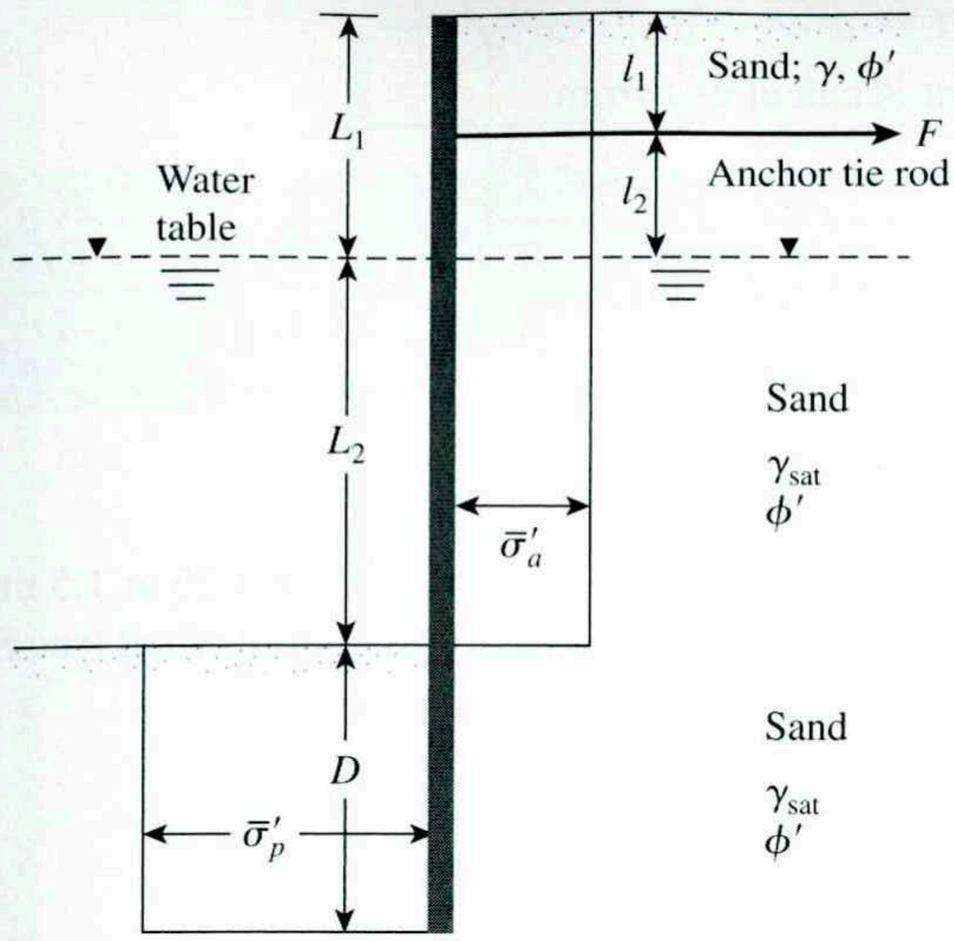

Figure 9.26 Computational pressure diagram method (*Note:* $L_1 + L_2 = L$)

Table 9.2 Range of Values for C and R [from Eqs. (9.75) and (9.76)]

Soil type	C[a]	R
Loose sand	0.8–0.85	0.3–0.5
Medium sand	0.7–0.75	0.55–0.65
Dense sand	0.55–0.65	0.60–0.75

[a] Valid for the case in which there is no surcharge above the granular backfill (i.e., on the right side of the wall, as shown in Figure 9.26)

The depth of penetration, D, anchor force per unit length of the wall, F, and maximum moment in the wall, M_{max}, are obtained from the following relationships.

Depth of Penetration

For the depth of penetration, we have

$$D^2 + 2DL\left[1 - \left(\frac{l_1}{L}\right)\right] - \left(\frac{L^2}{R}\right)\left[1 - 2\left(\frac{l_1}{L}\right)\right] = 0 \tag{9.79}$$

Anchor Force

The anchor force is

$$F = \bar{\sigma}'_a(L - RD) \tag{9.80}$$

Maximum Moment

The maximum moment is calculated from

$$M_{\max} = 0.5\overline{\sigma}'_a L^2\left[\left(1 - \frac{RD}{L}\right)^2 - \left(\frac{2l_1}{L}\right)\left(1 - \frac{RD}{L}\right)\right] \tag{9.81}$$

Note the following qualifications:

1. The magnitude of D obtained from Eq. (9.79) is about 1.25 to 1.5 times the value of D_{theory} obtained by the conventional free earth support method (see Section 9.9), so

$$\underset{\text{Eq. (9.79)}}{\underset{\uparrow}{D}} \approx \underset{\text{Eq. (9.68)}}{\underset{\uparrow}{D_{\text{actual}}}}$$

2. The magnitude of F obtained by using Eq. (9.80) is about 1.2 to 1.6 times the value obtained by using Eq. (9.66). Thus, an additional factor of safety for the actual design of anchors need not be used.
3. The magnitude of $M_{\max}$ obtained from Eq. (9.81) is about 0.6 to 0.75 times the value of $M_{\max}$ obtained by the conventional free earth support method. Hence, the former value of $M_{\max}$ can be used as the actual design value, and Rowe's moment reduction need not be applied.

Example 9.8

For the anchored sheet pile wall shown in Figure 9.27, determine (a) D, (b) F, and (c) $M_{\max}$. Use the CPD method; assume that $C = 0.68$ and $R = 0.6$.

Solution

Part a

$$\gamma' = \gamma_{\text{sat}} - \gamma_w = 19.24 - 9.81 = 9.43 \text{ kN/m}^3$$

From Eq. (9.77)

$$\gamma'_{\text{av}} = \frac{\gamma L_1 + \gamma' L_2}{L_1 + L_2} = \frac{(17.3)(3) + (9.43)(6)}{3 + 6} = 12.05 \text{ kN/m}^3$$

$$K_a = \tan^2\left(45 - \frac{\phi'}{2}\right) = \tan^2\left(45 - \frac{35}{2}\right) = 0.271$$

$$\overline{\sigma}'_a = CK_a\gamma'_{\text{av}} L = (0.68)(0.271)(12.05)(9) = 19.99 \text{ kN/m}^2$$

$$\overline{\sigma}'_p = R\overline{\sigma}'_a = (0.6)(19.99) = 11.99 \text{ kN/m}^2$$

From Eq. (9.80)

$$D^2 + 2DL\left[1 - \left(\frac{l_1}{L}\right)\right] - \frac{L^2}{R}\left[1 - 2\left(\frac{l_1}{L}\right)\right] = 0$$

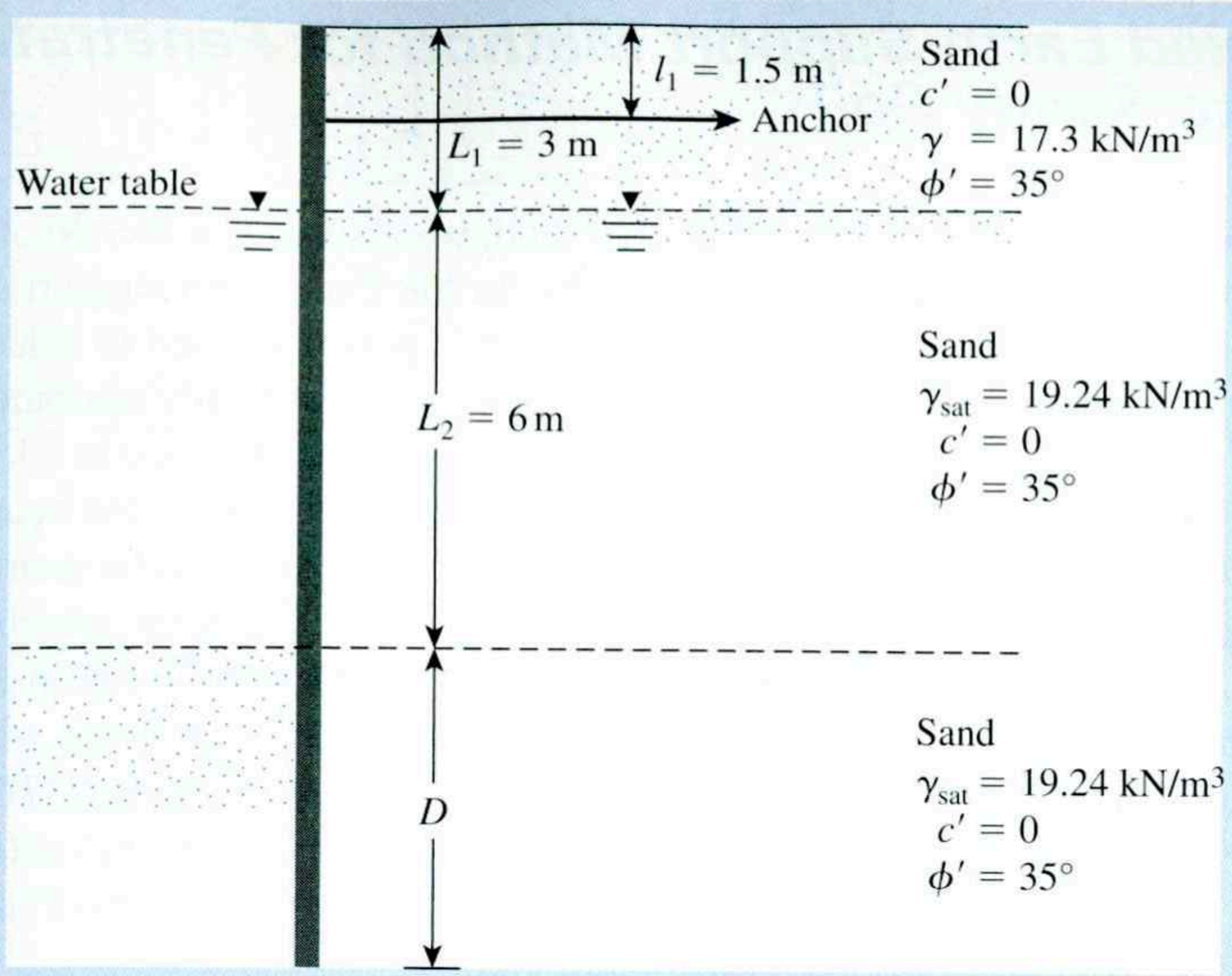

Figure 9.27

or

$$D^2 + 2(D)(9)\left[1 - \left(\frac{1.5}{9}\right)\right] - \frac{(9)^2}{0.6}\left[1 - 2\left(\frac{1.5}{9}\right)\right] = D^2 + 50D - 1000 = 0$$

Hence $D \approx$ **4.6 m.**

Check for the assumption of R:

$$R = \frac{L(L - 2l_1)}{D(2L + D - 2l_1)} = \frac{9[9 - (2)(1.5)]}{4.6[(2)(9) + 4.6 - (2)(1.5)]} \approx \mathbf{0.6—OK}$$

Part b

From Eq. (9.80)

$$F = \overline{\sigma}'_a(L - RD) = 19.99[9 - (0.6)(4.6)] = \mathbf{124.74\ kN/m}$$

Part c

From Eq. (9.81)

$$M_{max} = 0.5\overline{\sigma}'_a L^2\left[\left(1 - \frac{RD}{L}\right)^2 - \left(\frac{2l_1}{L}\right)\left(1 - \frac{RD}{L}\right)\right]$$

$$1 - \frac{RD}{L} = 1 - \frac{(0.6)(4.6)}{9} = 0.693$$

So,

$$M_{max} = (0.5)(19.99)(9)^2\left[(0.693)^2 - \frac{(2)(1.5)(0.693)}{9}\right] = \mathbf{201.6\ kN\text{-}m/m}$$

9.13 Fixed Earth-Support Method for Penetration into Sandy Soil

When using the fixed earth support method, we assume that the toe of the pile is restrained from rotating, as shown in Figure 9.28a. In the fixed earth support solution, a simplified method called the *equivalent beam solution* is generally used to calculate L_3 and, thus, D. The development of the equivalent beam method is generally attributed to Blum (1931).

In order to understand this method, compare the sheet pile to a loaded cantilever beam *RSTU*, as shown in Figure 9.29. Note that the support at T for the beam is equivalent to the *anchor load reaction* (F) on the sheet pile (Figure 9.28). It can be seen that the point S of the beam *RSTU* is the inflection point of the elastic line of the beam, which is equivalent to point I in Figure 9.28. It the beam is cut at S and a free support (reaction P_s) is provided at that point, the bending moment diagram for portion *STU* of the beam will remain unchanged. This beam *STU* will be equivalent to the section *STU* of the beam *RSTU*. The force P' shown in Figure 9.28a at I will be equivalent to the reaction P_s on the beam (Figure 9.29).

The following is an approximate procedure for the design of an anchored sheet-pile wall (Cornfield, 1975). Refer to Figure 9.28.

Step 1. Determine L_5, which is a function of the soil friction angle ϕ' below the dredge line, from the following:

ϕ' (deg)	$\dfrac{L_5}{L_1 + L_2}$
30	0.08
35	0.03
40	0

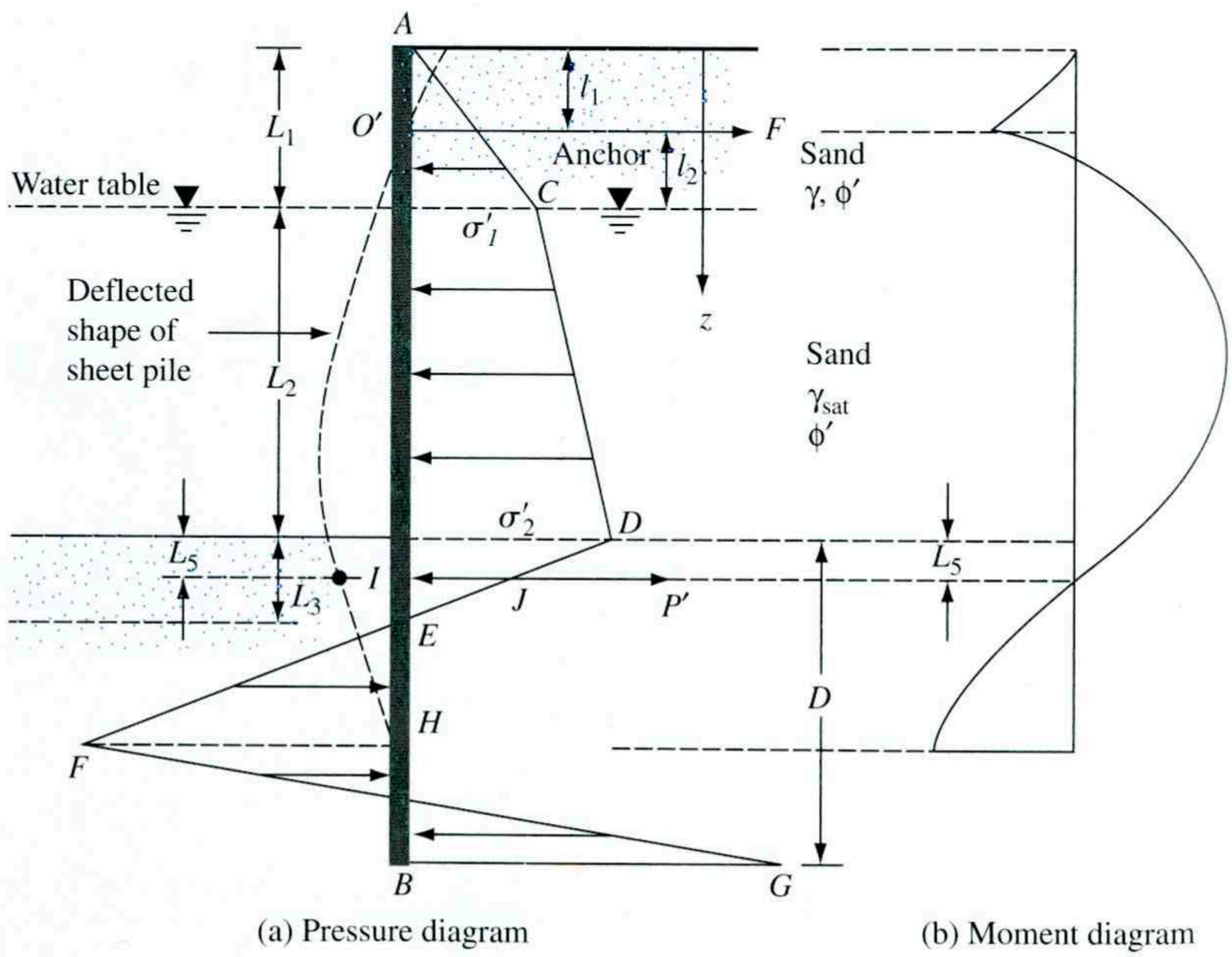

FIGURE 9.28 Fixed earth support method for penetration of sandy soil

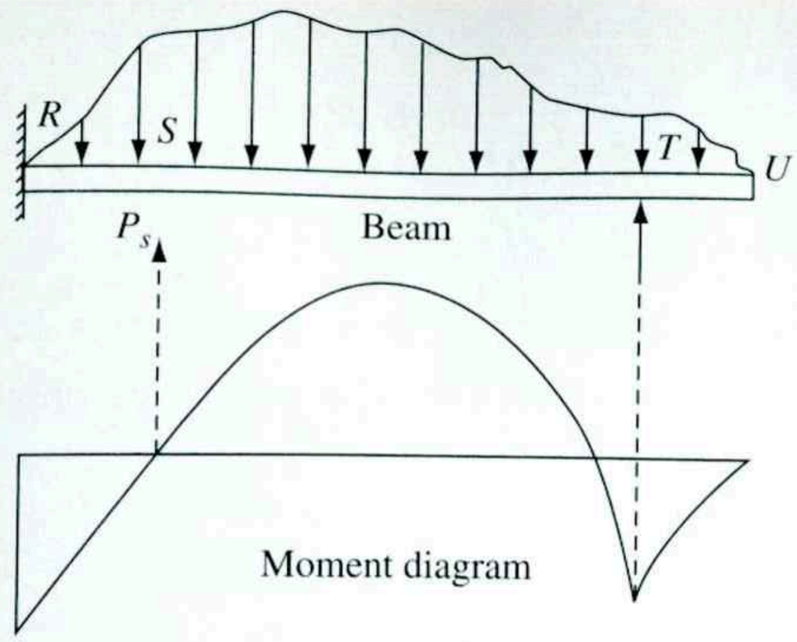

Figure 9.29 Equivalent cantilever beam concept

Step 2. Calculate the span of the equivalent beam as $l_2 + L_2 + L_5 = L'$.

Step 3. Calculate the total load of the span, W. This is the area of the pressure diagram between O' and I.

Step 4. Calculate the maximum moment, M_{max}, as $WL'/8$.

Step 5. Calculate P' by taking the moment about O', or

$$P' = \frac{1}{L'}\,(\text{moment of area } ACDJI \text{ about } O') \tag{9.82}$$

Step 6. Calculate D as

$$D = L_5 + 1.2\sqrt{\frac{6P'}{(K_p - K_a)\gamma'}} \tag{9.83}$$

Step 7. Calculate the anchor force per unit length, F, by taking the moment about I, or

$$F = \frac{1}{L'}\,(\text{moment of area } ACDJI \text{ about } I)$$

Example 9.9

Consider the anchored sheet-pile structure described in Example 9.5. Using the equivalent beam method described in Section 9.13, determine

a. Maximum moment
b. Theoretical depth of penetration
c. Anchor force per unit length of the structure

Solution

Part a

Determination of L_5: For $\phi' = 30°$,

$$\frac{L_5}{L_1 + L_2} = 0.08$$

$$\frac{L_5}{3.05 + 6.1} = 0.08$$

$$L_5 = 0.73$$

Net Pressure Diagram: From Example 9.5, $K_a = \frac{1}{3}$, $K_p = 3$, $\gamma = 16$ kN/m^3, $\gamma' = 9.69$ kN/m^3, $\sigma_1' = 16.27$ kN/m^2, $\sigma_2' = 35.97$ kN/m^2. The net active pressure at a depth L_5 below the dredge line can be calculated as

$$\sigma_2' - \gamma'(K_p - K_a)L_5 = 35.97 - (9.69)(3 - 0.333)(0.73) = 17.1 \text{ kN/m}^2$$

The net pressure diagram from $z = 0$ to $z = L_1 + L_2 + L_5$ is shown in Figure 9.30.

Maximum Moment:

$$W = \left(\frac{1}{2}\right)(8.16 + 16.27)(1.52) + \left(\frac{1}{2}\right)(6.1)(16.27 + 35.97)$$

$$+ \left(\frac{1}{2}\right)(0.73)(35.97 + 17.1)$$

$$= 197.2 \text{ kN/m}$$

$$L' = l_2 + L_2 + L_5 = 1.52 + 6.1 + 0.73 = 8.35 \text{ m}$$

$$M_{\max} = \frac{WL'}{8} = \frac{(197.2)(8.35)}{8} = \mathbf{205.8\ kN \cdot m/m}$$

Part b

$$P' = \frac{1}{L'}(\text{moment of area } ACDJI \text{ about } O')$$

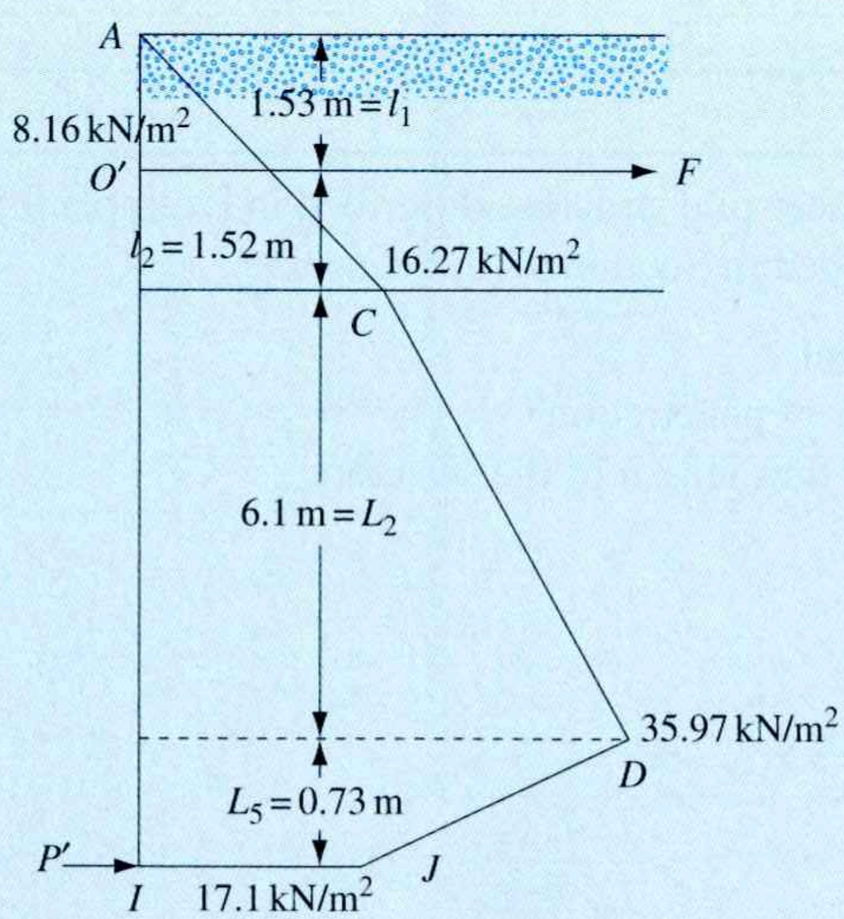

FIGURE 9.30

$$P' = \frac{1}{8.35}\left[\begin{array}{l}\left(\frac{1}{2}\right)(16.27)(3.05)\left(\frac{2}{3}\times 3.05 - 1.53\right) + (16.27)(6.1)\left(1.52 + \frac{6.1}{2}\right) \\ + \left(\frac{1}{2}\right)(6.1)(35.97 - 16.27)\left(1.52 + \frac{2}{3}\times 6.1\right) + \left(\frac{1}{2}\right)(35.97 + 17.1) \\ \times (0.73)\left(1.52 + 6.1 + \frac{0.73}{2}\right)\end{array}\right]$$

↑
Approximate

$= 114.48$ kN/m

From Eq. (9.83)

$$D = L_5 + 1.2\sqrt{\frac{6P'}{(K_p - K_a)\gamma'}} = 0.73 + 1.2\sqrt{\frac{(6)(114.48)}{(3 - 0.333)(9.69)}} = \mathbf{6.92\ m}$$

Part c

Taking the moment about I (Figure 9.30)

$$F = \frac{1}{8.35}\left[\begin{array}{l}\left(\frac{1}{2}(16.27)(3.05)\left(0.73 + 6.1 + \frac{3.05}{3}\right) + (16.27)(6.1)\left(0.73 + \frac{6.1}{2}\right)\right. \\ \left. + \left(\frac{1}{2}\right)(6.1)(35.97 - 16.27)\left(0.73 + \frac{6.1}{3}\right) + \left(\frac{1}{2}\right)(35.97 + 17.1)(0.73)\left(\frac{0.73}{2}\right)\right]\end{array}$$

↑
Approximate

$= \mathbf{88.95\ kN/m}$ ■

9.14 Field Observations for Anchor Sheet Pile Walls

In the preceding sections, large factors of safety were used for the depth of penetration, D. In most cases, designers use smaller magnitudes of soil friction angle, ϕ', thereby ensuring a built-in factor of safety for the active earth pressure. This procedure is followed primarily because of the uncertainties involved in predicting the actual earth pressure to which a sheet-pile wall in the field will be subjected. In addition, Casagrande (1973) observed that, if the soil behind the sheet-pile wall has grain sizes that are predominantly smaller than those of coarse sand, the active earth pressure after construction sometimes increases to an at-rest earth-pressure condition. Such an increase causes a large increase in the anchor force, F. The following two case histories are given by Casagrande (1973).

Bulkhead of Pier C—Long Beach Harbor, California (1949)

A typical cross section of the Pier C bulkhead of the Long Beach harbor is shown in Figure 9.31. Except for a rockfill dike constructed with 76 mm (3 in.) maximum-size quarry wastes, the backfill of the sheet-pile wall consisted of fine sand. Figure 9.32 shows the

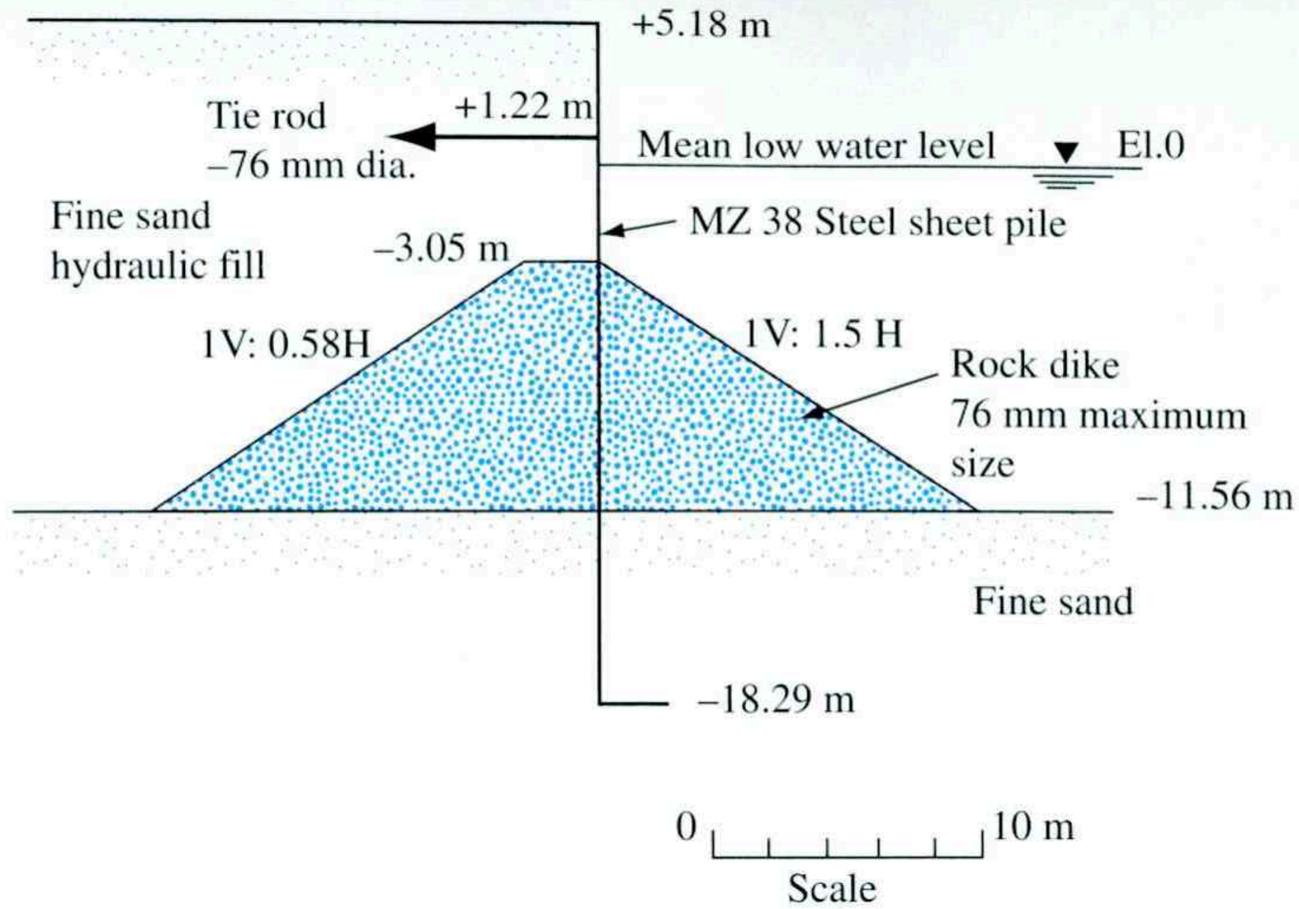

Figure 9.31 Pier C bulkhead—Long Beach harbor (Adapted after Casagrande, 1973)

variation of the lateral earth pressure between May 24, 1949 (the day construction was completed) and August 6, 1949. On May 24, the lateral earth pressure reached an active state, as shown in Figure 9.32a, due to the wall yielding. Between May 24 and June 3, the anchor resisted further yielding and the lateral earth pressure increased to the at-rest state (Figure 9.32b). However, the flexibility of the sheet piles ultimately resulted in a gradual decrease in the lateral earth-pressure distribution on the sheet piles (see Figure 9.32c).

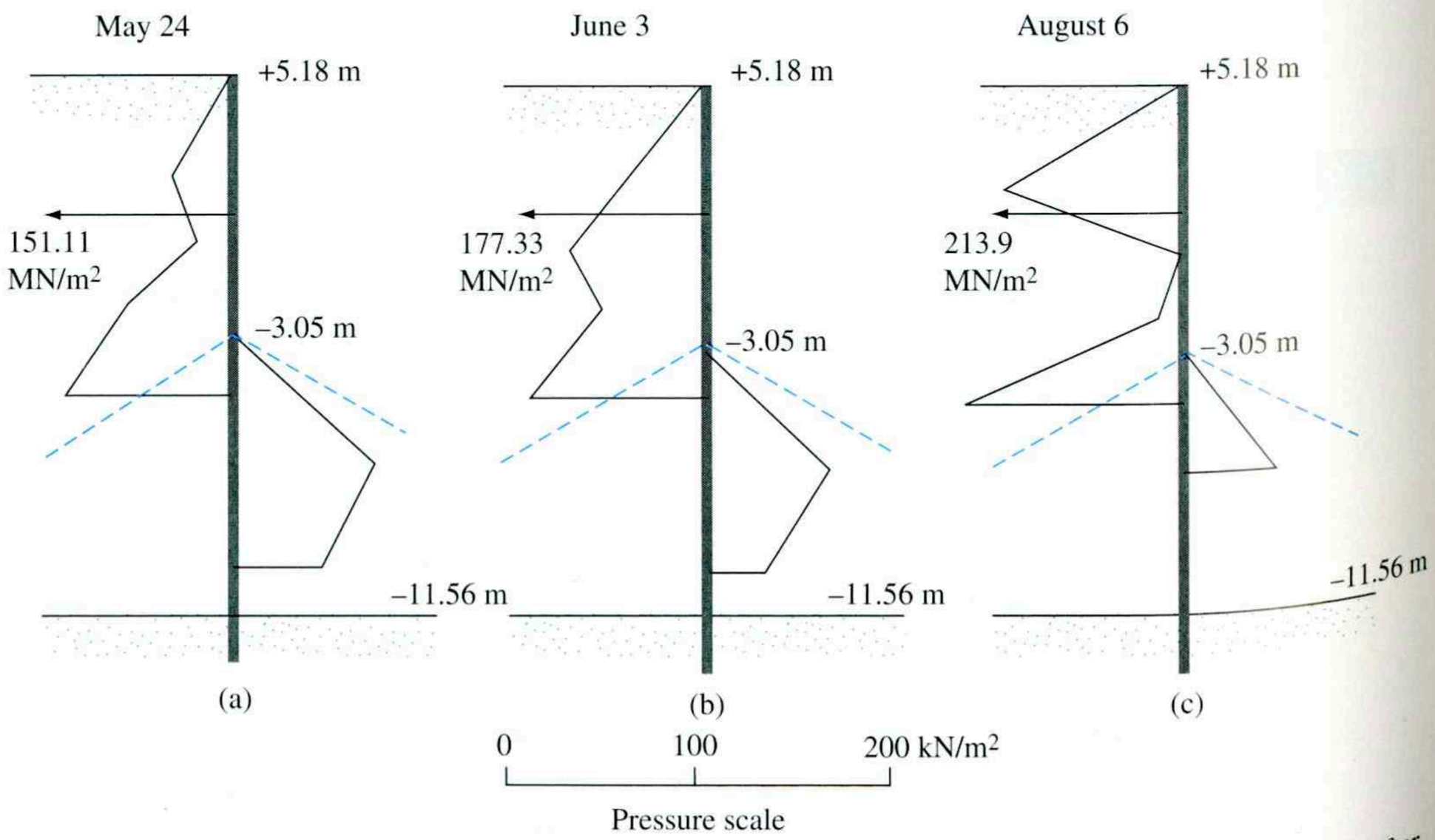

Figure 9.32 Measured stresses at Station 27 + 30—Pier C bulkhead, Long Beach (Adapted after Casagrande, 1973)

With time, the stress on the tie rods for the anchor increased as shown in the following table.

Date	Stress on anchor tie rod (MN/m^2)
May 24, 1949	151.11
June 3, 1949	177.33
June 11, 1949	193.2
July 12, 1949	203.55
August 6, 1949	213.9

These observations show that the magnitude of the active earth pressure may vary with time and depend greatly on the flexibility of the sheet piles. Also, the actual variations in the lateral earth-pressure diagram may not be identical to those used for design.

Bulkhead—Toledo, Ohio (1961)

A typical cross section of a Toledo bulkhead completed in 1961 is shown in Figure 9.33. The foundation soil was primarily fine to medium sand, but the dredge line did cut into highly overconsolidated clay. Figure 9.33 also shows the actual measured values of bending moment along the sheet-pile wall. Casagrande (1973) used the Rankine active earth-pressure distribution to calculate the maximum bending moment according to the free earth support method with and without Rowe's moment reduction.

Design method	Maximum predicted bending moment, M_{max}
Free earth support method	146.5 kN-m
Free earth support method with Rowe's moment reduction	78.6 kN-m

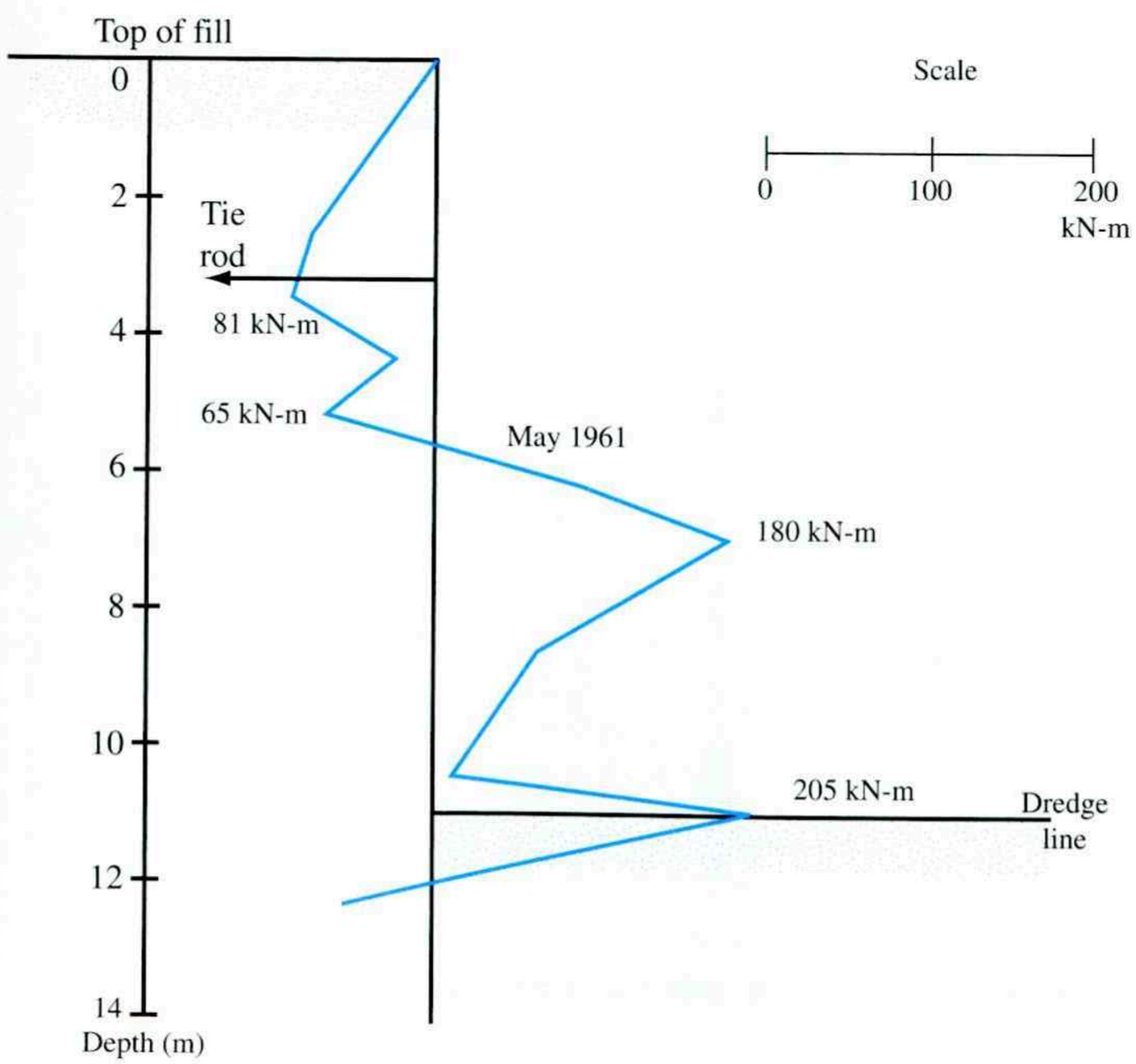

Figure 9.33 Bending moment from strain-gage measurements at test location 3, Toledo bulkhead (Adapted after Casagrande, 1973)

Comparisons of these magnitudes of M_{max} with those actually observed show that the field values are substantially larger. The reason probably is that the backfill was primarily fine sand and the measured active earth-pressure distribution was larger than that predicted theoretically.

9.15 Free Earth Support Method for Penetration of Clay

Figure 9.34 shows an anchored sheet-pile wall penetrating a clay soil and with a granular soil backfill. The diagram of pressure distribution above the dredge line is similar to that shown in Figure 9.12. From Eq. (9.42), the net pressure distribution below the dredge line (from $z = L_1 + L_2$ to $z = L_1 + L_2 + D$) is

$$\sigma_6 = 4c - (\gamma L_1 + \gamma' L_2)$$

For static equilibrium, the sum of the forces in the horizontal direction is

$$P_1 - \sigma_6 D = F \tag{9.84}$$

where

P_1 = area of the pressure diagram ACD
F = anchor force per unit length of the sheet pile wall

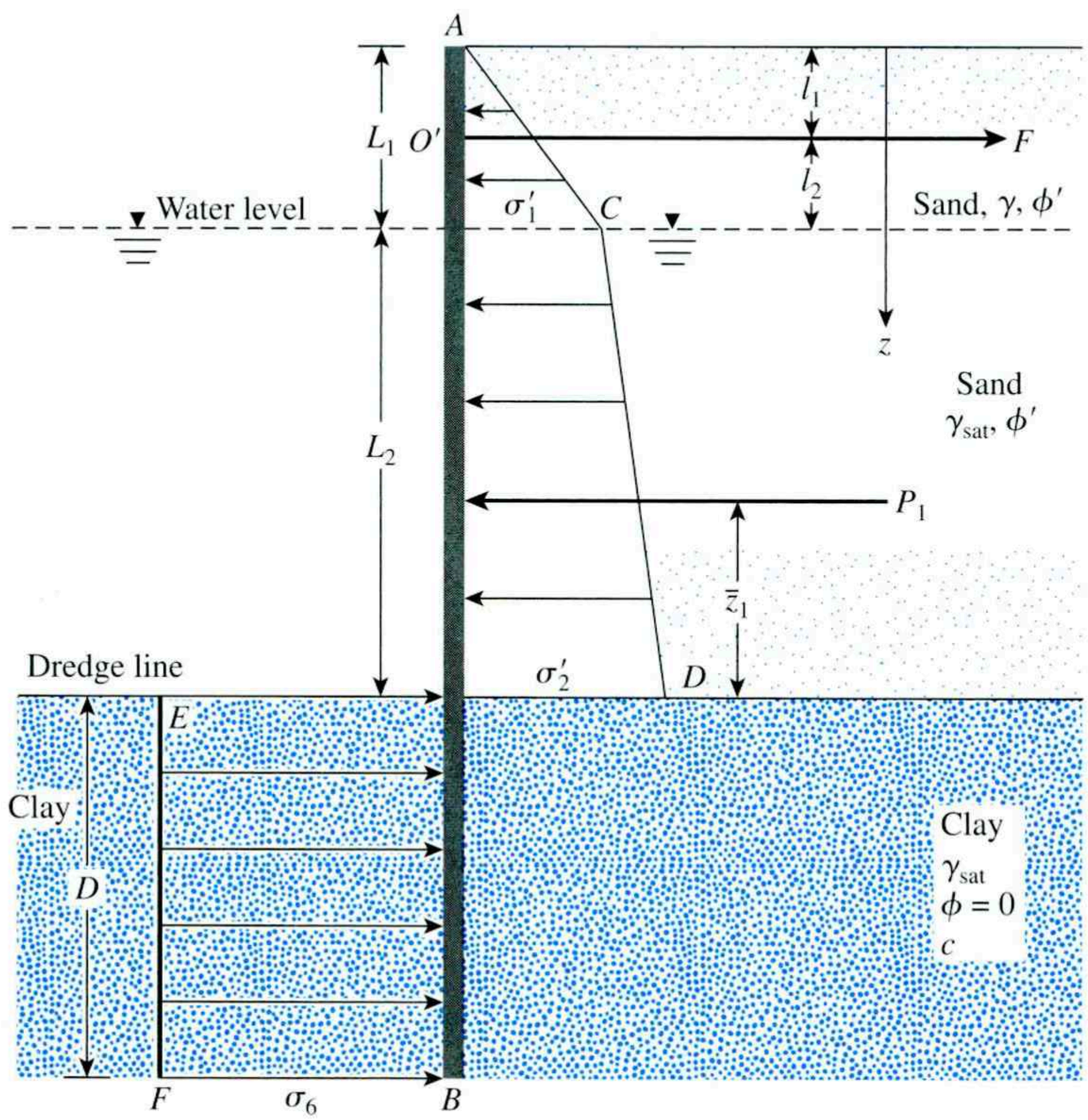

Figure 9.34 Anchored sheet-pile wall penetrating clay

Again, taking the moment about O' produces

$$P_1(L_1 + L_2 - l_1 - \bar{z}_1) - \sigma_6 D\left(l_2 + L_2 + \frac{D}{2}\right) = 0$$

Simplification yields

$$\sigma_6 D^2 + 2\sigma_6 D(L_1 + L_2 - l_1) - 2P_1(L_1 + L_2 - l_1 - \bar{z}_1) = 0 \tag{9.85}$$

Equation (9.85) gives the theoretical depth of penetration, D.

As in Section 9.9, the maximum moment in this case occurs at a depth $L_1 < z < L_1 + L_2$. The depth of zero shear (and thus the maximum moment) may be determined from Eq. (9.69).

A moment reduction technique similar to that in Section 9.11 for anchored sheet piles penetrating into clay has also been developed by Rowe (1952, 1957). This technique is presented in Figure 9.35, in which the following notation is used:

1. The stability number is

$$S_n = 1.25\frac{c}{(\gamma L_1 + \gamma' L_2)} \tag{9.86}$$

   where c = undrained cohesion ($\phi = 0$).

   For the definition of γ, γ', L_1, and L_2, see Figure 9.34.

2. The nondimensional wall height is

$$\alpha = \frac{L_1 + L_2}{L_1 + L_2 + D_{\text{actual}}} \tag{9.87}$$

3. The flexibility number is ρ [see Eq. (9.74a) or Eq. (9.74b)]
4. M_d = design moment
   $M_{\max}$ = maximum theoretical moment

The procedure for moment reduction, using Figure 9.35, is as follows:

Step 1. Obtain $H' = L_1 + L_2 + D_{\text{actual}}$.
Step 2. Determine $\alpha = (L_1 + L_2)/H'$.
Step 3. Determine S_n [from Eq. (9.86)].
Step 4. For the magnitudes of α and S_n obtained in Steps 2 and 3, determine $M_d/M_{\max}$ for various values of $\log \rho$ from Figure 9.35, and plot $M_d/M_{\max}$ against $\log \rho$.
Step 5. Follow Steps 1 through 9 as outlined for the case of moment reduction of sheet-pile walls penetrating granular soil. (See Section 9.11.)

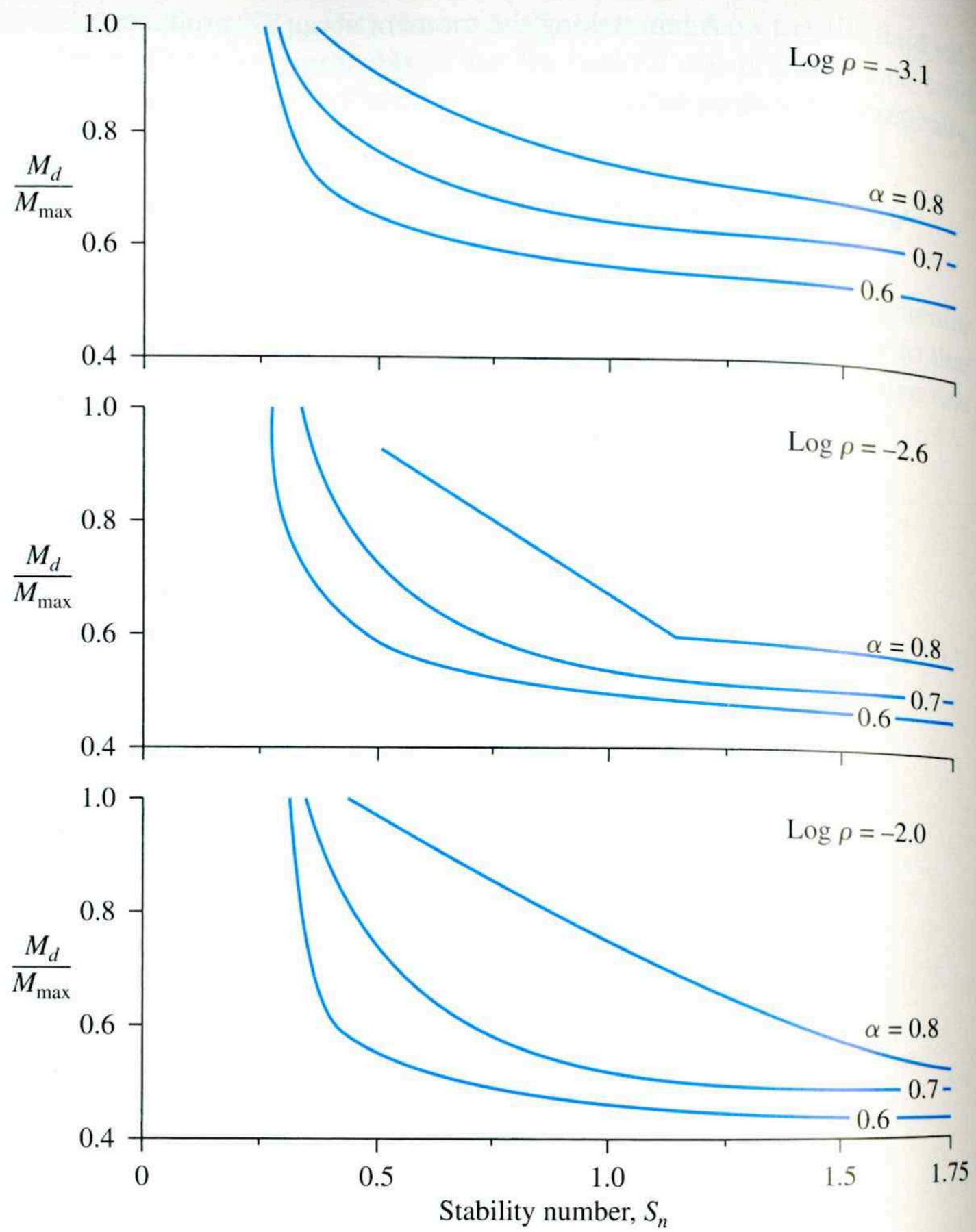

Figure 9.35 Plot of M_d/M_{max} against stability number for sheet-pile wall penetrating clay (From Rowe, P. W. (1957). "Sheet Pile Walls in Clay," *Proceedings*, Institute of Civil Engineers, Vol. 7, pp. 654–692.)

Example 9.10

In Figure 9.34, let $L_1 = 3$ m, $L_2 = 6$ m, and $l_1 = 1.5$ m. Also, let $\gamma = 17$ kN/m^3, $\gamma_{sat} = 20$ kN/m^3, $\phi' = 35°$, and $c = 41$ kN/m^2.

a. Determine the theoretical depth of embedment of the sheet-pile wall.
b. Calculate the anchor force per unit length of the wall.

Solution

Part a
We have

$$K_a = \tan^2\left(45 - \frac{\phi'}{2}\right) = \tan^2\left(45 - \frac{35}{2}\right) = 0.271$$

and

$$K_p = \tan^2\left(45 + \frac{\phi'}{2}\right) = \tan^2\left(45 + \frac{35}{2}\right) = 3.69$$

From the pressure diagram in Figure 9.36,

$$\sigma_1' = \gamma L_1 K_a = (17)(3)(0.271) = 13.82 \text{ kN/m}^2$$

$$\sigma_2' = (\gamma L_1 + \gamma' L_2) K_a = [(17)(3) + (20 - 9.81)(6)](0.271) = 30.39 \text{ kN/m}^2$$

$$P_1 = \text{areas } 1 + 2 + 3 = 1/2(3)(13.82) + (13.82)(6) + 1/2(30.39 - 13.82)(6)$$
$$= 20.73 + 82.92 + 49.71 = 153.36 \text{ kN/m}$$

and

$$\bar{z}_1 = \frac{(20.73)\left(6 + \frac{3}{3}\right) + (82.92)\left(\frac{6}{2}\right) + (49.71)\left(\frac{6}{3}\right)}{153.36} = 3.2 \text{ m}$$

From Eq. (9.85),

$$\sigma_6 D^2 + 2\sigma_6 D(L_1 + L_2 - l_1) - 2P_1(L_1 + L_2 - l_1 - \bar{z}_1) = 0$$

$$\sigma_6 = 4c - (\gamma L_1 + \gamma' L_2) = (4)(41) - [(17)(3) + (20 - 9.81)(6)] = 51.86 \text{ kN/m}^2$$

So,

$$(51.86)D^2 + (2)(51.86)(D)(3 + 6 - 1.5) - (2)(153.36)(3 + 6 - 1.5 - 3.2) = 0$$

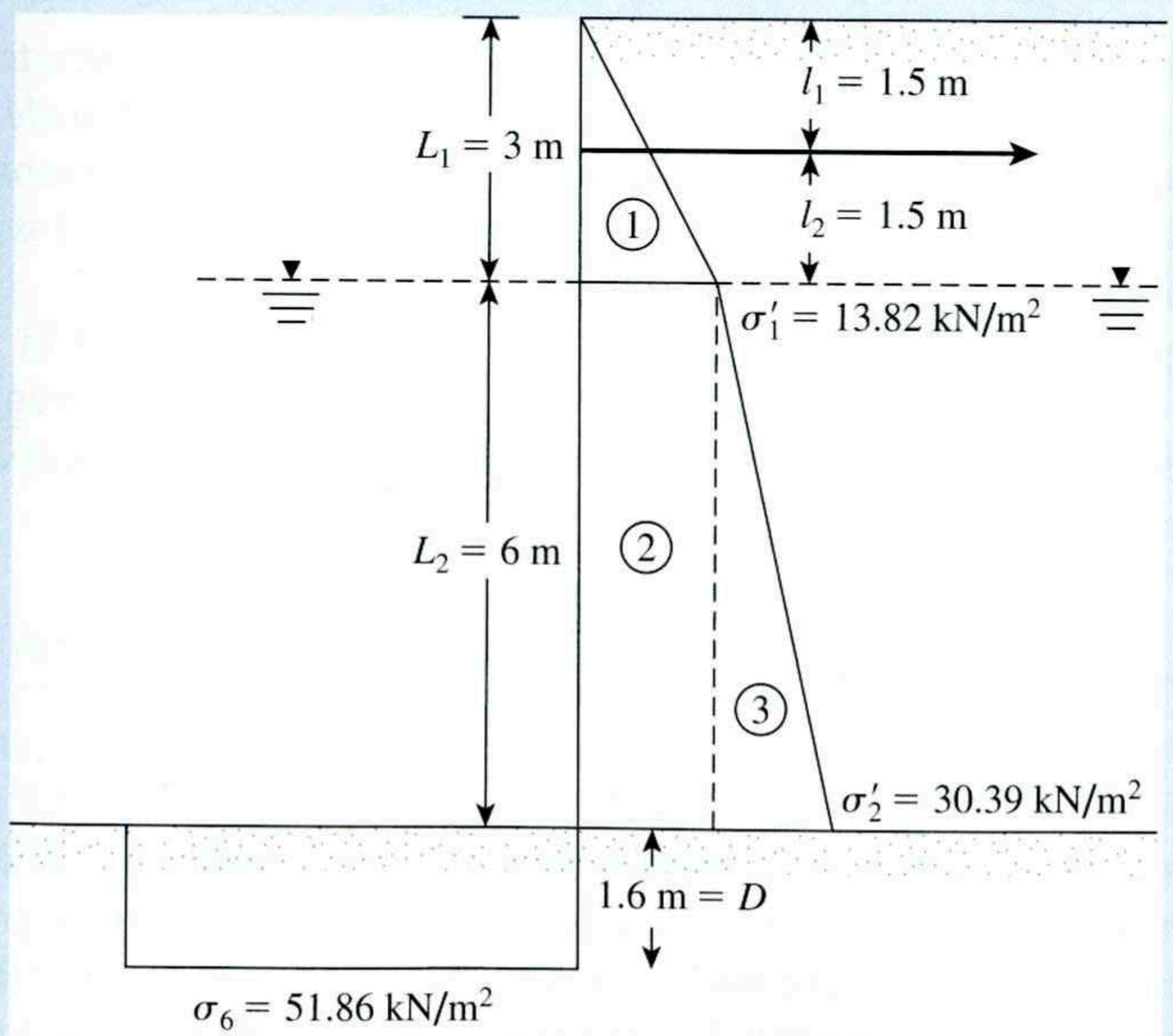

Figure 9.36 Free earth support method, sheet pile penetrating into clay

or

$$D^2 + 15D - 25.43 = 0$$

Hence,

$$D \approx \mathbf{1.6\ m}$$

Part b
From Eq. (9.84),

$$F = P_1 - \sigma_6 D = 153.36 - (51.86)(1.6) = \mathbf{70.38\ kN/m}$$

9.16 Anchors

Sections 9.9 through 9.15 gave an analysis of anchored sheet-pile walls and discussed how to obtain the force F per unit length of the sheet-pile wall that has to be sustained by the anchors. The current section covers in more detail the various types of anchor generally used and the procedures for evaluating their ultimate holding capacities.

The general types of anchor used in sheet-pile walls are as follows:

1. Anchor plates and beams (deadman)
2. Tie backs
3. Vertical anchor piles
4. Anchor beams supported by batter (compression and tension) piles

Anchor plates and beams are generally made of cast concrete blocks. (See Figure 9.37a.) The anchors are attached to the sheet pile by *tie-rods*. A *wale* is placed at the front or back face of a sheet pile for the purpose of conveniently attaching the tie-rod to the wall. To protect the tie rod from corrosion, it is generally coated with paint or asphaltic materials.

In the construction of *tiebacks,* bars or cables are placed in predrilled holes (see Figure 9.37b) with concrete grout (cables are commonly high-strength, prestressed steel tendons). Figures 9.37c and 9.37d show a vertical anchor pile and an anchor beam with batter piles.

Placement of Anchors

The resistance offered by anchor plates and beams is derived primarily from the passive force of the soil located in front of them. Figure 9.37a, in which AB is the sheet-pile wall, shows the best location for maximum efficiency of an anchor plate. If the anchor is placed inside wedge ABC, which is the Rankine active zone, it would not provide any resistance to failure. Alternatively, the anchor could be placed in zone $CFEH$. Note that line DFG is the slip line for the Rankine passive pressure. If part of the passive wedge is located inside the active wedge ABC, full passive resistance of the anchor cannot be realized upon

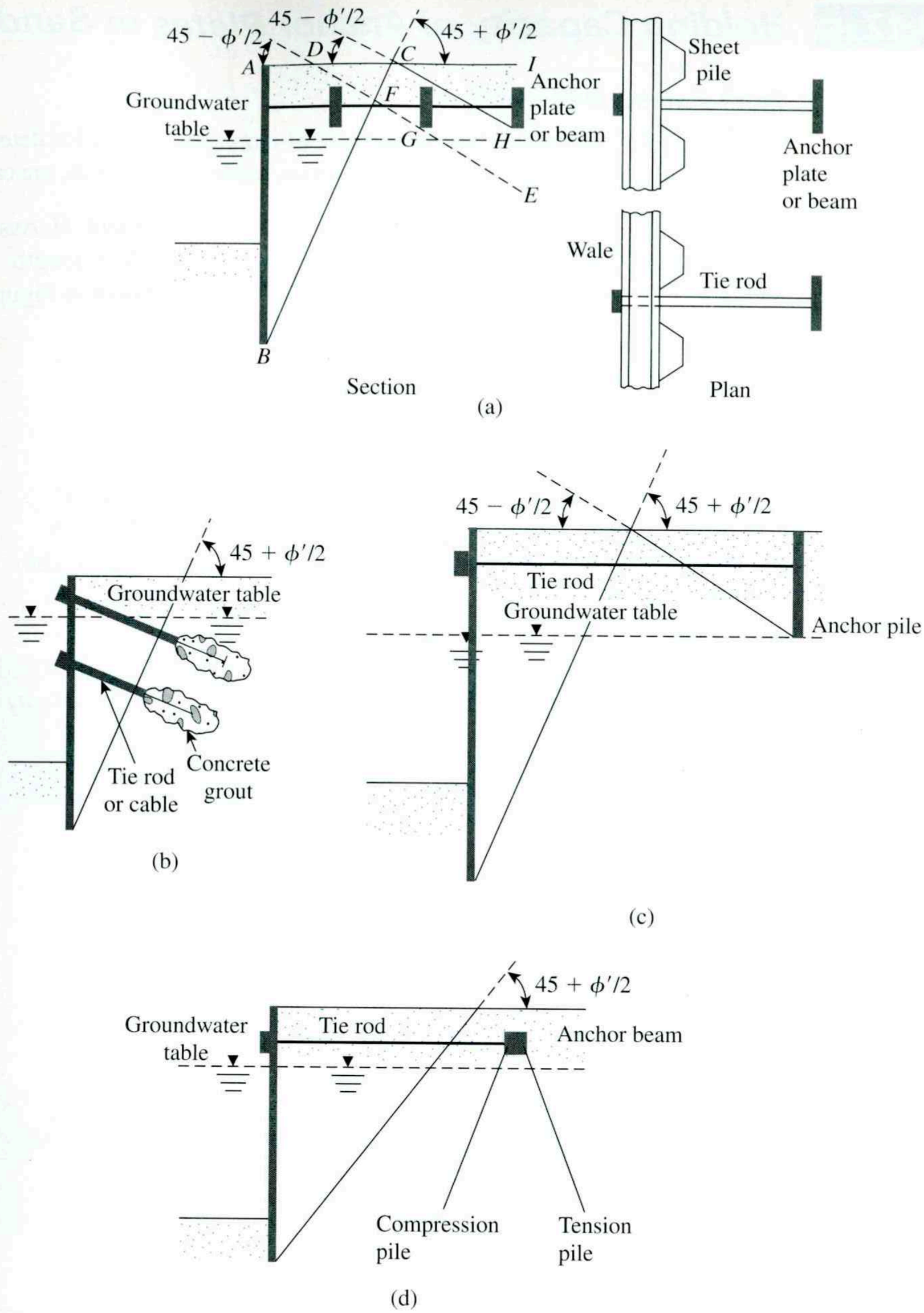

Figure 9.37 Various types of anchoring for sheet-pile walls: (a) anchor plate or beam; (b) tieback; (c) vertical anchor pile; (d) anchor beam with batter piles

failure of the sheet-pile wall. However, if the anchor is placed in zone *ICH*, the Rankine passive zone in front of the anchor slab or plate is located completely outside the Rankine active zone *ABC*. In this case, full passive resistance from the anchor can be realized.

Figures 9.37b, 9.37c, and 9.37d also show the proper locations for the placement of tiebacks, vertical anchor piles, and anchor beams supported by batter piles.

9.17 Holding Capacity of Anchor Plates in Sand

Semi-Empirical Method

Ovesen and Stromann (1972) proposed a semi-empirical method for determining the ultimate resistance of anchors in sand. Their calculations, made in three steps, are carried out as follows:

Step 1. **Basic Case.** Determine the depth of embedment, H. Assume that the anchor slab has height H and is continuous (i.e., B = length of anchor slab perpendicular to the cross section $= \infty$), as shown in Figure 9.38, in which the following notation is used:

P_p = passive force per unit length of anchor
P_a = active force per unit length of anchor
ϕ' = effective soil friction angle
δ' = friction angle between anchor slab and soil
P'_{ult} = ultimate resistance per unit length of anchor
W = effective weight per unit length of anchor slab

Also,

$$P'_{ult} = \tfrac{1}{2}\gamma H^2 K_p \cos\delta' - P_a \cos\phi' = \tfrac{1}{2}\gamma H^2 K_p \cos\delta' - \tfrac{1}{2}\gamma H^2 K_a \cos\phi'$$
$$= \tfrac{1}{2}\gamma H^2 (K_p \cos\delta' - K_a \cos\phi') \tag{9.88}$$

where

K_a = active pressure coefficient with $\delta' = \phi'$ (see Figure 9.39a)
K_p = passive pressure coefficient

To obtain $K_p \cos\delta'$, first calculate

$$K_p \sin\delta' = \frac{W + P_a \sin\phi'}{\frac{1}{2}\gamma H^2} = \frac{W + \frac{1}{2}\gamma H^2 K_a \sin\phi'}{\frac{1}{2}\gamma H^2} \tag{9.89}$$

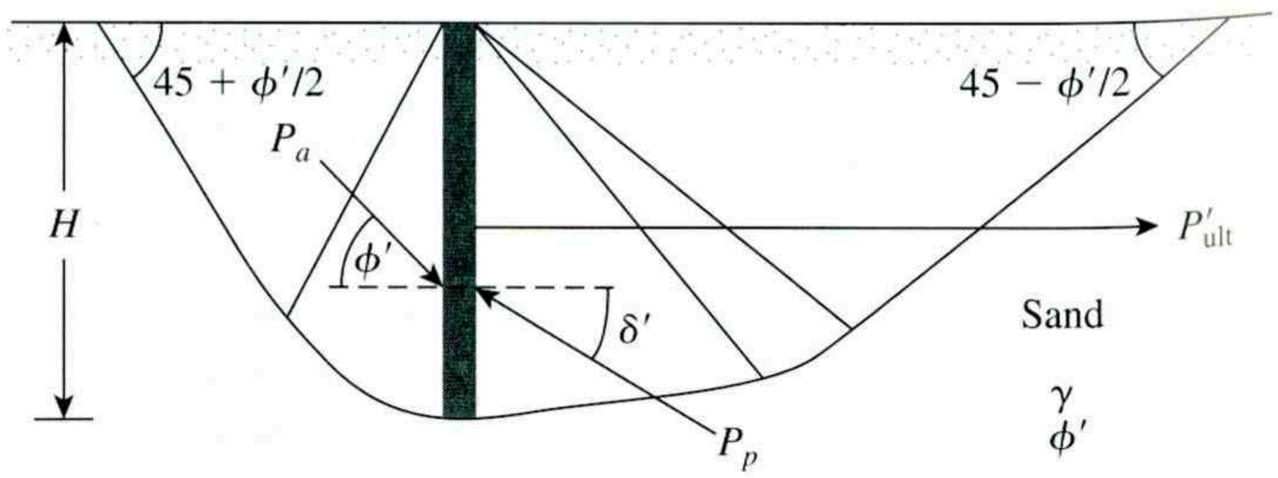

Figure 9.38 Basic case: continuous vertical anchor in granular soil

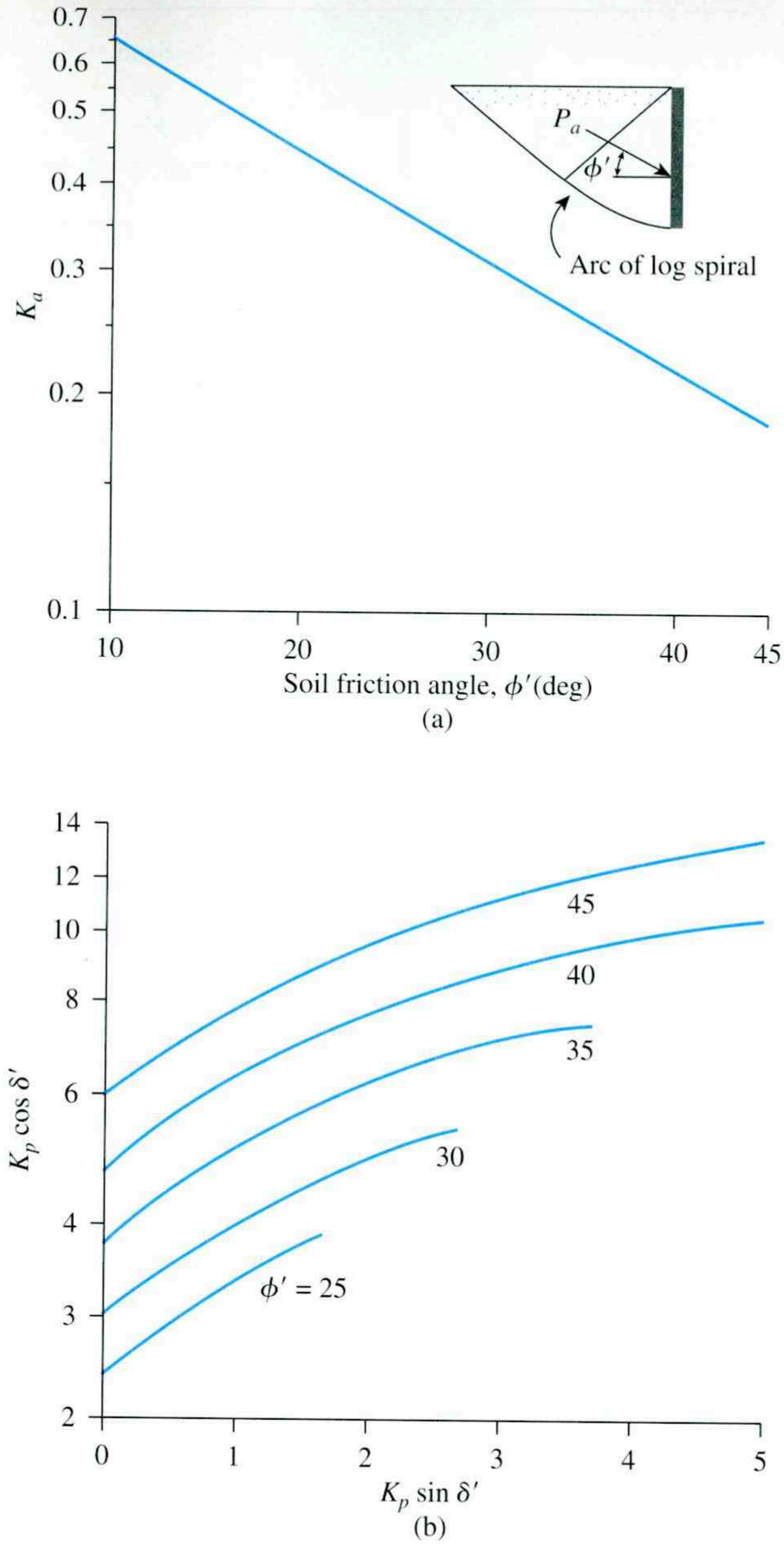

Figure 9.39 (a) Variation of K_a for $\delta' = \phi'$, (b) variation of $K_p \cos \delta'$ with $K_p \sin \delta'$ (Based on Ovesen and Stromann, 1972)

Then use the magnitude of $K_p \sin \delta'$ obtained from Eq. (9.89) to estimate the magnitude of $K_p \cos \delta'$ from the plots given in Figure 9.39b.

Step 2. **Strip Case.** Determine the actual height h of the anchor to be constructed. If a continuous anchor (i.e., an anchor for which $B = \infty$) of height h is placed in the soil so that its depth of embedment is H, as shown in Figure 9.40, the ultimate resistance per unit length is

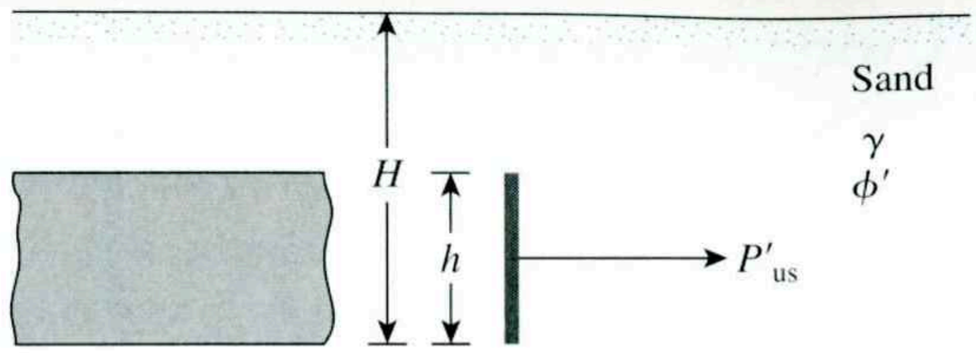

Figure 9.40 Strip case: vertical anchor

$$P'_{us} = \left[\frac{C_{ov} + 1}{C_{ov} + \left(\frac{H}{h}\right)}\right] \underset{\text{Eq. 9.88}}{\underset{\uparrow}{P'_{ult}}} \tag{9.90}$$

where

P'_{us} = ultimate resistance for the *strip case*
C_{ov} = 19 for dense sand and 14 for loose sand

Step 3. **Actual Case.** In practice, the anchor plates are placed in a row with center-to-center spacing S', as shown in Figure 9.41a. The ultimate resistance of each anchor is

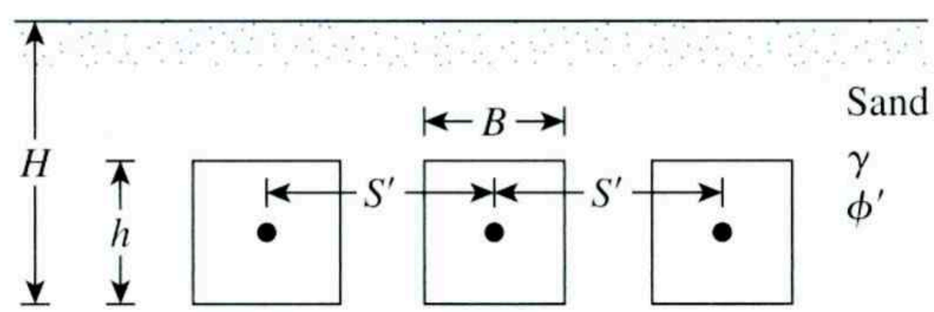

(a)

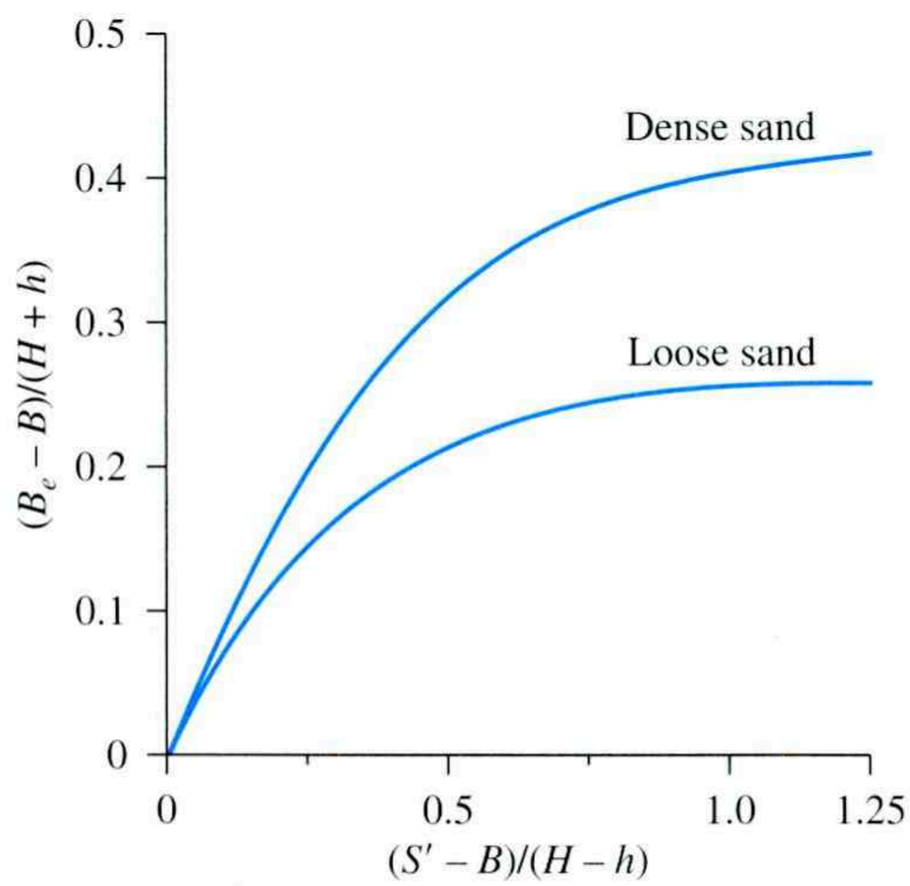

(b)

Figure 9.41 (a) Actual case for row of anchors; (b) variation of $(B_e - B)/(H + h)$ with $(S' - B)/(H + h)$ (Based on Ovesen and Stromann, 1972)

$$P_{ult} = P'_{us} B_e \tag{9.91}$$

where B_e = equivalent length.

The equivalent length is a function of S', B, H, and h. Figure 9.41b shows a plot of $(B_e - B)/(H + h)$ against $(S' - B)/(H + h)$ for the cases of loose and dense sand. With known values of S', B, H, and h, the value of B_e can be calculated and used in Eq. (9.91) to obtain P_{ult}.

Stress Characteristic Solution

Neely, Stuart, and Graham (1973) proposed a stress characteristic solution for anchor pull-out resistance using the *equivalent free surface* concept. Figure 9.42 shows the assumed failure surface for a strip anchor. In this figure, OX is the equivalent free surface. The shear stress (s_o) mobilized along OX can be given as

$$m = \frac{s_o}{\sigma'_o \tan \phi'} \tag{9.92}$$

where

m = shear stress mobilization factor
σ_o' = effective normal stress along OX

Using this analysis, the ultimate resistance (P_{ult}) of an anchor (length = B and height = h) can be given as

$$P_{ult} = M_{\gamma q} (\gamma h^2) B F_s \tag{9.93}$$

where

$M_{\gamma q}$ = force coefficient
F_s = shape factor
γ = effective unit weight of soil

The variations of $M_{\gamma q}$ for $m = 0$ and 1 are shown in Figure 9.43. For conservative design, $M_{\gamma q}$ with $m = 0$ may be used. The shape factor (F_s) determined experimentally is shown in Figure 9.44 as a function of B/h and H/h.

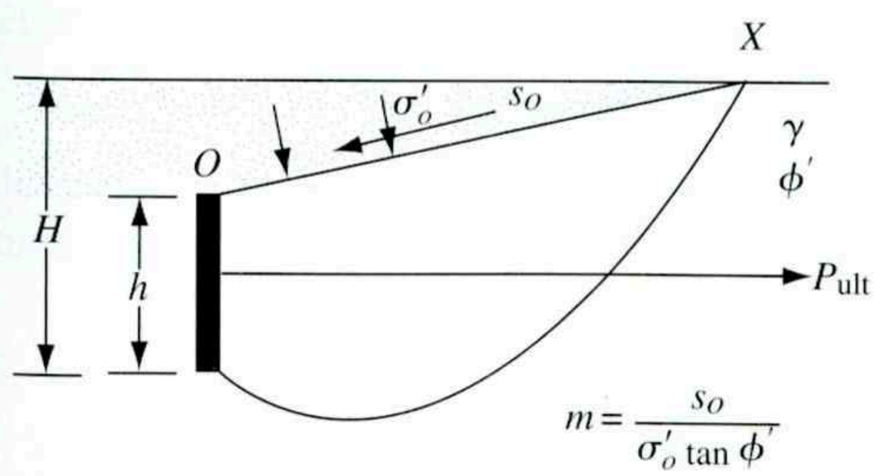

Figure 9.42 Assumed failure surface in soil for stress characteristic solution